RIPK1 down-regulation promotes tumor progression while enhancing the apoptotic response to TLR3 ligand in head and neck squamous cell carcinoma

by

Kevin Dylan McCormick

B.S. in Biology, Seton Hill University, 2007

M.S. in Infectious Diseases and Microbiology, University of Pittsburgh, 2011

Submitted to the Graduate Faculty of

School of Medicine in partial fulfillment of

the requirements for the degree of PhD in

Molecular Virology and Microbiology

University of Pittsburgh

2016

UNIVERSITY OF PITTSBURGH

SCHOOL OF MEDICINE

This dissertation was presented

by

Kevin Dylan McCormick

It was defended on

February 11, 2016

and approved by

Carolyn B. Coyne, PhD, Associate Professor

Saleem A. Khan, PhD, Professor

Pawel Kalinski MD, PhD, Professor

Thomas Smithgall, PhD, Professor

Jian Yu, PhD, Professor

Dissertation Advisor: Saumendra N. Sarkar, PhD, Assistant Professor

RIPK1 DOWN-REGULATION PROMOTES TUMOR PROGRESSION WHILE ENHANCING THE APOPTOTIC RESPONSE TO TLR3 LIGAND IN HEAD AND NECK SQUAMOUS CELL CARCINOMA

Kevin Dylan McCormick, PhD

University of Pittsburgh, 2016

Head and neck squamous cell carcinoma (HNSCC) is the most frequent malignancy of the aerodigestive tract and the limitations in current chemotherapeutic approaches have yielded a poor prognosis. Synthetic double stranded (ds) RNA, which activate toll-like receptor 3 (TLR3) and generate interferon regulatory factor 3 (IRF3)-mediated proapoptotic responses in cancer cells, are being investigated as potent adjuvants to chemotherapy. We had previously shown that cells derived from metastatic HNSCC were unable to activate prosurvival NF-κB in response to TLR3 ligand, resulting in an enhanced apoptotic response compared to cells from primary tumors. Here, we demonstrate that in metastatic tumor-derived cell lines, transcriptional downregulation of receptor interacting protein kinase 1 (RIPK1), an adaptor protein of the TLR3 pathway, enhances dsRNA-mediated apoptosis due to a loss of NF-κB activation. This is consistent with our observations supporting the reduction of RIPK1 expression during the tumor progression of HNSCC correlated with an increased promoter methylation in matched tumor samples from HNSCC patients. Treatment of metastatic tumor-derived cell lines with a hypomethylating agent rescued the expression of RIPK1, demonstrating that promoter methylation may be responsible for the downregulation of RIPK1. We show that silencing of RIPK1 enhances the tumor promoting properties in HNSCC cell lines by increasing the rate of migration, EGFR expression and anoikis resistance. As the downregulation of RIPK1 expression

contributes to the metastatic phenotype of HNSCC, but is essential for TLR3-NF-κB mediated pro-survival responses, we believe the results described here may open new prospects for using synthetic dsRNA to target metastatic tumor cells. In light of these findings, RIPK1 downregulation as a treatment biomarker, or combinational therapies with NF-κB-signaling inhibitors, could be used to enhance the immunotherapeutic efficacy of synthetic dsRNA. As the downregulation of RIPK1 has been observed in additional carcinomas, our findings suggest that synthetic dsRNA could be used as a broad anti-cancer therapy and that RIPK1 expression can be a useful indicator to predict the therapy response.

TABLE OF CONTENTS

TABLE OF CONTENTS VI

LIST OF TABLES XI

LIST OF FIGURES XII

ACKNOWLEDGEMENTS XIV

1.0 INTRODUCTION 1

1.1 HEAD AND NECK SQUAMOUS CELL CARCINOMA 1

1.1.1 Epidemiology of HNSCC 3

1.1.2 Molecular Biology of HNSCC: 5

1.1.2.1 High and Low Chromosome Instability 6

1.1.2.2 The Human Papilloma Virus 16

1.1.3 Current treatments for HNSCC: 17

1.2 HNSCC IMMUNOSURVEILLANCE AND IMMUNOEDITING: 20

1.2.1 Innate Immune Signaling in HNSCC 23

1.2.2 Toll-like Receptor Protein (TLR3): 27

1.2.2.1 TLR3-IRF3 signaling 29

1.2.2.2 TLR3-NF-κB signaling 30

1.2.2.3 TLR3 expression and function in HNSCC 31

1.2.2.4 TLR3 ligand as an immunotherapy for HNSCC 32

1.2.3 Receptor-interacting protein kinase 1 (RIPK1): 33
1.2.3.1 The role of RIPK1 in cancer 36
1.3 RATIONALE AND HYPOTHESIS 38
2.0 MATERIALS AND METHODS 42
2.1 CELL LINES AND TISSUES 42
2.2 ANTIBODIES AND IMMUNOHISTOCHEMISTRY 43
2.3 WESTERN BLOTTING ANALYSIS 43
2.4 LENTIVIRAL VECTORS 44
2.5 QUANTITATIVE PCR ANALYSIS OF GENE EXPRESSION 45
2.6 DNA METHYLTRANSFERASE INHIBITION ASSAY 46
2.7 ANOIKIS-RECOVERY ASSAY 46
2.8 MIGRATION ASSAY 47
2.8.1 Two-dimensional wound-healing (scratch) assay. 47
2.8.2 Three-dimensional transwell migration assay 47
2.9 ORTHOTOPIC XENOGRAFT MODEL 47
2.10 DATASETS AND STATISTICAL ANALYSIS 48
2.10.1 Datasets. 48
2.10.2 Statistical analysis. 49
3.0 AIM 1: ESTABLISH THE DOWNREGULATION OF RIPK1 EXPRESSION DURING THE TUMOR PROGRESSION OF HNSCC. 50
3.1 INTRODUCTION 50
3.2 RESULTS 52
3.2.1 Downregulation of RIPK1 in metastatic HNSCC cell lines. 52

3.3 DISCUSSION 56

4.0 AIM 2: ELUCIDATE THE MECHANISTIC CAUSE OF RIPK1 DOWNREGULATED EXPRESSION. 59

4.1 INTRODUCTION 59

4.2 RESULTS 60

4.2.1 There is promoter methylation in a CpG island -868 bases from the transcription start site of RIPK1. 60

4.2.2 Promoter methylation correlates with RIPK1 expression in resected tumor samples. 63

4.2.3 Hypomethylating treatment conditions restored the expression of RIPK1 in the PCI-15B metastatic tumor derived cell line. 64

4.3 DISCUSSION 65

5.0 AIM 3: INVESTIGATE THE BIOLOGICAL CONSEQUENCES OF RIPK1 DOWNREGULATION IN HNSCC: TUMOR PROGRESSION AND ENHANCED APOPTOTIC RESPONSE TO POLY(I):POLY(C) 67

5.1 INTRODUCTION 67

5.2 RESULTS 68

5.2.1 Modulation of RIPK1 expression changes *in vitro* tumor-promoting properties. 68

5.2.2 Ectopic expression of RIPK1 in OSC-19 cells in a mouse model. 72

5.2.3 Ectopic changes in RIPK1 expression modulates dsRNA-mediated apoptosis 75

5.2.4 Additive Apoptotic effect of poly(I):poly(C) cotreatment with HNSCC therapies in HNSCC cell lines 77
5.3 DISCUSSION 79
6.0 FINAL DISCUSSION 83
APPENDIX A : UNIQUE ANTIVITAL ROLES OF THE 2',5'-OLIGOADENYLATE SYNTHETASE ISOZYMES 92
A.1 INTRODUCTION 93
A.2 MATERIALS AND METHODS 97
A.2.1 CELL LINES AND 97
A.2.2 CRISPR/CAS9 KNOCKOUT 97
A.2.3 ANTIBODIES AND REAGENTS 98
A.2.4 WESTERN BLOTTING ANALYSIS 99
A.2.5 QUANTITATIVE PCR ANALYSIS OF GENE EXPRESSION 99
A.2.6 VIRUS INFECTION AND FLOW CYTOMETRY ANALYSIS 100
A.3 RESULTS 100
A.3.1 IFNγ signaling was defective in the THP-1 OAS1 knockout cell lines. 100
A.3.2 Downstream mediators of the IFNγ pathway are intact in OAS1 knockout cells. 101
A.3.3 Inhibition of the proteasome restores the induction of IRF1 upon IFNγ stimulation 103
A.3.4 Ectopic expression of mOas1b increases IRF1 stability upon IFNγ stimulation 104

A.3.5 IFNγ pretreatment of THP-1 OAS1 knockout cells elicited a less protective response against VSV-GFP infection. 105

A.4 DISCUSSION 107

APPENDIX B : SV40 LARGE T ANTIGEN INDUCTION OF ISGS IS DEPENDENT ON THE LT-INITIATED DNA-DAMAGE RESPONSE 110

B.1 INTRODUCTION 111

B.2 MATERIALS AND METHODS 112

B.2.1 Cells and reagents 112

B.2.2 Plasmids and viruses 112

B.2.3 QUANTITATIVE PCR ANALYSIS OF GENE EXPRESSION 112

B.3 RESULTS AND DISCUSSION 113

APPENDIX C : IRF4 REDUCED EXPRESSION INDUCES LYTIC REACTIVATION OF KSHV IN PRIMARY EFFUSION LYMPHOMA CELLS 115

C.1 INTRODUCTION 116

C.2 MATERIALS AND METHODS 117

C.2.1 Nuclear Extraction Protocol for the KSHV replication transactivator (RTA) expression assay 117

C.2.2 Quantitative real-time PCR assay for KSHV production 117

C.3 RESULTS AND DISCUSSION 119

APPENDIX D : LIST OF ABBREVIATIONS 121

BIBLIOGRAPHY 127

LIST OF TABLES

Table 1 HNSCC Related Matrix Metalloproteinases and Their Extracellular Matrix Substrates 15

Table 2 HNSCC cell lines used in this study 43

Table 3 Previously reported virus-specific antiviral activity of the OAS family 94

Table 4 Table of Abbreviations 121

LIST OF FIGURES

Figure 1 Schematic overview representing the anatomical sites effected by HNSCC 2

Figure 2 Detailed schematic of human toll-like receptor signaling: 26

Figure 3 TLR3 signaling: 28

Figure 4 Schematic representation of the multiple domains of RIPK1. 34

Figure 5 Downregulation of RIPK1 in metastatic head and neck cancer cell lines: 53

Figure 6 Downregulation of RIPK1 protein expression between metastatic and primary HNSCC resected patient-matched tumors: 54

Figure 7 Downregulation of RIPK1 mRNA expression between primary tumors and normal tissue from HNSCC resected matched-patient tumors: 55

Figure 8 RIPK1 expression is downregulated in primary tumors irrespective of HPV status: 56

Figure 9 Promoter methylation in a CpG island -868 bases from the transcription start site of RIPK1: 62

Figure 10 Promoter methylation correlates with RIPK1 expression in tumor samples: 63

Figure 11 Hypomethylating treatment restored the expression of RIPK1 in PCI-15B Metastatic cells: 64

Figure 12 Ectopic changes in the expression of RIPK1 in primary and metastatic HNSCC derived cell lines: 69

Figure 13 Silencing of RIPK1 in primary derived HNSCC cell lines enhances the rate of migration: 70
Figure 14 Silencing of RIPK1 expression enhanced the anoikis resistance: 71
Figure 15 Modulation of RIPK1 expression inversely correlates to the expression of EGFR: 72
Figure 16 Stable expression of RIPK1 in the OSC-19-luc HNSCC cell line does not suppress lymph node metastasis in the orthotopic xenograph mouse model: 74
Figure 17 Ectopic changes in RIPK1 expression modulates dsRNA-mediated apoptosis: 76
Figure 18 Induced RIPK1 expression mitigated dsRNA-mediated apoptosis: 77
Figure 19 Additive apoptotic effect with polyI:C cotreatments: 78
Figure 20 Schematic map showing chromosomal locations of the human and mouse OAS genes: 95
Figure 21 Loss of IRF1 induction in OAS1 knockout cell lines in response to IFNγ signaling: 101
Figure 22 IFNGR downstream mediators are intact in OAS1 knockout cells: 103
Figure 23 IRF1 proteasome degradation rate is increased in the OAS1 knockout cells: 104
Figure 24 IRF1 protein stability was increased in RAW cells expressing mOas1b: 105
Figure 25 IFNγ pretreatment of THP-1 OAS1 KO cells elicited a less protective response against VSV-GFP: 106
Figure 26 SV40 LT ISG induction is dependent on DDR activation: 114
Figure 27 Loss of IRF4 results in a robust induction of KSHV lytic gene expression and viral reactivation: 120

ACKNOWLEDGEMENTS

First and foremost, I would like to acknowledge my Committee members, Drs. Carolyn Coyne, Saleem Khan, Pawel Kalinski, Thomas Smithgall and Jian Yu, who have taken the time to attend numerous committee meeting and have contributed brilliant suggestions that guided my dissertation work. I would especially like to thank my dissertation advisor and PI Dr. Saumendra Sarkar for guiding me over the past four years. I know can I be overly cynical, which admittedly is my biggest fault, but Dr. Sarkar was able to show me how to look beyond the doubt and make "lemonade out of lemons."

I would also like to thank my previous mentors Dr. Jamie Fornsaglio for sparking my initial interest in scientific research. Without the opportunity to do an undergraduate senior research thesis I would have never been aware of research as a possible career path. Also from Seton Hill University I would like to recognize Sr. Susan Yocham and Dr. Bernadette Fondy for inspiring me to teach by giving me the opportunity to assist them in their biochemisty and ecology courses. From my previous studies, I would like to acknowledge Dr. Tianyi Wang for mentoring me during my Master's Thesis research and for inspiring me to continue my studies into a PhD.

I would like to thank my friend Jana Jacobs for her friendship throughout my studies. Our friendship began as lab mates in the Dr. Wang's lab and was bolstered through a shared unusual experience together. Without our relationship I would surely not have persevered. Also from Dr.

Wang's lab I would like to thank Dr. Shufeng Liu for teaching me about tissue culture and many lab methods and for being there when I needed him. I would also like to thank my current and previous lab mates from Dr. Sarkar's lab, Drs. Adriana Forero, Rolando Cuevas, Arundhati Ghosh and Jianzong Zhu for their assistance and guidance in experiments and suggestions for future directions.

Finally I would like to thank my parents, Barbara and David McCormick, who never stopped believing in me even in my darkest of hours. My sisters Jennifer Weinman and Melissa Young for their support and my loving wife Kathryn for her perseverance.

1.0 INTRODUCTION

1.1 HEAD AND NECK SQUAMOUS CELL CARCINOMA

Carcinomas are cancers of the epithelium and account for over 80 percent of all tumor-related deaths worldwide (*1*, *2*). Included in the exhaustive list of carcinomas are tumors of the gastrointestinal tract: the mouth, esophagus, stomach and small and large intestines, as well as cancers of the skin, mammary glands, pancreas, lung, liver, ovary, cervix, uterus, prostate, gallbladder and urinary bladder (*1*).

Attributable to the accumulation of genetic events and chromosome instability from long-term chronic exposure of the keratinocytes in the upper aerodigestive tract to tobacco and alcohol, squamous cell carcinoma (SCC) accounts for over 90% of head and neck cancers (*3*, *4*). Specifically the exposure to the mutagens benzo[a]pyrene and nitroamines in cigarette smoke, that produce guanine nucleotide transversions in critical tumor suppressor genes and acetaldehyde, a metabolite of alcohol consumption, increase the likelihood of developing this disease (*5*). Because of the exposure to these carcinogens, HNSCC primary tumors initially develop throughout the upper aerodigestive tract (oral cavity, oropharynx and larynx) **Figure 1**. Additionally, human papillomavirus (HPV) has been shown to be transmitted to the oral mucosa during oral sex and many HNSCC tumors have been shown to be HPV E6 and E7 positive, leading to the assertion that HPV is also a causative agent for HNSCC (*6*).

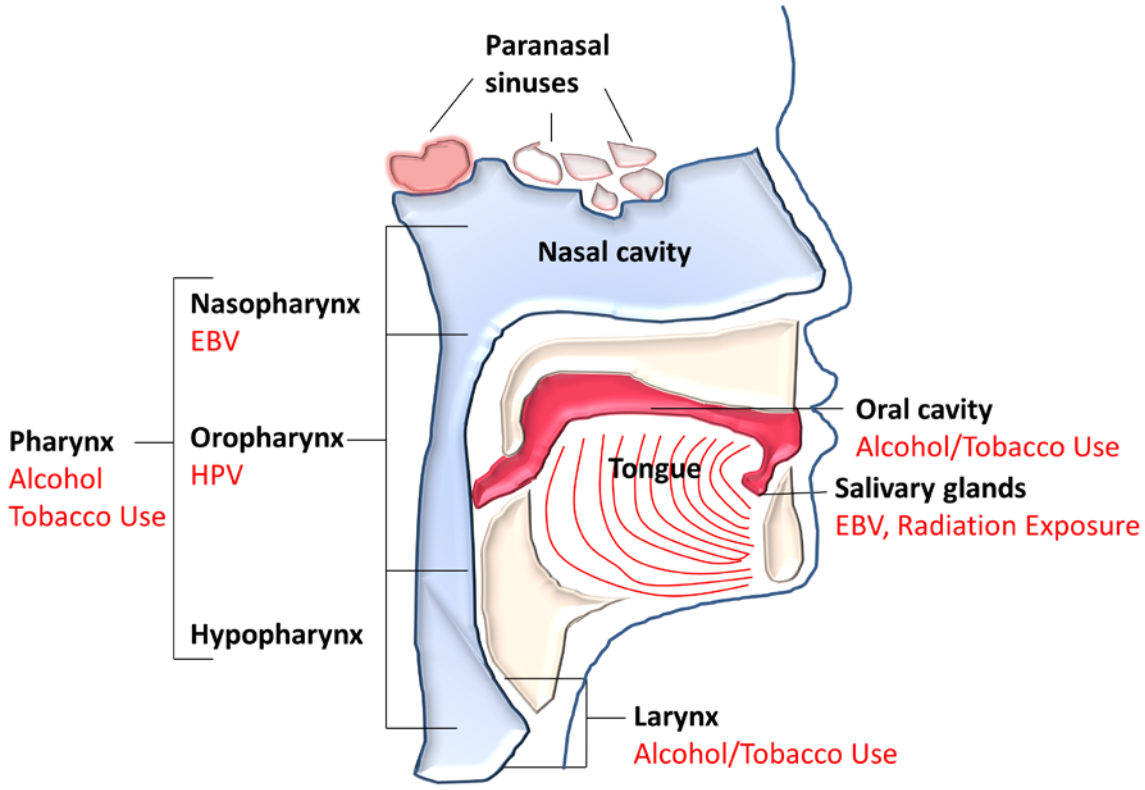

Figure 1 Schematic overview representing the anatomical sites effected by HNSCC

There are limitations in our understanding of the molecular factors that contribute to the multi-step tumorigenesis and tumor progression of carcinomas and HNSCC is certainly no exception. Because of this lack of knowledge and limitations in effective therapeutic strategies, over half of the patients with HNSCC die within 5 years of diagnosis (*7*, *8*). In addition, the majority of HNSCC cases are only diagnosed after the disease has metastasized to the lymph nodes where limitations in treatment further compound the poor prognosis (*7*). As a picture begins to emerge from research shedding light on the molecular drivers of tumorigenesis and tumor progression, we are beginning to develop more precise methods of treating patients through molecular profiling and targeted therapies (*8*).

1.1.1 Epidemiology of HNSCC

At almost 700,000 new cases each year, HNSCC is the sixth most common malignancy worldwide and accounts for most tumors of the upper aerodigestive tract (*7*, *9–11*). However, there are discrepancies in the incidence of HNSCC and in some countries, such as India, it accounts for over 60 percent of all malignancies (*12*). The high prevalence of HNSCC in India has been attributed to the risk factor of chewing areca nut or betel nut in a similar fashion of chewing tobacco in the US (*13*).

Interestingly, the incidence of HNSCC is three fold higher in men than women and the median age of diagnosis is above 60 years (*14*). As with many other diseases in the US, there is an ethnic disparity in the incidence of HNSCC and the disease is twice as common in African-Americans as their European-American counterparts (*14*, *15*). Furthermore, European-Americans have an improved five year survival rate of 59.1% compared to 16.9% in African-Americans (*14*, *15*). Additionally, there appears to be a correlation between socioeconomic class and the incidence of HNSCC as individuals in a lower-class tend to be more susceptible to this disease (*16*, *17*).

In the United States, the disease incidence appears to be decreasing over time, which is believed to result from a decline in the amount of smokers (*18*). It is intriguing that while the incidence of smoking related HNSCC incidence is on the decline, through smoking cessation, it has been reported that there is a significant increase in the amount of HPV positive HNSCC (*18*). HPV infection is the most common sexually transmitted disease in the world and, in the US alone, 20 million people are currently infected and 6.2 million acquire a new infection each year (*19*). Moreover, half of all sexually active Americans will be infected with genital HPV in their lives (*19*).

Due to the high prevalence of HPV, it is now estimated that 70-90% of newly diagnosed HNSCC cases in the US are HPV positive and it has been reported that HPV is found in 40-90% of all HNSCC cases in the developed world (*20*, *21*). HPV positive HNSCC patients tend to be Caucasian, tobacco-free and are typically younger than HPV negative HNSCC patients (*22*). There is some reassurance in the fight against HNSCC as HPV positive tumors respond better to standard treatments and there is a more favorable prognosis in HPV positive HNSCC as the 2-5 year survival rates are much higher in these patients (*23*). Moreover, with the recent advances in HPV vaccination it is thought that this will contribute the overall reduction in new cases.

The majority of HNSCC cases remain undiagnosed until the disease has already metastasized to the cervical lymph nodes. However, there are premalignant oral lesions that have been associated with HNSCC including leukoplakia (white patches in the mouth that cannot be rubbed off) and erythroplakia (red patches that cannot be diagnosed as any other disease). Although both conditions are attributed to tobacco use, leukoplakia is much more common being present in up to five percent of the population (*4*). Both conditions have been shown to transform into HNSCC with leukoplakia progressing to malignancy in 1-3% of the cases and erythroplakia progressing in up to 50% of cases in 5 years (*24*). In addition to reducing future tumor burden, cessation of smoking has been shown to reduce these premalignant lesions (*24*).

It has been suggested that these premalignant lesions are specifically associated with HPV (*25*). However, of the 964 leukoplakia biopsies that have been analyzed in the literature, only 31.1% contained HPV DNA of any type, and of the 32 cases that were diagnosed with erythroplakia, only 9 contained HPV 16 DNA (*25*). Yet, there are premalignant and benign tumors associated with HPV positive cancer as HPV often presents itself as warts or papillomas of the skin and upper respiratory tract (*26*). Unfortunately, in the majority of those who are

diagnosed with HNSCC there is no warning sign and the disease is not diagnosed until there has been metastasis to the lymph node resulting in a poorer prognosis (*8*).

1.1.2 Molecular Biology of HNSCC:

HNSCC is a heterogeneous disease, which includes three major subclasses of genetic classification (*3*). The vast majority (80%) of HNSCC is HPV negative and caused by the accumulation of genetic and epigenetic changes from chronic environmental exposure to carcinogens, most commonly to tobacco products and excessive alcohol consumption (*3*). The 80% of HPV negative tumors are further differentiated into tumors with high chromosome instability (CIN) (65%) and low CIN (15%) presumably the immortal telomerase positive and mortal telomerase negative HNSCC cases respectively (*4*). The third etiology of HNSCC cases, as previously mentioned, are caused by persistent infection with HPV and together account for the remaining 20% (*4*). However, some estimates of HPV positive HNSCC tumors are as high as 36% (*27*).

The molecular profiling of these diseases has shown that these classes can have distinct, and sometimes overlapping, changes in signaling pathways and response to therapies (*28*). For example, somatic mutations in the tumor suppressor *TP53* gene are found in 60-80% of HPV negative HNSCC, whereas *TP53* is also inactivated in HPV positive HNSCC albeit through degradation by HPV E6 protein (discussed in detail below) (*29*). Similarly the retinoblastoma protein (Rb) pathway is often inactivated in both HPV negative and positive tumors. In addition, the activation of telomerase is common in 80% of HNSCC and is not specific to HPV negative tumors. Moreover, it has been shown that changes in growth factor signaling through epithelial

growth factor receptor (EGFR) expression, common in both HPV positive and negative tumors, negatively correlates with clinical outcomes in both cases (*30*). Interestingly, there is limited data providing an explanation of the cell manipulation caused in low CIN tumors.

1.1.2.1 High and Low Chromosome Instability The molecular mechanisms driving tumor progression in HNSCC largely follow the classic cancer hallmarks as proposed by Hanahan and Weinburg in their well-known cancer review articles (*31, 32*). These hallmarks are based on molecular evidence that has emerged in the past 30 years, supporting the multiple hit theory of tumorigenesis and tumor progression. It has long been postulated, based on mathematical modeling, that there are an estimated 6 hits which drive most cancers into fully malignant diseases (*33, 34*). According to Hanahan and Weinburg the initial 6 hallmark capabilities acquired by a cell to become malignant are: 1) sustaining proliferative signaling, 2) evading growth suppressors, 3) resisting cell death, 4) inducing angiogenesis, 5) enabling replicative immortality and, finally, 6) activating invasion and metastasis. Interestingly, they postulated that although all of these hits are necessary but they may not occur in the same order.

Sustaining proliferative signaling

The growth of normal tissues is carefully controlled by the release and detection of growth-promoting signals that instruct the cell to progress through the cell cycle. As such, normal cells are unable to proliferate without some form of stimulatory signals. Cancer cells deregulate and often circumvent these signals in order to proliferate independently of this homeostatic regulation.

Enhanced expression of cell surface receptors, which sense proliferative signals, are often responsible for the sustained stimulation needed for cancer cells to grow (*29*). The enhanced

expression of growth receptors facilitate the cells in becoming hyper-responsive to ambient levels of growth factors present within the tumor site. As previously mentioned, EGFR initiates one such pro-growth signaling pathway that appears to be crucial in driving proliferative signals in HNSCC and thus, EGFR is overexpressed in 80% of cases (*35–37*). EGFR is a receptor tyrosine kinase that signals through the Ras-MAPK, phospholipase C and PI3K-PTEN-AKT and mTOR pathways to induce proliferation, survival and protein translation. It is therefore unsurprising that in addition to the overexpression of EGFR, there are often mutations in the downstream mediators of this pathway, including mutations leading to constitutively active PI3K and AKT or defective PTEN (*29*).

Evasion of Growth Suppressors

In addition to deregulating the homeostatic control of proliferative signaling, cancer cells must evade growth suppressors. This is accomplished by preventing anti-proliferative signals, which act to block the advancement through the G1 phase of the cell cycle, from acting on the cell. In the case of HNSCC, it appears that the transforming growth factor-β (TGFβ) pathway is one of the most important suppressors of cell growth, and thus the TGFβ receptor and downstream Smad proteins are often downregulated or mutated in HNSCC (*38*).

After binding to the TGFβ binding type II receptor (TRII), TGFβ signaling is activated by the formation of a heterotetrameric complex composed of a TRII dimer and a dimer of the signaling type I receptor (TRI) (*39, 40*). This serine/threonine kinase receptor complex then recruits the downstream Smad proteins and, after R-Smad is phosphorylated by TRII, they form heterodimers and homodimers and translocate into the nucleus. This leads to the induction of genes that enhance apoptosis and limit cell proliferation, such as the cell-cycle inhibitors like cyclin-dependent kinase inhibitors *CDKN2B, CDKN1A* and *CDKN1C* (*39, 41*). These factors are

responsible for blocking the cyclin:CDK complexes that facilitate the initiation of cell cycle progression by phosphorylating pRb and triggering its release from the E2F transcription factors.

Interestingly, in addition to enhancing apoptotic signaling and inhibiting progression into the cell cycle, it has also been shown that TGFβ signaling may also down-regulate the expression of hTERT through Smad3 negative regulation (*39*). This suggests that the loss of the TGFβ signaling in cancer cells may not only contribute to the evasion of growth suppression, but also in the immortalization of cancer cells (discussed in more detail below) (*39*, *42*, *43*). Additionally, as previously mentioned, loss of TGFβ alters the phosphorylation patterns of downstream pRb. However, the homeostatic function of pRb is often perturbed in HNSCC, suggesting that there are overlapping patterns in evading growth suppressing signals (discussed in more detail below).

Evading cell death

Disruption of the normal homeostatic control of cell growth and death by genetic, metabolic and signaling aberrations is a hallmark of tumorigenesis (*44*, *45*). There are several mechanisms that elicit cell death including, caspase dependent intrinsic (internal crisis signals) and extrinsic apoptosis (death receptor signals), anoikis (loss of attachment), necrosis, necroptosis (i.e. programmed necrosis differentiated from physical or chemical “accidental” injury induced necrosis), pyroptosis (inflammasome mediated caspase-1-dependent cell death), autophagic cell death, mitotic catastrophe etc. (*46–48*). Fortunately, many oncogenic events that promote tumor development also increase the sensitivity of cells to death inducing stimuli including chemotherapeutic drugs (*44*). The apoptotic and necroptotic pathways are the major cell viability regulators, and the activation or restoration of these pathways offers potential therapeutic targets to induce tumor cell death (*46*).

In the past, the characterization of *in vitro* cell death has been largely based on morphological characteristics, i.e. apoptosis leads to DNA fragmentation and membrane blebbing, whereas necrosis is characterized by swelling of the endoplasmic reticulum, mitochondria and cytoplasm, leading to rupture of the cell membrane (*48*). However, deeper insights into the molecular pathways that regulate cell death have led to more precise and quantitative biochemical techniques. Nevertheless, there are still overlapping molecular mechanisms in cell death and thus, there has been exhaustive work to extrapolate biochemical techniques to differentiate a particular cell death pathway (*48*). In fact, as more molecular mechanisms have been elucidated, the number of cell death pathways has continued to increase.

Apoptosis is a programmed cell death pathway that exists as a quality control mechanism to eliminate cells that are no longer needed or that present a potential threat to the body such as infected or cancerous cells (*49*). Although apoptosis can be initiated by either external or internal signals, both pathways converge and initiate the intracellular proteolytic cascade mediated by caspases (caspases may also mediate pro-inflammatory signaling in addition to apoptosis). Caspases are a family of proteases which have a cysteine at their active site and act to cleave specific target proteins at aspartic acids (*50*). The caspase proteins exist as inactive procaspases, which are activated by proteolytic self-cleavage (*50*).

Extrinsic apoptosis can be initiated through activation of a number of extracellular signals including, growth/survival factor depletion, hypoxia, radiation and loss of cell-matrix interactions (*50*). Additionally, there are external cell receptors harboring a death domain that activate apoptosis such as the Fas and TNF receptor. Upon ligand binding, these receptors recruit a number of intracellular adaptor proteins (most vital to the process is FADD) that recruits and triggers the formation of initiator procaspase-8, forming a death-inducing signaling complex

(DISC), which in turn activates down-stream executioner caspases (reviewed in sections below) (*51*).

Likewise, in intrinsic apoptosis, there are several internal signals which can activate initiating caspases including, DNA damage (produced by cell-cycle checkpoint defects or exogenous toxins), telomere malfunction and inappropriate proliferative signals produced by oncogenic mutations (*52*). The intrinsic form of apoptosis is also known as mitochondrial apoptosis because it depends on factors released from the mitochondria such as cytochrome *c*, which is released in response to signals mediated by the activity of the Bcl-2 family of proteins, dictated by the balance of pro-apoptotic (Bax, Bak, Bid, Bim) or anti-apoptotic (Bcl-2, Bcl-XL, Bcl-W) factors (*32*).

After cleavage and activation, the extrinsic and intrinsic initiator caspases will cleave the executioner procaspases 3, 6 and 7 (*51*). These executioner caspases then cleave several proteins, an act that yields one of three of the following outcomes: (1) destroying the protein's activity, (2) triggering its activity by removing inhibitory domains or (3) creating a dominant–negative form of the protein. These cleaved proteins then directly contribute to the apoptotic state where cellular membranes are disrupted, the cytoplasmic and nuclear skeletons are broken down, the cytosol is extruded, the chromosomes are degraded, and the nucleus is fragmented (*32*).

A number of genes and proteins are deregulated in HNSCC, which act to either enhance cell survival signals or directly inhibit the apoptosis pathway. For example p53, one of the master initiators for apoptosis, is often mutated or down-regulated in HNSCC. Additionally, the PI3K-AKT pathway triggers the inactivation of pro-apoptotic molecules such as BAD and caspase-9 by phosphorylation. In addition to the PI3K and AKT proteins being over-expressed, and sometimes constitutively activated, PTEN, the phosphatase that removes phosphate groups

from PI3K, is often lost or mutated in HNSCC (*29*). Moreover, the external death ligand induction of apoptosis can be suppressed through the over-expression of the FLICE-inhibitory protein (FLIP), which interferes with caspase 8 activation (*53*, *54*).

Necroptosis morphologically resembles necrosis (unregulated cell death), but is a regulated active type of cell death that requires many of the same signals, both intrinsic and extrinsic, as apoptosis; however, it occurs under conditions of caspase inhibition. Necroptosis is differentiated from apoptosis by morphological changes, as characterized by swelling of the endoplasmic reticulum, mitochondria and the cytoplasm, which results in the rupture of the cellular membrane.

The best characterized initiators of necroptosis are those downstream mechanisms of death domain receptor ligands including TNF, though, more recent evidence suggests that the Toll-like receptors 3 and 4 can trigger this form of cell death (these pathways are discussed in detail below). In short, the death domain receptor recruits the protein kinase RIPK1 which, after being polyubiquitinated, activates the pro-inflammatory NF-κB signaling and the downstream execution of either apoptosis or necroptosis. Polyubiquitinated RIPK1 can interact with RIPK3, resulting in the phosphorylation of MLKL and its downstream lysis of the cellular membrane (*55*). A similar mechanism exists in the NF-kB signaling, TLR3 and TLR4 pathways, though there are differences in the activity of the RIPK1 kinase domain (as described in sections below). Because of its capacity to induce cell death, TNF was thus one of the first molecules to be demonstrated to induce hemorrhagic necroptosis in cancer cells. Unfortunately, because TNF elicits a strong inflammatory response and thus yielding a high level of toxicity, TNF did not fulfill expectations to be useful in treating tumor cells (*56*, *57*).

Inducing angiogenesis

Tumors are able to alter energy metabolism and often use the glycolysis pathway, even in the presence of oxygen, in order to grow more than a few millimeters. Tumors must therefore recruit blood vessels for the delivery of nutrients and oxygen supply to compensate for the loss of ATP during glycolysis as well as to dispose of catabolites (*29*, *31*, *58*, *59*). In the case of HNSCC as with other tumors neo-angiogenesis is accomplished by the overproduction of pro-angiogenic factors. The most potent of these factors secreted by HNSCC cancer cells for the recruitment of new blood vessels is vascular endothelial growth factor (VEGF) and therefore this factor has been shown to be up-regulated in most HNSCC cases (*60*).

The close proximity of these newly established blood vessels within the tumor presents a new opportunity for growth advantage through nutrient and oxygen delivery and also a potential avenue for the dissemination of the mutant cells from the primary site to metastasis. It is therefore unsurprising that this factor is considered a hallmark of tumorigenesis and progression as VEGF is associated with the prognosis of HNSCC including disease outcome and associated with increased rates of metastasis (*61*, *62*).

Limitless Replication potential: enabling replicative immortality

Due to DNA damage incurred over time and shortening of telomeric DNA through cell proliferation, differentiated squamous cells have a limited replication potential and are not immortal. The first obstacle that a cell must overcome is senescence by deregulating the checkpoint proteins in the p53 and pRb pathways. It is unsurprising therefore that *TP53* mutations are found in 60-80% of all HNSCC cases and the majority of WT *TP53* cases are HPV E7 positive (*29*, *63*). The pRb pathway is also perturbed, usually by mutations in $p16^{INK4A}$ (*CDKN2A*), cyclin D1 (*CCND1*) or with the expression of HPV E6 (*29*). Additionally, as with

most cancers, to prevent senescence and crisis induced by telomere shortening, telomerase activity is detectable in 80% of HNSCC cases analyzed and it has been suggested that the remaining 20% most likely undergo the TERT independent process of telomere lengthening or alternative lengthening of telomeres (ALT) (*64–66*).

Activating Invasion and Metastasis: HNSCC EMT and Lymph Node Metastasis

Metastasis is the process of the dissemination of cancerous cells from the primary tumor site to distal organs (*67*). At the time of diagnosis, the majority of HNSCC patients will exhibit locoregional or distal metastasis, primarily to the cervical lymph nodes and as with many other cancers due to this late stage diagnosis of HNSCC, metastasis correlates with poor survival rates (*68*). Invasion of HNSCC into distal tissues is a complex multistep process where chemotactic responses drive the migration of cells first into the basement membrane, through the extracellular matrix (ECM), into regional vasculature, followed by extravasation at the metastatic site (*68*). In addition, even after traversing the extracellular matrix, the cancerous cells must survive in circulation in either the blood or lymphatic systems, before and after reaching the lymph nodes.

This passage of metastasis begins with the process known as the epithelial-mesenchymal transition wherein cancerous cells acquire the phenotypes of mesenchymal cells such as fibroblasts (*1*). During this process, tumor cells alter their epithelial characteristics including loss of cytokeratin, tight junctions, polarity and acquire new phenotypic changes including a fibroblast shape, motility and invasiveness, increased resistance to apoptosis and anoikis, protease secretion, fibronectin secretion and, most vital to EMT, the loss E-cadherin expression with gain of the mesenchymal adherens junction protein, N-cadherin (*1*).

The first barrier HNSCC tumor cells must surmount to break away from the primary site and migrate into distant tissues is the basement membrane and the ECM (*68*). The ECM is an

intricate network of macromolecules, comprised primarily of proteins and polysaccharides, structured into a meshwork that fills the extracellular space within tissues and largely determines the tissues physical properties (*69*). The components of the ECM are mainly produced locally by cells within the matrix such as fibroblasts. The two main classes that encompass the ECM are, polysaccharide chains called glycosaminoglycans (GAGs), that are covalently linked to proteins (proteoglycans), which include: collagen, elastin, fibronectin and laminin (*69*). The collagens make up the majority of the components of the ECM and are the most abundant proteins in animals, constituting 25% of the total protein mass (*1*).

Migration through these sites requires the proteolytic degradation of the ECM components by actin polymerization driven subcellular structures, termed invadopodia, that mimic the normal podosomes of macrophages, osteoclasts and smooth muscle cells (*68*). The invadopodia are comprised of a central filamentous (F)-actin core that is regulated by a number of assembly molecules including those of the Arp2/3 complex (*70*). They are enriched with a number of migration factors including actin regulatory proteins, adhesion molecules, signaling proteins and remodeling proteins, but the most important factor localized to the invadopodia, that facilitate traversing through the basement membrane and excavate passageways in the ECM, are the matrix metalloproteases (MMPs) (Table 1). MMPs are zinc-dependent metalloproteases that are synthesized as latent enzymes and are later activated by the release of propeptide domains (*71*). Once activated, the MMPs cleave ECM components such as collagen, proteoglycans and glycoproteins. Interestingly, in addition to the secretion of MMPs by neoplastic epithelial cells, the cancerous cells often rely on the recruitment of stromal cells such as macrophage, mast and fibroblast cells, which will aid in the secretion of these MMPs (*71*).

Table 1 HNSCC Related Matrix Metalloproteinases and Their Extracellular Matrix Substrates

Name of MMP	Alternative Name of MMP	Expression	Major ECM Substrate
MMP-1	**Collagenase-1**	**Fibroblasts>tumor cells, macrophages and endothelial cells**	**Fibrillar collagens**
MMP-2	**Gelatinase**	**Fibroblasts>tumor cells and macrophages**	**Collagen IV, denatured collagens**
MMP-3	**Stromelysin-1**	**Fibroblasts>tumor cells, macrophages and endothelial cells**	**Proteoglycans, glycoproteins (laminin, fibronectin, vitronectin)**
MMP-7	**Matrilysin**	**Fibroblasts and macrophages**	**Similar to MMP-3**
MMP-9	**Gelatinase B**	**Fibroblasts and endothelial cells**	**Similar to MMP-2**
MMP12	**Metalloelastase**	**Fibroblasts and tumor cells**	**Elastin**
MMP-14	**MT1-MMP**	**Fibroblasts and tumor cells**	**Fibrillar collagens, gelatins**

Note: Table 1 Adapted from Rosenthal *et al* and Robert Weinburg's *The Biology of Cancer* (*1*, *71*)

Of the MMPs overexpressed in carcinomas, MT1-MMP appears to be the most critical enzyme in degrading the ECM (*71*). Unsurprisingly therefore, it has been shown that MT1-MMP is overexpressed in HNSCC and that the expression profile is upregulated by aberrant growth factor signaling, most notably EGFR and MET proto-oncogene receptor tyrosine kinase (cMET) signaling pathways that are known to be over activated in HNSCC either by mutation or overexpression (*72–74*). MT1-MMP unlike the other MMPs, is not secreted by cells, but rather, is cleaved intracellularlly by the proprotein convertase furin, which is also overexpressed in HNSCC, and then expressed on the cell surface as an active protease (*71*, *75*, *76*). MT1-MMP is also produced by stromal cells that can become activated in the presence of invading cells in the ECM.

1.1.2.2 The Human Papilloma Virus In addition to HNSCC caused by exposure to environmental carcinogens, it has also been associated with HPV infection. Hundreds of HPV genomes have been sequenced to date and there have been 148 types identified to infect humans. Almost 33% of HPV types have been associated with HNSCC and cervical cancer. These types are further characterized by high- and low- associated cancer risk including the high-risk types: 16, 18, 26, 31, 33, 35, 39, 45, 51, 52, 53, 56, 58, 59, 66, 68, 73, and 82 and low-risk infections including 6; 11; 40; 42; 54; 55; 61; 62; 64; 67; 69; 70; 71; 72; 81; and 82 subtype IS39, 83, 84, and 89 (cp6108) (*77*).

HPV are small (52-55nm), circular dsDNA (group I), nonenveloped viruses belonging to the *Papillomaviridae* family. There are eight open reading frames in the HPV genome encoding for three functional components known as the early (E) region, the late (L) region and long control region (LCR) (*25*). The E region codes for proteins that are essential for replication, associated with cellular transformation and for the control of viral transcription, while the L encodes for the L1 and L2 structural proteins that make up the viral capsid. Finally the LCR is responsible for viral replication and virus gene transcription (*26*, *78*).

The cancerous nature of HPV can be directly attributed to its manipulation of the factors governing cell cycle checkpoints during its productive replication cycle. HPV is host-specific and tissue specific, infecting the basal transitory-amplifying cells of the epithelium. After the entry into these cells, presumably through damage of the upper-epithelium layers, the HPV genomes are established as extrachromosomal elements in the nucleus and the copy number of the genome is amplified 50-100 times per cell (*78*). During cell division the genome is distributed between the daughter cells and as these daughter cells differentiate into the upper

squamous layers, the initially infected basal cell continues to be a reservoir for further cell divisions.

Because the virus in the infected basal cells is not actively producing viral progeny, the cells at this stage are not lysed by the virus and continue to proliferate, allowing the virus to persist in this layer of cells for periods as long as years. Since HPV rely on cellular enzymes to replicate their genome, as the infected daughter cells exit the cell cycle and begin to differentiate, the HPV encoded proteins must act to inhibit the blockage of the complete cell cycle exit and induce S-phase. This is principally accomplished, at least in high cancer risk HPV infectious cycles, through the modulation of pRb and p53 checkpoint proteins, by the virally encoded proteins E6 and E7, respectively (*79–82*). As previously mentioned, the HPV types that are attributed to these cancers can be classified as either high- or low-risk risk viruses, dependent on the capability of the viral E7 protein to bind with p53 and thus induce its degradation. In carcinomas, it has been shown that the whole viral genome or fragments thereof are integrated into the chromosomal DNA of expanding cells (*83*, *84*). The integration of the viral genome into cells facilitates the constitutive expression of the genes E6 and E7 and the persistent deregulation of the cell cycle.

1.1.3 Current treatments for HNSCC:

The treatment regimen of HNSCC varies depending on diagnosis, with approximately 40 percent of patients undergoing surgical resection (*85*, *86*). For those with unresectable tumors, concurrent chemoradiotherapy (CRT), i.e. radiation combined with cisplatin-chemotherapy, (a platinum based drug that binds to and causes crosslinking of DNA and thus induces apoptosis in cells), is recommended (*8*). Unfortunately, a meta-analysis of 87 trials recently revealed that the

survival benefit for chemotherapy is only 4.5% for a five year period and only slightly higher for concurrent chemotherapy at 6.5% (*87, 88*). In addition to cisplatin, there have been additional potential HNSCC chemotherapeutics that have made it into clinical trials including the mitotic inhibitors (taxanes) however, there was no significant benefit over the use of cisplatin and therefore little progress has been made to find better therapeutics for treating HNSCC (*87).*

As elevated EGFR expression has been associated with most HNSCC an EGFR monoclonal antibody, cetuximab, is the single exception for novel HNSCC therapy treatments to emerge and can be used either in second-line therapy after failure of platinum-based chemotherapy or in first-line therapy in combination with platinum-based chemotherapy (*8*). Unfortunately, it has been shown that treatment with combined cetuximab and cisplatin only improves the five year median survival of HNSCC patients by a medium of two months, compared to monotherapy (*89, 90*). However, a similar study found the survival rate for cotreatment with cetuximab and radiotherapy improved the five year survival rate to 49 months compared to 29 months for radiation alone (*30, 91*).

In addition to cetuximab, additional EGFR downstream mechanisms have been targeted. The cytoplasmic tyrosine kinase of EGFR has been targeted in clinical trial with a number of small molecule kinase inhibitors such as gefitinib, erlotinib or lapatinib, although, due to limited efficacy, these therapies have not been FDA approved for the treatment of HNSCC (*30*). Unlike cancers such as non-small cell lung cancer, where EGFR is often mutated and therefore these tyrosine kinase inhibitors are much more effective, EGFR is seldom mutated in HNSCC and is rather overexpressed, making resistance to EGFR inhibitors common due to the activation of downstream pathways (*30*). Nevertheless, there have been attempts to target the downstream

pathways including PIK3-Akt signaling, with a number of combined and pan-class inhibitors, however none have yet to succeed in clinical trials (*30*).

Recently it was shown that, in addition to EGFR, MET levels are also elevated in the majority of HNSCC and that treating HNSCC cell lines with MET inhibitors yielded more additive cell death effects when combined with cisplatin or the EGFR tyrosine kinase inhibitor erlotinib treatments (*92*). However, no clinical trials of MET inhibitors have been conducted to date. Because of their critical roles in the metastasis of carcinomas, several MMP inhibitors have been taken to Phase III clinical trials, however none of them have been tested on HNSCC and overall they have been found to have limited clinical benefit (*71, 93, 94*). Nevertheless, because of a lack of efficacy of these therapies, of the almost 500,000 new cases that develop each year over 300,000 cases result in death (*8, 12*).

Molecular profiling of select patient populations, who are physiologically more susceptible to certain chemotherapies and immunotherapies, (predictive biomarkers) is offering novel strategies for treating HNSCC. These predictive biomarkers are being investigated to overcome the limitation in current treatments and also to develop new drugs for the improved therapeutic agents in oncology (*95*). Among the novel predictive biomarkers including EGFR and MET mentioned above, TLR3 expression has been shown to positively correlate with the efficacy of synthetic dsRNA (poly(I):poly(C)) to eliminate cancer cells (*95, 96*). Though, in addition to causing growth arrest and apoptosis in cancer cells, TLR signaling has been shown to induce pro-inflammatory responses and therefore its application for targeted immunotherapy has not yet proven effective. To improve the efficacy of poly(I):poly(C) as an adjuvant, additional factors contributing to these discrepancies need to be addressed.

1.2 HNSCC IMMUNOSURVEILLANCE AND IMMUNOEDITING:

In addition to the 6 canonical hallmark mechanisms required for a cell to become malignant (as described above), avoiding immunosurveillance presents an additional challenge for tumors and is widely accepted as the 7th hallmark of cancer (*97*, *98*). The theory of cancer immunosurveillance predicts that the innate and adaptive immune systems work together to detect the presence of a developing tumor and, in most cases, destroy these precursors before they become clinically apparent (*98*). However, emerging evidence suggests that cancer immunosurveillance represents only one step of a broader process, termed cancer immunoediting, whereby a developing tumor must proceed sequentially through three distinct phases termed elimination, equilibrium and escape (*99*). This model stresses the dual host-protective versus tumor-sculpting actions of the immune system in cancer (*97*, *99*).

The basis of cancer immunosurveillance, or tumor "elimination," is that cancer cells express antigens (neoantigens) that differentiate them from their nontransformed counterparts (*97*). These neoantigens are released, through means such as necroptosis, and captured by dendritic cells (DCs) for antigen processing (*100*). The activated DCs then function as antigen presenting cells (APCs) whereby they present the captured neoantigens on HLA class I and HLA class II molecules to T cells (*100*). This presentation drives the priming and activation of cytolytic T lymphocytes (CD8+T cells) that function to eliminate premalignant cells presenting the neoantigen by HLA class I (*100*, *101*). The magnitude of the immune response is determined at APC stage, with a critical balance representing the ratio of T effector cells versus T regulatory cells being vital to the final outcome (*100*). Also contributing to the elimination process, are natural killer cells (NK cells) that work in concert with CD8+ T cells to kill cells that no longer express self-antigens or express stress-signaling proteins (*100*).

For an effective anticancer T cell response, the priming of T cells must be accompanied by immunogenic signals including numerous cytokines, chemokines and additional cellular factors that are released by tumor cells (*100*). Thus the immunologic rejection of a developing tumor likely requires an integrated response involving both the innate and adaptive arms of the immune system (*99*). However, the precise mechanism in which the immune system is alerted to the presence of neoantigen in a developing tumor has not been completely elucidated (*100*). It is thought stress-associated or damage-associated molecular patterns (DAMPs) from the innate immune activation, and bridge the generation of adaptive immunity (*102*). Of these signals, the interferons (IFNs), both type I (IFN-α/β) and type II (IFN-γ), have emerged as critical components of the cancer elimination process, and work is ongoing to define their respective roles in promoting antitumor immune responses (*103*, *104*).

The essential role of IFN-γ in cancer elimination is well-documented *in vivo* (*103*, *105–107*). It has been shown that IFN-γ receptor (IFNGR1) knockout mice, tumor cells with dominant-negative IFNGR1 mutations, and tumor cells treated with IFN-γ-neutralizing antibodies have all been shown to have compromised tumor rejection (*103, 105–107*). IFNGR1 is expressed on nearly all cells and IFN-γ signaling causes an exhaustive list of cellular effects in both innate and adaptive immune cells as well as tumor cells, which is discussed in detail in a comprehensive review by Schroder and colleges (*105*). However, because of the cross-talk and overlapping function of the Type I (IFNα/β) and II IFNs, several studies have recently emerged demonstrating the essential roles IFNα/β. For example, both type I and II IFN up-regulate HLA class I presentation to enhance the quality and diversity of antigen that is presented to CD8+ T cells. IFNα/β have been shown to play a central role in the process of immunoediting by enhancing the maturation, co-stimulatory activity and by increasing the capacity of dendritic

cells to present neoantigens (*104*). Additionally, it was shown that Type I IFN signaling caused the release of chemokine (C-X-C motif) ligand 10 (CXCL10), which is a potent chemo-attractant for adaptive and innate immune cells (*108*).

In the equilibrium phase of the immunoediting process, rare tumor variants begin to survive the elimination process (*109*). In this phase the adaptive immune system prevents tumor cell outgrowth and also begins to sculpt the immunogenicity of the cancerous cells (*109*). Thus, in the equilibrium phase, the immune system maintains the tumor cells in a state of dormancy (*110*). Tumor antigens are either no longer detected or recognized as "self" by DCs and T cells in the equilibrium phase, thereby creating T regulatory cell responses rather than effector responses (*111*). Moreover, the elimination of a tumor in this phase is restricted by a deficiency of infiltrating effector T cells and by suppressive factors present in the tumor microenvironment that cause effector T cells to become exhausted (*111*).

In the final step of tumor immunoediting, tumor cells escape immunosurveillance. This phase occurs following the selection of the tumor cells that are more fit to survive after the immuneselection or by establishing conditions within the tumor microenvironment that facilitate tumor outgrowth (*109*). There are multiple ways by which tumor cells can escape immunosurveillance. In addition to secreting factors that lead to induction of a Th2 proinflammatory response over Th1 T cell response, HNSCC tumors are able to escape immune destruction by concealing the presentation of irregular proteins that should be recognized as neoantigens by the adaptive immune system (*112*). One of the well-established mechanisms whereby cells evade elimination by the adaptive immune system is through the loss of HLA I antigen presentation. HLA class I expression has been shown to be down-regulated in approximately 50% of HNSCC cases and has been associated with lymph node metastasis (*113*–

115). This was shown to be caused by a loss of HLA components such as HLA heavy chain and beta2-microglobulin (β2m) that form the class I-β2m-antigen complex (*113–115*).

In addition to evading interferon signaling and exhausting the CTL and NK cells, deregulated innate immune signals can contribute to a cancer promoting tumor microenvironment (*112*). Of the innate immune pathways correlated with tumor progression of HNSCC, up-regulated activity of NF-κB, and the downstream cytokines and chemokines that promote growth and recruit pro-inflammatory cells, has been shown to be important for evading immune destruction of the tumor (*112, 116).* The pro-inflammatory cytokines and chemokines, interleukin (IL)-1, IL-6, granulocyte/monocyte-colony stimulating factor (GM-CSF) and chemokine CXCL1 have been shown to contribute to tumor progression in a number of models including HNSCC (*112, 116–118*). Secretion of these factors results in a potent proinflammatory response that leads to enhanced myeloid and monocyte leukocyte infiltration and thus, a more pronounced Th2 dominant pattern with increased IL-2, IL-12, IFNγ and tumor necrosis factor α (TNFα) and elevated IL-4 and TGFβ (*117, 118*). The presence of Th2 T cells leads to a more robust inflammatory response and a downregulation of the recruitment and activation of CTL cells (*100*).

1.2.1 Innate Immune Signaling in HNSCC

Mammalian cells possess surveillance sensors known as pattern recognition receptors (PRR) used for the detection of pathogen associated molecular patterns (PAMPs) derived from invading pathogens and damage-associated molecular patterns (DAMPs), in both extracellular and intracellular environments (*119*). These sensors initiate both the innate immune response and

later, prime the adaptive immune response required to eliminate the invading pathogen or damaged cells. There are four major groups of PRRs categorized by their structural features; Toll-like receptors (TLRs), retinoic acid-inducible gene I-like receptors (RLRs), nucleotide-binding oligomerization domain-like receptors (NLRs), and C-type lectin receptors (CLRs) (*120*).

TLRs recognize numerous conserved PAMPs including the nucleic acids dsRNA (TLR3), ssRNA (TLR7 and 8), ssDNA (TLR9) and the pathogen ligands bacterial lipopolysaccharides (TLR4), flagellin (TLR5) and lipopeptides (TLR2-TLR1, 6 or10), whereas RLR are only found in the cytoplasm and are RNA helicases that recognize nucleic acids (*121*). Also in the cytoplasm of cells are the NLRs that recognize several DAMPs and PAMPS including nucleic acids, changes in ion concentration, microbial peptides (including toxins) and polysaccharides, reactive oxygen species etc. The NLRs form inflammasomes that work in concert with the TLR and RLRs by activating the secretion of downstream pro-inflammatory cytokines via caspase-1 activation (*122*).

Activation of the TLR receptors, by PAMP or DAMP binding, initiates a signaling cascade which leads to the induction of both IFN and proinflammatory cytokines (*121*). The induced IFN is secreted and, upon binding to IFN receptors, stimulates the phosphorylation of JAK-STAT signaling that leads to the production of IFN-stimulated genes (ISGs) and thus the establishment of an anti-viral and –microbial state (*121*). Because the activation of these receptors results in the induction of a robust immune response, there has been an interest in utilizing ligands for these sensors to eliminate cancer cells directly, through apoptosis, or through priming the adaptive immune response favor of the CTL activation (*109*).

The TLRs are class I transmembrane glycoproteins and are characterized by extracellular domains containing a varying number of leucine-rich-repeat (LRR) motifs (*123*). These LRR motifs are involved in protein-protein interactions and ligand recognition. TLRs also contain a single transmembrane α-helix and a conserved cytoplasmic domain containing a Toll/interleukin-1 receptor (TIR) domain, which is involved in signaling adaptor recruitment (*124*). In humans there are a 10 TLRs (TLR1-10) that differ in their subcellular localization, ligand specificity, downstream signaling adaptors, and in the cellular responses they induce (**Figure 2**) (*124*).

Based on subcellular localization the TLRs can be divided into two groups. The heterodimers of TLR2–TLR1, TLR2-TLR6 or TLR2–TLR10 and homodimers of TLR5 and TLR4 bind to their respective ligands at the cell surface, whereas TLR3, TLR7–TLR8, and TLR9 localize to the endosomes and sense nucleic acids (*123*). However, TLR4 is an exception to this localization pattern as it may sense LPS at the cell surface as well as in endosomes (*123*).

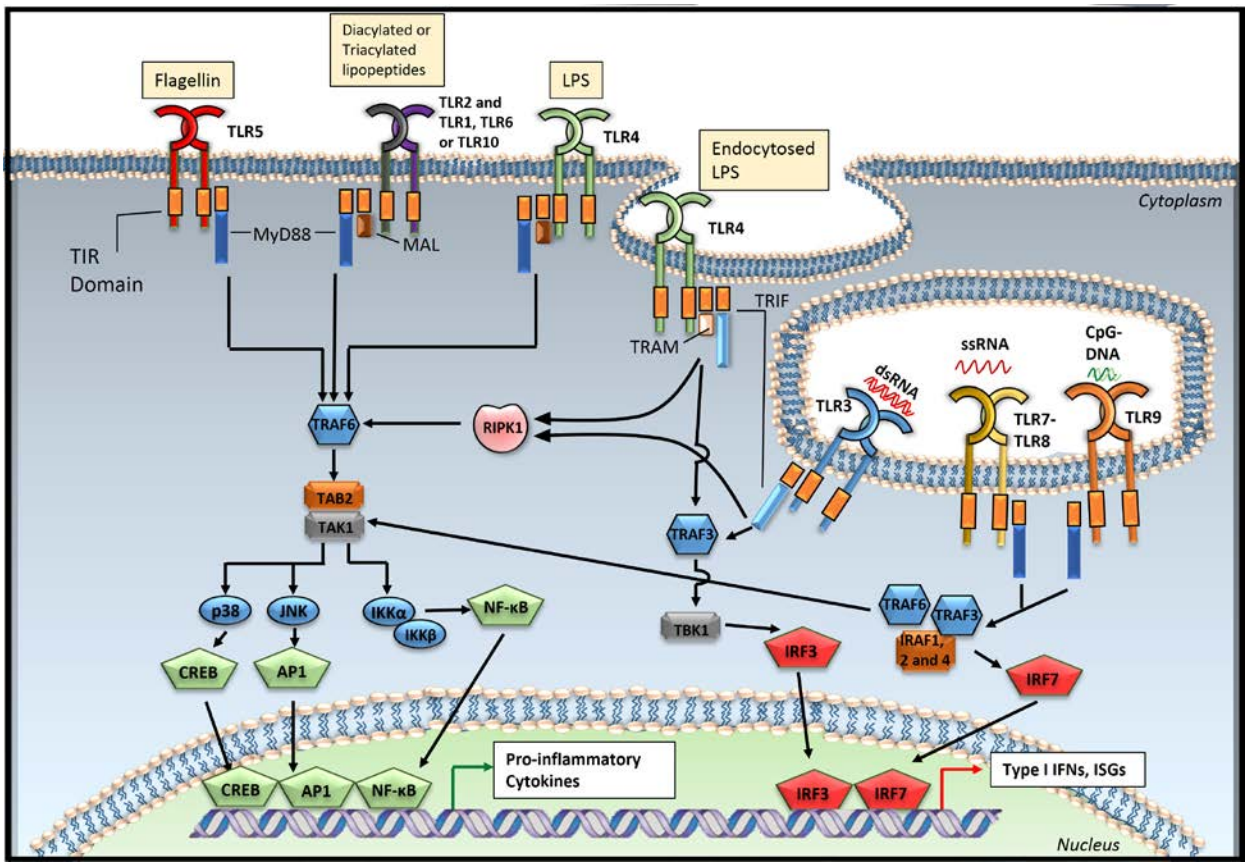

Figure 2 Detailed schematic of human toll-like receptor signaling: Homodimers of TLR4, TLR5 and heterodimers of TLR2 and TLR1, TLR6 or TLR10 sense their respective ligands at the cell surface. Following this, the TIR domains of these TLRs recruit the adapter MyD88 either directly (TLR5) or via the recruitment of the adapter MAL (TLR4 and TLR2). The recruitment of MyD88 at the cell surface leads to a downstream signaling cascade and the activation of pro-inflammatory cytokines. Similarly, homodimers of TLR3, TLR4, TLR9 and heterodimers of TLR7 and TLR8 sense nucleic acids in endosomal compartments. TLR7-TLR8 and TLR9 recruit MyD88, whereas TLR3 and TLR4 signal through a unique adaptor, TRIF, causing the activation of pro-inflammatory cytokines as well as Type I IFN. Figure adapted from O'Neill *et al.* (*123*)

Upon ligand binding, the TLRs activate downstream signaling pathways by recruiting either of the two adaptor molecules TIR domain-containing adaptor (TRIF, also known as TICAM-1) or myeloid differentiation primary response gene 88 (MyD88) (*121*). Each of the TLRs signal through Myd88 with the exception of TLR3, which exclusively recruits TRIF, as discussed in detail below (*121*, *125*). In addition to its dual signaling at the cell surface as well as in endosomes, activated TLR4 is able to recruit the adaptors MYD88-adaptor-like protein

(MAL) and TRIF-related adaptor molecule (TRAM), which facilitate the interaction of TLR4 with both MyD88 and TRIF respectively (*123*).

The engagement of TRIF and MyD88 with the activated TLR receptor stimulates the downstream signaling pathways, which involve the recruitment of the adaptor molecules TNF receptor-associated factors (TRAFs) and IL-1R-associated kinases (IRAKs) (*123*). This interaction causes the activation of the mitogen-activated protein kinases (MAPKs) JUN N-terminal kinase (JUN) and p38 and to the activation of transcription factors (*123*). These transcription factors induce the production of pro-inflammatory cytokines (via cAMP response element-binding protein (CREB), activating *protein*-1 (AP-1) and NF-κB activation) and type I IFN and ISG (through IRF3 and IRF7 activation) leading to the anti-viral and –microbial state. Although TRIF and MyD88 recruitment drives the activation of NF-κB and IRF, it is thought that MyD88 signaling causes a more pronounced NF-kB pro-inflammatory response, while TRIF signaling leads to a more enhanced IRF3 activation (*121*).

1.2.2 Toll-like Receptor Protein (TLR3):

TLR3 is made up of an N terminal ectodomain (ECD) formed by 23 LRRs, a transmembrane domain spanning the endosomal membrane and a C terminal TIR domain (*126*, *127*). Viral dsRNA is recognized by TLR3 through the ECD in endosomes of cells, which induces TLR3 to dimerize and recruit the adaptor protein TRIF (**Figure 3**) (*128–130*). Upon recruitment, TRIF oligomerizes and activates two divergent pathways leading to the activation of IRF3 through its N terminal TIR domain and NF-κB through both its N and C terminal domains (*131*). The activation of these transcription factors leads to the induction of type I IFN, cytokine/chemokine

production and dendritic cell maturation, which enables the activation of CTL and NK cells leading to a robust antiviral response (*130*).

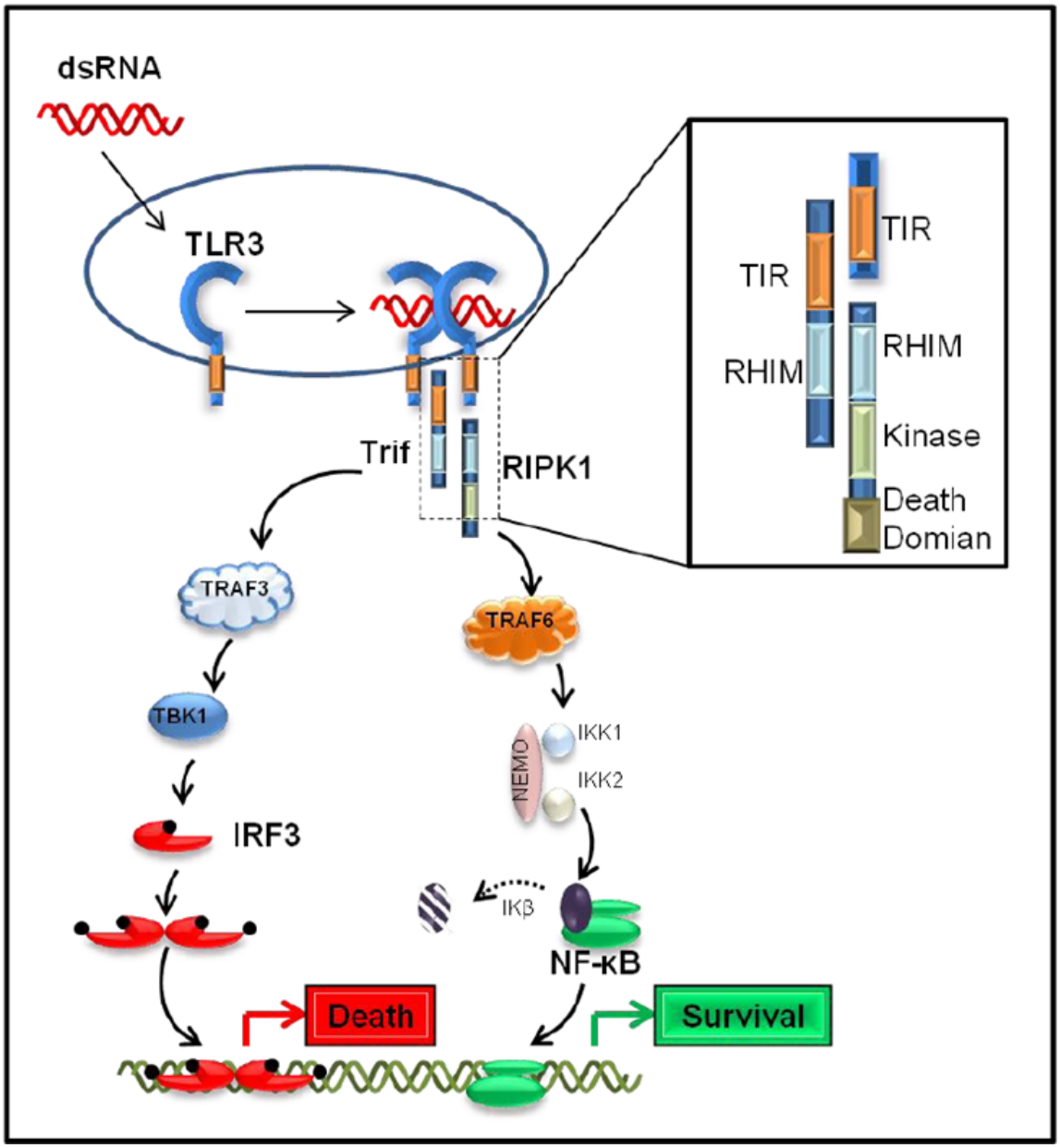

Figure 3 TLR3 signaling: TLR3 senses viral dsRNA in endosomal compartments. After binding to dsRNA TLR dimerizes and, by its TIR domain, recruits the adaptor molecule TRIF. TRIF then engages with TRAF3 and, through its RHIM domain, also engages with RIPK1 and TRAF6. This interaction leads to two divergent downstream signaling pathways, which culminate in either a pro-death (IFN) or pro-survival (NF-kB inflammation) response.

1.2.2.1 TLR3-IRF3 signaling TRIF is expressed at low levels in cells and after its recruitment to activated TLRs, it oligomerizes and forms speckled structures that co-localize with downstream signaling molecules (*132*, *133*). It was proposed that the oligomerized TRIF recruits the ubiquitin ligase TRAF3 through interactions between the N terminus TIR domain of TRIF (*134*). The autoubiquitination of TRAF3 is then required for the recruitment of TBK1 (TANK-binding kinase 1) and IκB kinase-related kinase-ε (IKKε) which are thought to be the main kinases that phosphorylate IRF3 in response to viral infection and stimulation of TLR3 (*121*, *135–137*). However, there is still no evidence of a direct interaction between TRIF and TRAF3, and it has also been shown that in addition to the recruitment of TBK1 through TRAF3, TBK1 can directly interact with the N terminal domain of TRIF to activation IRF3 (*138*). Additionally, it has been shown that the cytoplasmic domain of TLR3 is tyrosine-phosphorylated upon activation, which recruits PI3K and that this activation is required for the complete phosphorylation and activation of IRF3 (*139*)

Unlike most of the proteins in the IRF family, IRF3 is constitutively expressed and resides in the cytosol in latent form. Upon recruitment of the IRF3 kinases, TBK1 and IKKε to the TIRF-TRAF3 complex, specific serine residues in the C-terminal (regulatory) region are phosphorylated, IRF3 forms a dimer enabling it to translocate and interact with the co-activators CREB-binding protein (CBP) or p300 to form a holocomplex in the nucleus (*140–143*). This holocomplex then binds to interferon-stimulated response elements (ISRE) in the DNA and begins transcribing type I interferon and numerous ISGs, including ISG54, ISG56 and ISG60 inducing a potent antiviral state in infected cells (*144*). In addition to IFN and ISG induction, IRF3 has been suggested to trigger apoptosis in response to activation through a number of mechanisms. Recently it was shown that IRF3 contains a BH3 domain, which together with the

pro-apoptotic protein Bax, co-translocates to the mitochondria and the results in activation of the mitochondrial apoptotic pathway (*145*).

1.2.2.2 TLR3-NF-κB signaling In addition to IRF3 signaling, as previously mentioned, NF-κB is also activated upon TLR3 stimulation. Under normal physiological conditions, NF-κB is sequestered in the cytosol by its interaction with the Inhibitor of κB protein (IκB). In addition to recruiting TRAF3 to the TRIF complex, it was also shown that TRAF6 interacts with the N terminus of TRIF and is recruited to the speckled signaling structures upon TLR stimulation. It was therefore proposed that TRAF6 was required to activate NF-kB signaling, as it has been shown that overexpression of a dominate negative TRAF6 or the mutation of TRIF so that it no longer interacts with TRAF6, is sufficient to block NF-κB signaling (*146*, *147*). It was later shown that the TRIF-TRAF6 complex recruits the transforming growth factor activated protein kinase 1 (TAK1), a member of the MAP family and TAB2 (*146*). TAK1 and TAB2 are phosphorylated on the membrane, followed by the formation and translocation of TRAF6-TAK1-TAB2 from the membrane to the cytosol, where this complex then phosphorylates IKKα and IKKβ, which in turn phosphorylate IκB, leading to its degradation and nuclear translocation of NF-κB (*147–149*).

However, the essential role of TRAF6 in TLR3 signaling was later shown to be controversial. In follow-up experiments others showed that in cell lines TRAF6 deletion does not ablate NF-kB signaling, nor does the deletion of the N terminus of TRIF, which is thought to be required from TRAF6 recruitment (*134*, *150*, *151*). Upon investigating the activation of NF-kB through the C terminus, it was discovered that TRIF also contains a RIP homotypic interaction motif (RHIM). It was revealed that rather than recruiting TRAF6, RIPK1 is also recruited to the

TRIF complex upon TLR3 stimulation and that its recruitment is required for the degradation of IκB and activation of NF-κB (*152*, *153*).

1.2.2.3 TLR3 expression and function in HNSCC As previously discussed, the main function of TLR3 is thought to be the endosomal sensing of viral dsRNA. However, because TLR3 activation causes IRF3-mediated proapoptotic responses as well as NF-κB-mediated inflammatory signals, there has been an interest in investigating the role of TLR3 signaling in cancer. Subsequently, TLR3 has been shown to be expressed in many types of cancer tissue including HNSCC (*154–163*). Furthermore, it was recently shown that a TLR3 polymorphism (rs5743312) is associated with poor overall survival rates in advanced oral cancer (*164*). Although the molecular consequences this polymorphism have not been elucidated, its effect on patient survival demonstrates the significance of TLR3 signaling in HNSCC.

Several studies have shown that TLR3 expression in HNSCC is associated with anti-tumor properties and that its activation causes an increase in apoptosis (*154–157*). It was shown that treatment of HNSCC cells with TLR3 ligand induced apoptosis through the down-regulation of survivin.(*155*). Moreover, we have previously observed that TLR ligand caused an enhanced apoptotic response in HNSCC metastatic tumor tissue (*156*). Additionally, it was shown that stimulation of HNSCC cells with TLR3 ligand caused an decrease in cell migration (*157*). In a comprehensive study of the TLR3 signaling in OSCC, He *et al.* found that poly(I):poly(C) stimulated robust responses including upregulated cytokine expression, decreased cell viability, suppression of cell proliferation and decreased cell migration (*154*).

However, because of its dual role in activating NF-κB, TLR3 expression has also been shown to contribute to the metastatic phenotype by enhancing c-MYC-mediated proliferation and was shown to be associated with invasive HNSCC (*158*). Enhanced TLR3 expression in

HNSCC patients was significantly correlated with tumors that were poorly differentiated and with perineural invasion (*159*). Moreover, they found that poly(I):poly(C) stimulation promoted CCL5-mediated migration in HNSCC cell lines. In addition, a recent proteomic approach revealed that TLR3 stimulation of HNSCC cell lines caused a decrease in the expression of calreticulin, which inhibits cell proliferation (*160, 161*) and an increase in profilin-1, which has been shown to enhance angiogenesis, ECM invasion and MMP2 secretion (*162, 163*).

Because of these conflicting studies, the precise role of TLR3 in the tumor progression of HNSCC has not been completely elucidated. Further investigation of the downstream signaling molecules that determine the overall cellular response to TLR3 ligand may help explain these differing observations.

1.2.2.4 TLR3 ligand as an immunotherapy for HNSCC Of the TLRs that have been tested as potential immunotherapies, it is thought that there is potential for the use of TLR3 ligands for the treatment of carcinomas (*119*). The activation of this pathway with poly(I):poly(C) has shown to be a strong inducer of type I IFN and leading to the induction of an adaptive immune response. In addition, TLR3-IRF3 activation has been shown to induce apoptosis through a direct interaction between phosphorylated IRF3 and the pro-apoptotic protein Bax in infected and cancerous cells (*145*, *155*, *156*, *165*, *166*).

Accumulating *in vivo* evidence regarding the anticancer role of TLR3 has come from a number of studies (*95*, *167–171*). TLR3-/- mice are more prone to breast cancer tumor development and progression (*95*). Using this mouse model it was also shown that there is a decreased relapse following dsRNA treatment in TLR3-positive compared to the TLR3-/- breast cancers (*95*, *170*). Furthermore, TLR3 ligands have been shown to cause growth arrest and apoptosis in prostate cancer cells in a xenograft mouse model (*171*). Additionally, between 1970

and 1990 six random oncology clinical trials were conducted on the efficacy of using dsRNA for the treatment of numerous tumor types including gastric, bladder, breast, and melanoma (*167–169*). However, the results of these studies were varied, 2 showed a significant clinical benefit and 3 showed a more favorable outcome with the administration of dsRNA (*95*).

There are currently 23 clinical trials for the use of poly(I):poly(C) as an adjuvant in combination with chemotherapies and immunotherapies for treating a number of cancers including: colorectal, ovarian, breast, lung, prostate, melanoma, myeloma, leukemia, glioblastoma, brain, cervical and liver cancers (*172*). However, because of limitations in our understanding of the molecular mechanisms that dictate the pro-inflammatory (pro-cancer) versus pro-interferon (pro-death) and how these pathways may be perturbed in HNSCC, a consensus has not been reached as to whether there is any major clinical benefit of this treatment (*173*).

In addition to TLR3 expression, numerous proteins play a role in defining the downstream signaling by mediating the pro-survival NF-κB and pro-apoptotic IFN regulatory factor 3 (IRF3) signaling responses to poly(I):poly(C). A better understanding of the mechanism of TLR3-mediated apoptosis and its potential involvement in controlling tumor metastasis could lead to improvements in current treatment.

1.2.3 Receptor-interacting protein kinase 1 (RIPK1):

The kinase RIPK1 belongs to the RIP family of serine threonine kinases that play a role in both the innate and adaptive immune responses (*174*). RIPK1 consists of an N-terminal kinase domain, an intermediate domain, a RIP homotypic interaction motif (RHIM), and a C-terminal death domain (DD) motif (**Figure 4**) (*46*). The intermediate domain of RIPK1 contains a site that

is subject to K63-linked ubiquitination (K377), which is recognized by many of the ubiquitin-binding proteins involved in NF-kB signaling (*175*). The RHIM domain interacts with multiple proteins also containing the RHIM domain such as TRIF, RIPK3 and DNA-dependent activator of IRFs (DAI). The six helical bundle, making up the death domain of RIPK1, is also found in FAS, TNFR1, FAS-associated death domain protein (FADD and TNFR1-associated death domain protein (TRADD) (*175*, *176*).

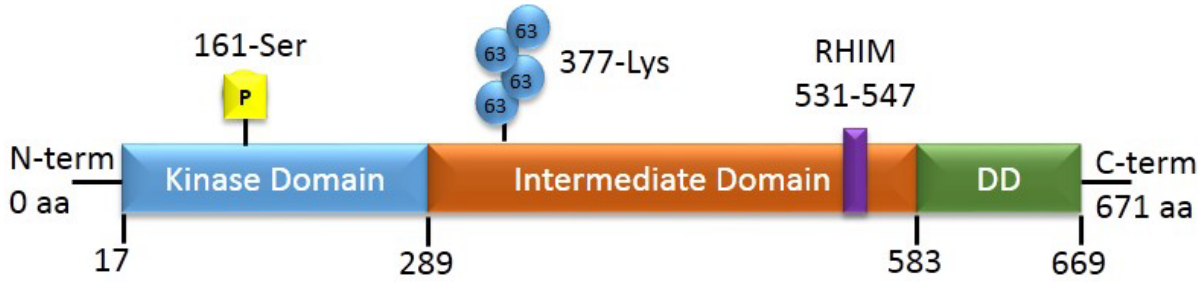

Figure 4 Schematic representation of the multiple domains of RIPK1.

Because of its multiple domains and interaction motifs, the overall expression levels of RIPK1 in a cell have a significant role in defining the outcome of a number of pathways. For instance, it was revealed that RIPK1 regulates inflammation signaling (NF-κB activation) in response to TNF and TLR ligands, through both kinase-dependent and independent manners respectively. Furthermore, RIPK1 has been shown to play a critical role in the necroptotic cell death pathway induced by a number of receptors including: TNFα receptor 1 (TNFR1) (*177*), TNFα related apoptosis-inducing ligand receptor (TRAIL) (*178*), TLR3 and 4 (*153*, *179*, *180*), and RIG-I (*174*, *181*). However, in the majority of cells, stimulation with these ligands does not result in cell death as it was revealed that RIPK1 plays a role in not only contributing to necroptosis, but also conversely preventing apoptosis.

RIPK1 is probably best known for its canonical role in TNF signaling including its function in mediating inflammatory responses, commencing necroptosis and inhibiting apoptosis. Upon ligand binding to TNFR1 or TRAIL, these receptors trimerize and recruit a membrane-associated complex, named complex I, containing TRADD, RIPK1 and several E3 ubiquitin ligases including cIAP1 and cIAP2 (*46*, *182*). The recruitment of the ubiquitin ligases to the complex leads to RIPK1 polyubiquitination at Lys377 (*46*). This polyubiquitination begins the pro-inflammatory response by recruiting TAB2/3 and TAK1 that activate NF-κB signaling as discussed above (*46*, *182*). After internalization of complex 1 a second complex begins to form mediated by the recruitment of FADD (*182*). The downstream signaling pathways that are activated now are contingent on the proteins that are recruited to complex II leading to 1) the formation of complex IIa via the recruitment of caspase 8 resulting in the induction of apoptosis or the recruitment of RIPK3 or 2) the formation of complex IIb and activation of necroptosis (*182*).

It has widely been accepted, although somewhat controversial (*183*), that ubiquitination of RIPK1 during TNFα signaling contributes to the IκB kinase (IKK)/mitogen-activated protein kinase (MAPK)-dependent NF-κB activation that drives inflammatory cytokine production (*184*, *185*). This suggests a possible mechanism of how RIPK1 can prevent caspase-8-induced apoptosis, as it has been shown that NF-kB signaling increases the cellular FLICE-like inhibitor protein (cFLIP) levels in response to TNF and TRAIL signaling, and that cFLIP is the inhibitor for caspase 8 dimerization (*53*, *186–188*).

Although RIPK1 is essential in inducing necroptosis through TNFα signaling, its expression has been shown to be vital to the survival of the cell. RIPK1 can directly mitigate TNF-caspase-8-mediated apoptosis and TLR3-RIPK3-mixed lineage kinase domain-like protein

(MLKL) mediated necroptosis (*189*). Several groups have recently revealed that RIPK1 null mice die at birth from systemic inflammation and that the neonatal lethality is caused by systemic inflammation from cell death (*184*, *189–192*). This death can be prevented by also deleting RIPK3 and caspase 8, suggesting that RIPK1 acts to directly inhibit these pathways. These findings suggest that RIPK1 may limit inflammatory signals by inhibiting TLR3-RIPK3-MLKL mediated necroptosis in addition to its role promoting NF-kB-mediated inflammation (*184*, *189–192*).

1.2.3.1 The role of RIPK1 in cancer Given the duality of RIPK1 in promoting and limiting inflammatory signals as well as preventing and contributing to cell death, it is unsurprising that RIPK1 has been found to be both up- and down-regulated in cancers (*27*, *193–198*). Recently it was shown that RIPK1 up-regulated and, through the increased activation of the NF-kB proinflammatory response, this overexpression contributes to the growth and invasive properties in a number of cancers including melanoma, gallbladder, colorectal adenocarcinoma, and non-small cell lung cancer (*193–196*). However, RIPK1 expression has also been shown to be down-regulated in several other types of cancer including breast, OSCC, and colon cancer, as discussed below (*27*, *197*, *198*).

The Death Domain of RIPK1 Downregulates EGFR expression

Upon investigating the expression levels of RIPK1 and EGFR in breast cancer cell lines, Ramnarain *et al.* found that there was a strong correlation between the loss of RIPK1 and the overexpression of EGFR (*27*). With an EGFR-promoter driven luciferase assay, this group discovered that the overexpression of RIPK1 by transfection of mouse embryonic fibroblast cells (MEFs) increased the levels of EGFR transcription. This finding was surprising given that

RIPK1 lacks a DNA binding domain and therefore had not been shown to increase the expression of transcription factors necessary for the expression of EGFR. To investigate the mechanism these researchers then went on to make mutations in the RIPK1 gene and found that the loss of the RIPK1 DD completely ablated the downregulation of EGFR. Examination of the EGFR transcription factors revealed that Sp1 forms a complex with RIPK1, interruptible with the deletion of the DD, that limits the induction of Sp1 stimulated genes (*27*). As EGFR is known to be ubiquitously overexpressed in 90% of HNSCC cancers, this finding could suggests a mechanism responsible for at least some of the oncogenes high levels (*29*, *35*).

RIPK1 in DNA damage-induced p53-independent cell death

In addition to the roles of RIPK1 previously mentioned in prompting cell death through TNF, TRAIL and Fas in concert with the accumulation of reactive oxygen species, it was shown that RIPK1 is essential for the DNA damage-induced TNFR- and p53-independent cell death response (*178*, *199–201*). This study revealed that cell death elicited by the c-Jun N-terminal kinase/stress-activated protein kinase pathway is mediated by the activation of JNK by RIPK1 in response to DNA damage (*200*). This finding could have strong implications for the survival of cancerous cells in HNSCC as they are often p53 defective (mutations or HPV E7-mediated degradation) and have high chromosome instability, as previously discussed.

Reduction of RIPK1 Expression Increases Resistance to Anoikis

Anoikis, literally meaning “the state of being without a home,” is a form of cell death that is induced by anchorage-dependent cells losing its epithelial cell-matrix interactions (*202*). This form of cell death must be circumvented, therefore, for a cancerous cell to complete the EMT transformation and breakaway from the primary tumor site in order to metastasize to distant

organs. The detachment of cells from the ECM has been shown to suppress the focal adhesion complex (FAK)-mediated survival signaling and, conversely, the overexpression of a constitutively active FAK has been shown to rescue cells from anoikis. It was shown that RIPK1 interacts with both the Fas-mediated anoikis pathway and the FAK-mediated survival pathway and that the downregulation or loss of RIPK1 expression causes cells to be sensitive to anoikis inducing conditions (*203*). Later it was shown by the same authors that a sirtuin-3 (SIRT3), a nicotinamide adenine dinucleotide-dependent deacetylase that is mitochondrial associated and therefore regulates cell death and metabolism, is downregulated by RIPK1 expression and that RIP suppression inhibits anoikis induced by SIRT3 (*198*).

1.3 RATIONALE AND HYPOTHESIS

HNSCC is the most frequent malignancy of the aerodigestive tract and because of limitations with chemotherapy over half of those diagnosed with this cancer succumb to the disease (*29*). Synthetic dsRNA, which act as ligands for the activation of TLR3 and generate IRF3-mediated proapoptotic responses in cancer cells, have been used as potent adjuvants to chemotherapy (*167–169*). It has been shown that TLR3 expression and activation in HNSCC is associated with up-regulated cytokine expression, decreased cell viability, suppression of cell proliferation and decreased cell migration (*154–157*). However, because of its dual role in activating NF-κB, TLR3 expression has also been shown to contribute to metastatic characteristics including enhanced proliferation, invasion and migration in HNSCC (*158–163*). Because of these conflicting studies, the precise role of TLR3 in the tumor progression of HNSCC has not been

completely elucidated. Further investigation of the downstream signaling molecules that determine the overall cellular response to TLR3 ligand may help explain these opposing conclusions. We postulated that variations in the molecular landscape of HNSCC may tip the balance of the TLR3-signaling axis and impact the ultimate cellular response to TLR3 ligand. Defining these molecular changes would lead to improvements in the therapeutic use of synthetic dsRNA to eliminate cancer cells.

Using paired cell lines derived from autologous primary and metastatic HNSCC, we previously showed that the cells derived from metastatic tumors were unable to activate NF-κB while the pro-apoptotic IRF3 signaling remained intact (*156*). Consequently, stimulation of the cells from metastatic tumors with poly(I):poly(C) resulted in an enhanced apoptotic response due to the imbalance in downstream signaling (*156*). As NF-κB activation and activity remained intact downstream of other signaling pathways, we postulated that RIPK1, an adapter molecule upstream of TLR3-NF-κB signaling, is lost or mutated during tumor progression into metastasis (*174*).

Taken together, **we hypothesized that the RIPK1 expression could be downregulated in HNSCC cells and that this reduction contributes to the metastatic phenotype, while causing an enhanced apoptotic response to poly(I):poly(C) treatment.** In this investigation we sought to:

SPECIFIC AIM 1: Establish the downregulation of RIPK1 expression during the tumor progression of HNSCC. Recently it was shown that RIPK1 amplification contributes to the growth and invasive properties in number of cancers including melanoma, gallbladder, colorectal adenocarcinoma, and non-small cell lung cancer (*193–196*). However, RIPK1 expression has also been shown to be down-regulated in several other types of cancer including

breast, OSCC, and colon cancer, as discussed below (*27*, *197*, *198*). To determine if RIPK1 is downregulated during the tumor progression of HNSCC, we will compare the mRNA and protein expression between cell lines derived from primary and metastatic tumors. We will also obtain clinical samples from resected patient HNSCC tumors that will be used to validate if the downregulation of RIPK1 correlates with disease progression *in vivo*.

SPECIFIC AIM 2: Elucidate the mechanistic cause of RIPK1 downregulated expression. Moriwaki *et al.* showed that both RIPK1 and RIPK3 are down-regulated during tumor progression of colon cancer and that these genes were suppressed by hypoxia, but not by epigenetic DNA modification (*197*). However, a more recent study showed that RIPK3 is downregulated in breast cancer from genomic methylation near its transcriptional start site (*204*). We plan to analyze CpG island methylation data from patient-matched normal and primary tissue to determine if changes in RIPK1 downregulation correlates with promoter methylation. Additionally, we will culture our metastatic-derived cell lines in hypomethylating conditions to determine if a reduction in promoter methylation rescues the expression of RIPK1 in these cells.

SPECIFIC AIM 3: Investigate the biological consequences of RIPK1 downregulation in HNSCC tumor progression and elucidate its role in the enhanced apoptotic response to poly(I):poly(C). The contribution of downregulated RIPK1 expression to tumor progression has been demonstrated in a number of studies, which have revealed an increase in the resistance to anoikis, decreased DNA damage-induced p53-independent apoptosis and an up-regulation of EGFR expression (*27*, *197*, *198*). To elucidate the biological consequences of reduced RIPK1 expression, we will make ectopic changes in the expression of RIPK1 by restoring the expression of RIPK1 in our metastatic cell lines and silencing RIPK1 expression in our primary derived cell lines. These cell lines will be used to determine the

biological consequences of altered RIPK1 expression in the context of metastatic cell characteristics. Finally, they will be used to determine if RIPK1 downregulation is responsible for our previously observed enhanced apoptotic response to poly(I):poly(C).

2.0 MATERIALS AND METHODS

2.1 CELL LINES AND TISSUES

The HNSCC cell lines were derived from the primary tumors and metastatic lymph nodes and characterized at the University of Pittsburgh as described before (*156, 205*). The cell lines were authenticated within the last six months by HLA typing and STR DNA profiling as described before (*206*), and monitored regularly to be free of mycoplasma contamination. All cell lines were cultured in DMEM, (Lonza) containing 10% FBS (Atlanta Biologicals) and penicillin/streptomycin (Lonza) at 37°C in a humidified 5% CO_2 atmosphere. Pairs of primary and metastatic HNSCC tissues were isolated from patients during surgery as per University of Pittsburgh IRB-protocol 99-069. Additional cell lines were used in this study (provided in Table 2).

Table 2 HNSCC cell lines used in this study

Cell Line	Pri/Met	HPV Status	p53	Tumorgenicity	References
PCI-6A	**Primary**	**Negative**	**?**	**yes**	(*207*)
PCI-6B	**Metastatic**	**Negative**	**?**	**yes**	(*207*)
PCI-15A	**Primary**	**Negative**	**ND, OE, A273C mis**	**yes, 30%**	(*207*, *208*)
PCI-15B	**Metastatic**	**Negative**	**ND, OE, A273C mis**	**yes, 70%**	(*207*, *208*)
UM-SCC-22A	**Primary**	**Negative**	**ND, OE, T220C mis**	**yes, 100%**	(*207*, *208*)
UM-SCC-22B	**Metastatic**	**Negative**	**ND, OE, T220C mis**	**no, 0%**	(*207*, *208*)
OSC-19-luc	**Metastatic**	**Negative**	**D,null L164STP Mis/SS**	**yes, 100%**	(*208*, *209*)
UMSCC2	**Primary**	**Negative**	**WT**	**yes**	(*210*, *211*)
UPCI-SCC90	**Primary**	**Positive**	**WT**	**yes**	(*212*, *213*)
SCC47	**Primary**	**Positive**	**WT**	**yes**	(*212*)
93VU-147T	**Primary**	**Positive**	**WT**	**yes**	(*212*)

Note: ND= Non-disruptive mutation, OE = overexpressed, D=disruptive mutation

2.2 ANTIBODIES AND IMMUNOHISTOCHEMISTRY

IHC was performed on formalin fixed, paraffin-embedded prospective tissue microarrays (0.6mm cores) containing paired primary and metastatic tumors and stained with RIPK1 antibody (BD Transduction Laboratories). Antibodies against the cleaved PARP were purchased from Cell Signaling Technology and actin from Santa Cruz Biotechnology. Polyinosinic:polycytidylic acid [p(I):p(C)] (GE Healthcare) was dissolved to a final concentration of 1μg/μl in PBS before use. 5-Aza-2′-deoxycytidine was obtained from Sigma.

2.3 WESTERN BLOTTING ANALYSIS

To prepare whole cell lysates, cells were washed in ice-cold PBS, scraped and collected in lysis buffer (20 mM HEPES pH 7.4, 1 % Triton-X 100, 150 mM NaCl, 1.5 mM $MgCl_2$, 12.5 mM b-

glycerophosphate, 2 mM EGTA, 10 mM NaF, 2 mM DTT, 1 mM Na_3VO_4, 1 mM PMSF plus 1x protease inhibitors). Protein lysates were quantified using the Quick Start™ Bradford 1x Dye Reagent (BioRad). Equal amounts of protein extracts were subjected to 8% SDS–polyacrylamide gel electrophoresis and transferred onto a polyvinylidene difluoride membrane. Membranes were blocked with 5% nonfat dry milk for twenty minutes and incubated with primary antibody for 1 hour followed by 3 subsequent 5 minute washes. After washing, the membrane was covered in horseradish peroxidase–conjugated secondary antibody for 1 hour at room temperature. After further washing, membranes were treated with 1ml of the Enhanced Chemiluminescence (ECL) reagent and exposed onto film and then developed.

2.4 LENTIVIRAL VECTORS

Doxycycline inducible lentiviral vectors were generated by performing LR recombination between pENTR/D-TOPO FLAG-RIPK1-HA and pInducer 20 destination vector (*214*). Lentiviruses were packaged in 293T and pseudotyped with VSV G protein as before (*156*). Briefly, $2x10^6$ 293T cells were seeded in a 10 cm plate and incubated overnight at 37oC. The transfection solution was prepared by combining a total of 10µg plasmids (1.2:1:0.8 ratio of gene vector, pCMV-Δ8.9 gag/pol and VSV-glycoprotein) with 30µl of lipofectamine2000 in 1ml of OPTI-MEM. After 20 minute incubation, the lipo-DNA solution was added dropwise to the 293T cells. The transfection was allowed to incubate for 24 hours before the media was replaced with fresh DMEM. At 48 and 72 hours post-transfection the supernatant was filtered using 0.45nm syringe filters. Transduction of PCI-15B and OSC-19 cells was carried out overnight at 37^{o}C in the presence of 1µg/ml polybrene. Cells were selected with 1µg/ml Puromycin to

establish stable cell lines. Similarly, the PCI-15A cells stably expressing shRIPK1 were generated by packaging the pLKO-shRNA-RIPK1 plasmid and selecting with 1µg/ml Puromycin.

2.5 QUANTITATIVE PCR ANALYSIS OF GENE EXPRESSION

Total RNA was purified using TRIzol reagent (Invitrogen) and treated with DNase I (DNA Free kit, Ambion). Briefly, the cells were washed with 1XPBS and then 1ml of TRIzol was added directly to the well and the cells were incubated for 5 minutes. The TRIzol containing cell lysate was then transferred to 1.5ml tubes and 200µl of chloroform was added to the suspension. The mixture was then vortexed and centrifuged at 13,000g for 15 minutes at 4^{o}C. The top clear layer of the centrifuged sample contained the total RNA and was carefully transferred into new tubes containing 500µl of isopropanol. The isopropanol-RNA mixture was incubated for 10 minutes at RT to allow the RNA to precipitate out of solution. The RNA was then pelleted by centrifugation at 13,000g for 10 minutes at 4^{o}C. The pelleted RNA was then washed with 500µl 75% ethanol and re-suspended with 30µl of RNase free water.

Total RNA (1µg) was used for reverse transcription using iScript cDNA synthesis kit (Bio-Rad) and subjected to real-time PCR using a CFX96 real time system (Bio-Rad) according to manufacturer's instructions. Primers for RIPK1 (forward 5'-CTGGGCTTCACACAGTCTCA-3' reverse 5'-GTCGATCCTGGAACACTGGT-3') and RPL32 were as previously reported (*215*). PCR amplification of each gene was normalized to that of RPL32.

2.6 DNA METHYLTRANSFERASE INHIBITION ASSAY

Cells were seeded $2x10^5$ per well in 12 well plates. After 24 hours the cells were treated with 0, 1, 5, 10 or 15 μM 5-Aza-2′-deoxycytidine. The media was changed every 24 hours for 72 hours and replaced with fresh 5-Aza-2′-deoxycytidine. After 72 hours incubation, the cells were harvested for RT-qPCR and western blot analysis.

2.7 ANOIKIS-RECOVERY ASSAY

Twenty-four well plates were coated with 200μl poly-2-hydroxyethyl methacrylate (poly-HEMA) (10mg/ml) diluted in 75% ethanol three times allowing the reagent to dry before reapplying. After the wells had dried, $5x10^5$ cells were plated and incubated in the poly-HEMA coated wells for 48 hours. After the 48 hours incubation, the cells were pipetted several times to break up aggregates that had formed from growing in suspension conditions and then the cells were transferred to 6 well plates for recovery. Cells were recovered for 24 and 96 hours before they were fixed with a 50/50 mixture of methanol and water containing 4% crystal violet. Images of the stained plates were taken using a pc scanner.

2.8 MIGRATION ASSAY

2.8.1 Two-dimensional wound-healing (scratch) assay.

PCI-15A-shCTRL and PCI-15A-shRIPK1 were seeded $2x10^5$ cells per well in 12 well plates and were incubated until reaching ~100% confluence (24 hours). The cell monolayer was then "scratched" once with a p-200 pipet tip causing an approximately 1mm wound in the monolayer. Microscopic phase contrast images were taken immediately after, and 12 hours post-wound and the migration distance was quantified.

2.8.2 Three-dimensional transwell migration assay.

To assay the three-dimension migration of our PCI-15A-shCTRL and PCI-15A-shRIPK1 cell lines, cells were seeded in BDbiocoat 8.0 micron fibronectin inserts (pre-coated with Human Fibronectin (HFN), which promotes cell attachment) and the number of migrated cells was quantified and values normalized to BDbiocoat 8.0 micron control inserts according to the manufacturers protocol.

2.9 ORTHOTOPIC XENOGRAFT MODEL

Bioluminescence imaging was performed to monitor the time course to metastasis of OSC-19-luc tumor cells stably expressing pcDNA3-CTRL or pcDNA3-RIPK1. These cells were harvested from subconfluent cultures by trypsinization and, after washing with PBS, $1x10^5$ cells were

injected into the lateral tongues of nude mice. The mice were imaged once before tumor implantation (day 0). After the implantation of tumor cells the mice were imaged with bioluminescence imaging starting on day 4 after implantation and were followed by imaging 1–2 times per week until day 11. For bioluminescence imaging, the mice were injected intraperitoneally with a 150 mg/kg dose of D-luciferin (Biosynth) in phosphate-buffered saline, anesthetized with 2.5% isoflurane, and imaged with a charge-coupled device camera–based bioluminescence imaging system (IVIS 100; Caliper; exposure time, 1–5 min; binning, 16; field of view, 12; f/stop, 1; open filter). Signal was displayed as photons/s/cm^2/sr.

2.10 DATASETS AND STATISTICAL ANALYSIS

2.10.1 Datasets.

The Cancer Genome Atlas was used for both datasets in this study (promoter methylation and expression)(*216*). For TCGA expression data, we downloaded level 3 RNAseqV2 data for the N=30 patient samples with both normal solid tissue and primary solid tumor. After consolidating the RSEM values for RIPK1 and actin from each of these samples into an excel chart, we normalized the RSEM value of RIPK1 to that of actin. Similarly, TCGA methylation data was downloaded and beta values were consolidated into a spreadsheet according to patient matched normal solid tissue and primary solid tumor.

2.10.2 Statistical analysis.

Statistical analyses were carried out using GraphPad Prism. * $P < 0.05$, ** $P < 0.01$, *** $P < 0.005$ and **** $P < 0.001$ represent statistical significance by two-tailed paired Student's t test analysis. Wherever applicable, plots show mean with standard error bars. When correlating the expression and methylation data, we used the Pearson's correlation coefficient using an n=20 (df = 18) one-tailed test for negative correlation with a critical value of -0.468

3.0 AIM 1: ESTABLISH THE DOWNREGULATION OF RIPK1 EXPRESSION DURING THE TUMOR PROGRESSION OF HNSCC.

3.1 INTRODUCTION

While investigating the *in vitro* efficacy of treating HNSCC cell lines with TLR ligands, we previously observed an enhancement of apoptosis in response to poly(I):poly(C) in cells derived from metastatic tumors as compared to those derived from autologous primary tumors (*156*). We theorized that there could be several reasons why there was an enhanced apoptosis in the metastatic cells. One of the most likely explanations was that there was an altered expression of TLR3 in these cells that elicited more pronounced signaling, as the up-regulation of TLR3 expression has been previously reported to correlate to the efficacy of poly(I):poly(C) in the treatment of breast cancers (*95*). However, when we investigated the mechanistic cause for this observation, we found no statistically significant difference in the expression of TLR3 or TRIF (*156*). As it had been shown that IRF3 signaling is able to both directly and indirectly induce apoptosis, we reasoned that there could be an amplification of this signaling arm of the TLR3 pathway (*156*). However, when we analyzed IFNβ induction, a transcription factor downstream of the IRF3 activation, we again found no significant difference (*156*).

As we did not see a difference in the expression of TLR3 or TRIF, nor the downstream activation of IRF3, we reasoned that there could be a difference in the TRIF-RIPK1 mediated NF-κB signaling arm of TLR3. Theoretically, a loss in NF-κB signaling would enhance the apoptotic response as NF-κB signaling has been shown to induce pro-inflammatory and pro-survival genes upon activation (*217*). After analyzing IL-8 induction, a downstream NF-κB stimulated gene, we found that there was induction of its expression in the primary, but not metastatic cells in response to TLR3 and TLR4 ligands (*156*). Conversely, we observed that when we treated these cells with, IL-1β, an alternative NF-κB activating cytokine, we saw that there was induction of IL-8 in both cell types (*156*). Moreover, when we treated the metastatic cells with IL-1β there was a degradation of IκBα. The complete ablation of NF-κB signaling (IL-8 induction) in TLR4 was perplexing, because NF-κB is activated thru MyD88 as well as TRIF mediated TLR4-NF-κB activation. However, we believe the complete loss in TLR4-NF-κB could be partially explained by the significant reduction of TLR4 receptor expression in the metastatic cells causing them to be less sensitive to LPS ligand (*156*). Additionally it is conceivable that in addition to the defect in the TRIF mediated NF-κB activation, there could also be a defect in MyD88 signaling in the HNSCC derived cell lines.

These data suggested there was a defect in the activation of NF-κB by TLR3 signaling and that its activity was intact in RIPK1 independent activation of NF-κB through IL-1β signaling. We therefore hypothesized that a defect in NF-κB signaling, known to induce pro-survival and pro-inflammatory signals, could be responsible for our observed apoptotic response in metastatic cells. To evaluate this hypothesis, we treated the cells with poly(I):poly(C) in the presence of IL-1β and we found that the alternative induction of NF-kB was sufficient to rescue the observed phenotype (*156*). Additionally through a gain-of-function approach we used Bay11,

an inhibitor of prosurvival NF-κB, to treat the primary HNSCC cells and showed that in response to dsRNA the primary cell line now had an enhanced apoptosis. We concluded that the enhancement of apoptosis could therefore be caused by a defect in NF-κB signaling causing an imbalanced TLR3 signaling axis in favor of IRF3 resulting in apoptosis. However, the molecular mechanistic explanation for this lack of NF-κB activation by TLR3 signaling in metastatic tumor derived cells remained to be uncovered. In the following section we describe the identification of RIPK1 as the mediator of this differential TLR3 response.

3.2 RESULTS

3.2.1 Downregulation of RIPK1 in metastatic HNSCC cell lines.

Given the above observation (*156*), we hypothesized that the adaptor protein RIPK1, which is uniquely involved in the NF-κB activation through TLR3 might be involved in this differential response. We immunoblotted whole-cell lysates from paired primary (PCI-15A & PCI-6A) and matched metastatic tumor derived cell lines (PCI-15B & PCI-6B) and observed that metastatic cells showed a marked decrease of RIPK1 protein (**Figure 5A**). This finding validated previous studies which suggested RIPK1 levels are reduced during tumorigenesis as a result of alternative mechanisms (*27*, *198*, *200*). Additionally, we analyzed the mRNA levels in the autologous pair of the tumor-derived HNSCC cell line (PCI-15) and we discovered that mRNA levels of RIPK1 are also downregulated between metastatic (15B) and primary (15A) cell lines suggesting that the downregulation of RIPK1 could occur on the transcriptional level (**Figure 5B**).

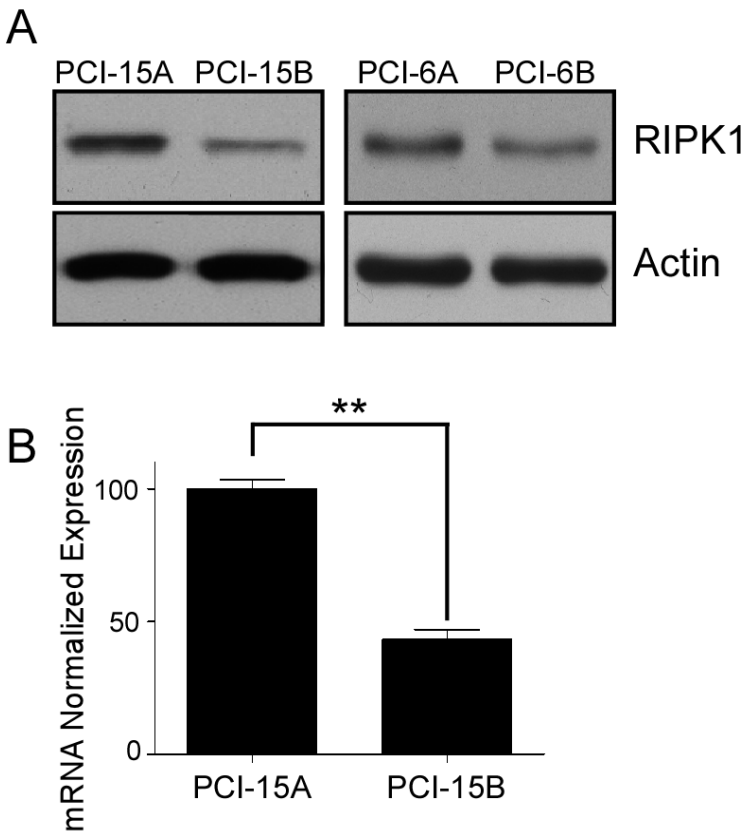

Figure 5 Downregulation of RIPK1 in metastatic head and neck cancer cell lines: Whole-cell lysates from autologous paired primary (PCI-15A & PCI-6A) and metastatic (PCI-15B & PCI-6B) tumor derived cell lines were immunoblotted with anti-RIPK1 and anti-actin antibodies (A). (B) qRT-PCR analysis of RIPK1 mRNA expression levels in PCI-15A and PCI-15B total RNA. Following the normalization of each sample with the internal control RPL32, RIPK1 mRNA levels are shown as % expression with respect to PCI-15A. Each bar represents mean and SD from triplicate samples.

3.2.2 The downregulation of RIPK1 expression in HNSCC correlates with disease progression *in vivo*.

To validate our *in vitro* evidence suggesting that RIPK1 protein is downregulated in HNSCC, we probed tissue microarrays (TMAs) created from resected primary and metastatic tumors with a RIPK1 antibody. Immunohistochemistry (IHC) of these samples showed a decrease in the expression of RIPK1 between the primary tumor (left image) and the matched metastatic tumor (right image) (**Figure 6**, upper panel**).** Quantitative analysis of a number of these IHC images

showed a significant decrease in the protein levels of RIPK1 from resected metastatic tumors compared to primary tumors (**Figure 6**, lower graph).

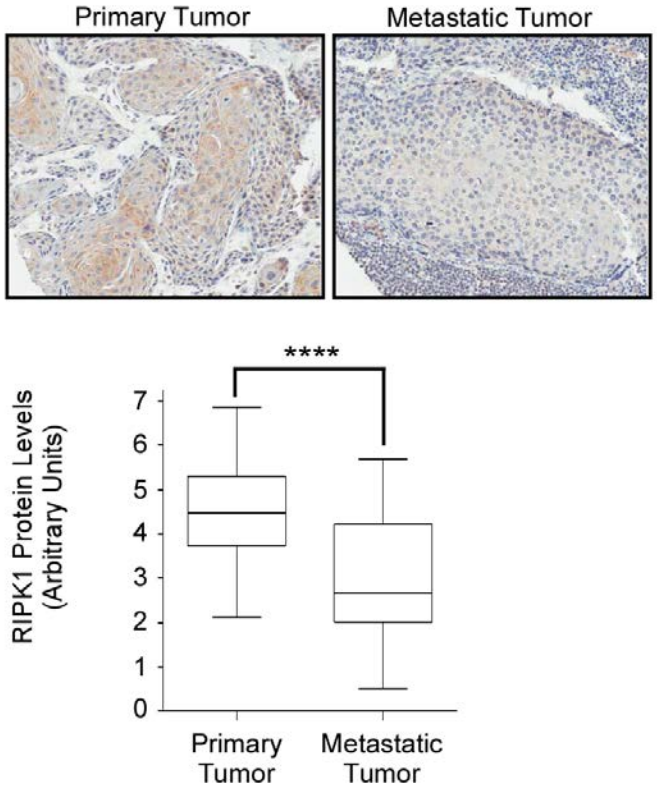

Figure 6 Downregulation of RIPK1 protein expression between metastatic and primary HNSCC resected patient-matched tumors: (A) Resected primary (n=90) and metastatic (n=32) tumors from patients with HNSCC were mounted and stained with RIPK1 antibody. A representative sample is shown in (A, upper panel) where nuclei are stained with hemalun (blue) and the tumor cells are scored for RIPK1 expression levels by a pathologist (A, lower graph).

We were able to validate the loss in RIPK1 protein expression in our HNSCC derived cell lines using immunohistochemistry on resected patient samples. However, we were unable to obtain RNA from these clinical samples. To validate our mRNA *in vitro* data and determine if there is a loss of RIPK1 mRNA loss during tumorigenesis, we sought to utilize one of the publically available online HNSCC datasets. We accessed the Cancer Genome Atlas (TCGA) to obtain HNSCC transcriptome data provided for normal and primary paired (from the same patient) samples. Here we also observed a reduction in the RIPK1 mRNA expression in these

samples (**Figure 7**). This suggests that RIPK1 expression is not only downregulated during the transition between primary tumor and metastatic tumor, but also during the transition between normal tissue and primary tumor lesion formation. This finding suggests that RIPK1 may play a role in the cellular transition during tumorigenesis as well as tumor progression.

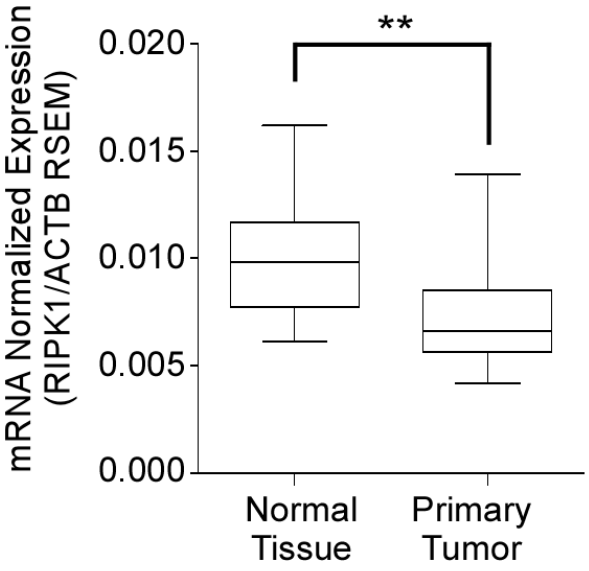

Figure 7 Downregulation of RIPK1 mRNA expression between primary tumors and normal tissue from HNSCC resected matched-patient tumors: RIPK1 mRNA expression RNAseq[2] data in HNSCC patient paired normal solid tissue and primary solid tumors (n=30) provided by The Cancer Genome Atlas. This data was provided as RNA-Seq gene expression estimation with read mapping uncertainty (RSEM) and the RSEM of RIPK1 was normalized to the RSEM of Actin.

Also provided in the TCGA was clinical data on HPV status of the patients. There are often overlapping and divergent molecular pathway aberrations between HPV positive and negative HNSCCs (*29*). For example, it has been shown that HPV positive tumors are typically *TP53* wild type and HPV negative tumors are mainly *TP53* mutant (*29*). However, in both cases the p53 pathway is inactivated, although through the expression of the HPV viral oncogene E6, rather than *TP53* mutation, in HPV positive tumors (*29*). Interestingly, there is a more favorable prognosis with both HPV positive and *TP53* wild type tumors and it has been suggested that

HPV-positive tumors form a distinct group within HNSCCs (*29*). Because of this it is thought that there may be different pathways that are altered in these tumors through amplification, mutation or downregulation (*29*). To determine if there is an etiological distinction in the reduction of RIPK1, we segregated the normal and primary samples according to their HPV status. We found that there was a significant decrease in the RIPK1 levels in both cases irrespective of HPV status (**Figure 8**).

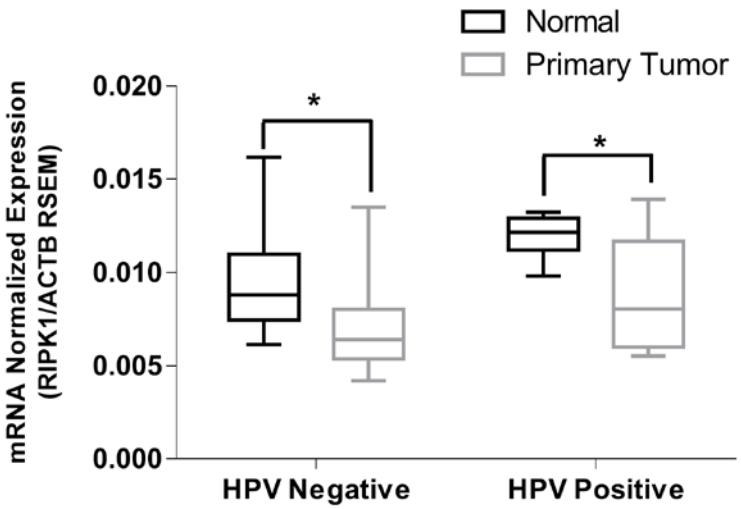

Figure 8 RIPK1 expression is downregulated in primary tumors irrespective of HPV status: Clinical information provided by TCGA on HPV status in patient samples was used to separate the HPV negative (n= 18) and HPV positive (n=6) patients. RIPK1 mRNA expression RNAseq[2] data was then analyzed between these groups. This data was provided as RNA-Seq gene expression estimation with read mapping uncertainty (RSEM) and the RSEM of RIPK1 was normalized to the RSEM of Actin.

3.3 DISCUSSION

Previously we had observed a defect in NF-κB signaling in metastatic cells in response to TLR3 ligands, leading to a more pronounced apoptosis in these cells compared to their primary counterparts (*156*). While investigating the defect in NF-kB signaling we analyzed the expression of the upstream mediators of this pathway. Here we show that RIPK1 was

downregulated at both mRNA and protein levels in the metastatic compared to autologous primary cell lines. Because RIPK1 is required for TLR3-mediated pro-survival NF-kB signaling, we reasoned that this could explain why we observed an enhanced apoptotic response in metastatic cells (*27*).

To validate this finding *in vivo* we used immunohistochemistry of HNSCC tumor microarrays from resected patient primary and metastatic samples. We found that the RIPK1 protein levels were reduced in the clinical specimens suggesting that this is a finding that can be recapitulated in patients as well as in cell lines. This finding also validated the use of our cell lines in elucidating the mechanistic defect in RIPK1 and the contributions that a loss of RIPK1 might have on tumor progression. Although a few studies have suggested that RIPK1 levels are downregulated during tumorigenesis, to our knowledge this is the first clinical data showing this occurrence in HNSCC (*27*, *198*, *200*, *203*, *218*, *219*).

We also validated our protein data at the mRNA level. Expression profiling data from patient samples is provided on cancer databases such as the TCGA. However at the time of this study, the only data provided by the TCGA on HNSCC was from normal solid tissue and primary solid tumor, and not metastatic tumor samples. Upon analysis of this data for RIPK1 mRNA expression we found that RIPK1 expression is also reduced during the initial phases of tumorigenesis, i.e. normal solid tissue expressed relatively higher levels of RIPK1 mRNA than tumor samples. This finding suggests that the initial RIPK1 loss could be contributing to tumorigenesis and further down-regulation may increase the tumor progressive capabilities of the cancer cells.

The loss of RIPK1 expression between normal solid tissue and primary tumor and then subsequent loss after primary tumors metastasize, suggests that RIPK1 could act as a tumor

suppressor gene. After observing this phenomena we wanted to first determine the mechanistic cause contributing to the reduced RIPK1 expression and second what are the consequences on a cell phenotype after losing this expression. As the protein and mRNA levels were both lower in the metastatic cells, we theorized that the downregulation was probably transcriptionally regulated. Additionally as the downregulation of RIPK1 expression in HNSCC correlates with disease progression *in vivo*, we speculated that a reduction of RIPK1 contributes to tumor promoting properties.

4.0 AIM 2: ELUCIDATE THE MECHANISTIC CAUSE OF RIPK1 DOWNREGULATED EXPRESSION.

4.1 INTRODUCTION

Epigenetic modifications enable cells to control DNA transcription by turning on or off coding sequences in order to drive appropriate gene expression. The epigenetic landscape is thus continuously modified by extracellular and intracellular factors to maintain homeostasis. Aberrant epigenetic modifications can have profound effects on gene expression in a cell and that these types of modifications are common during tumorigenesis. DNA promoter methylation is one such epigenetic change able to alter gene expression profiles.

The function of methylation in relation to gene expression was first observed by J. D. McGhee and G. D. Ginder in the 1980s (*220*). These researchers compared the methylation status in cells with differential gene expression using restriction enzymes that were specific to methylated sites (*221*). Their work was later validated by treating cells with 5-azacytidine, a chemical analog for the nucleoside cytosine, which are integrated into growing DNA strands and severely inhibit the action of the DNA methyltransferase enzymes that normally methylate DNA.

DNA methylation consists of covalent attachments of methyl groups to the 5’ position of cytosine residues in CG dinucleotides, which are typically clustered in what are known as “CpG islands,” or DNA sequences of ~200 base pairs that are GC rich, often containing greater than

50% GC content. The methylated cytosines are also found in “CpG shores” which are within 2kb of the vicinity of CpG islands (*222*). The exact mechanism of promoter methylation in controlling gene expression has not been fully elucidated, but it is thought that methylated promoters alter the binding affinity of transcription factors.

As we observed a decrease in both the protein as well as mRNA levels in our autologous primary and metastatic HNSCC cell lines, we hypothesized that the downregulation may be at the transcriptional level. As it is well-established that abnormal DNA methylation is widespread in cancer and plays an important role in oncogenesis, we reasoned that promoter methylation may contribute to the RIPK1 downregulation (14). Although other studies have shown that both RIPK1 and RIPK3 are down-regulated during tumor progression of colon cancer, it was shown that these genes were suppressed by hypoxia, but not by epigenetic DNA modification (*197*). However, in support of the notion that RIPK1 may be down-regulated by promoter methylation, it was recently revealed that the mechanistic cause of RIPK3 reduced expression in breast cancer is through promoter hypermethylation (*204*).

4.2 RESULTS

4.2.1 There is promoter methylation in a CpG island -868 bases from the transcription start site of RIPK1.

In addition to the mRNA data previously shown, the TCGA database also provides DNA methylation status of HNSCC resected normal solid tissue and paired primary solid tumor analyzed with the Illumina Infinium HumanMethylation450 platform. After accessing this data

from N=30 paired samples, we found that there was an increase in RIPK1 promoter methylation (beta value) in the -868 probe position from the RIPK1 transcription start site (**Figure 9)**. We included promoter methylation from all of the CpG islands provided for RIPK1 as well as a related gene (*RIPK2*) and a housekeeping gene (*ACTN*) to show that although alterations in promoter methylation may be widespread in tumorigenesis, this method has the sensitivity to detect relevant changes in a specific gene.

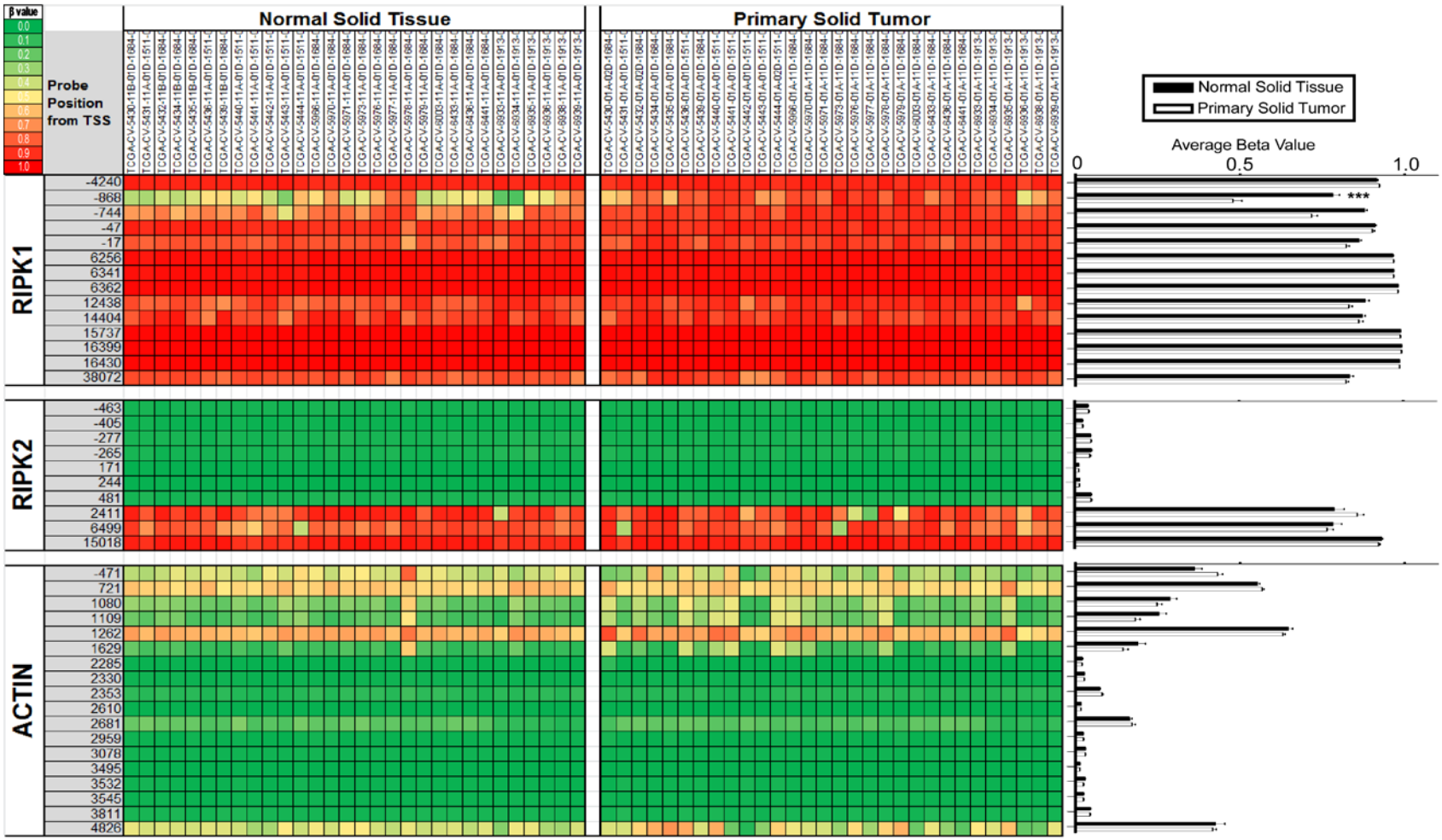

Figure 9 Promoter methylation in a CpG island -868 bases from the transcription start site of RIPK1: RIPK1 CpG island methylation data from HNSCC patient paired normal solid tissue and primary solid tumors (n=30) analyzed with Illumina Infinium HumanMethylation450 was provided on The Cancer Genome Atlas (A). Graphic representations of the average beta values in normal vs primary samples for each of the CpG islands are provided (A, right). The beta value is the ratio of the methylated probe intensity and the overall intensity and therefore 1.0 (red) relates to higher methylation and 0 (green) to lower methylation.

4.2.2 Promoter methylation correlates with RIPK1 expression in resected tumor samples.

As we had obtained mRNA expression (**Figure 7**) and CpG methylation datasets (**Figure 10A)** from the matched patients, we were able to test the correlation between these two parameters. We plotted the difference in RIPK1 promoter methylation (beta value) versus the difference in mRNA expression (RNAseq RSEM value) between normal tissue and primary tumors from the same patient. After plotting these data, we used the Pearson's correlation coefficient with an N of 20 as an indicator of correlation. As shown in **Figure 10B**, we found a strong negative correlation between the increases in promoter methylation verses the decrease in RIPK1 expression.

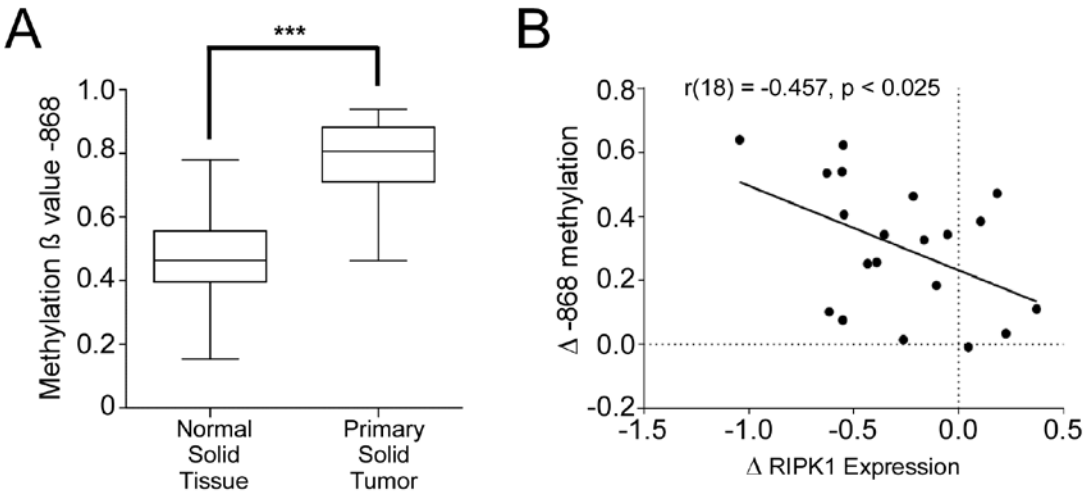

Figure 10 Promoter methylation correlates with RIPK1 expression in tumor samples: The significant difference observed the RIPK1 CpG islands -868 from the transcription start site from Fig. 9 was represented here more clearly as a box-and-whisker blot (A). (B) Correlation between the changes in methylation status at -868 from paired normal and primary samples to the matched change in expression between paired normal and primary samples (same patient TCGA methylation vs RNAseq2 data). Statistical values represent Pearson's correlation coefficient using an n=20 (df = 18) one-tailed test for negative correlation with a critical value of -0.468.

4.2.3 Hypomethylating treatment conditions restored the expression of RIPK1 in the PCI-15B metastatic tumor derived cell line.

To experimentally validate the TCGA correlative data, we treated the HNSCC cell line PCI-15B with a hypomethylating reagent. 5-aza-2'-deoxycytidine is a chemical analogue of the cytosine nucleoside that causes an inhibition of DNA methyltransferase during DNA replication. Treatment of the HNSCC cell line PCI-15B with an increasing dose of 5-aza-2'-deoxycytidine should cause a reduction in the levels of promoter methylation. The dose response in **Figure 11A** and **Figure 11B** shows that the expression of RIPK1 mRNA and protein correlates to the increasing concentration of 5-aza-2'-deoxycytidine.

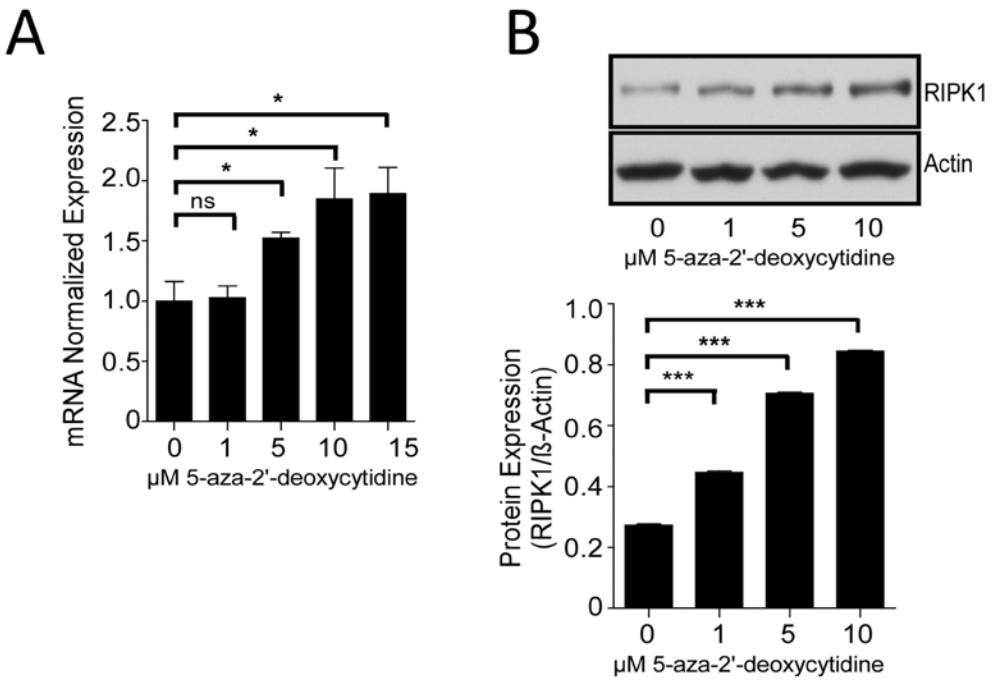

Figure 11 Hypomethylating treatment restored the expression of RIPK1 in PCI-15B Metastatic cells: PCI-15B metastatic cells were treated with an increasing concentration of the DNA methyltransferase inhibitor (5-aza-2'-deoxycytidine) and the mRNA and protein levels were quantitated by qRT-PCR (C) and immunoblotting (D) respectively. Bars represent the mean and SD from triplicate readings of the representative blot provided in (D, upper panel)

4.3 DISCUSSION

After analyzing the methylation data for HNSCC provided by the TCGA, we found that there was an increase in the amount of promoter methylation at a specific CpG island -868 bases upstream of the TSS in the RIPK1 promoter region. However, we did not observe any promoter methylation in the additional genes we investigated, including RIPK2 and Actin (**Figure 9)**, as well as RIPK3 and RIPK4 (data not shown). Thus, we reasoned that this methylation could be responsible for the observed downregulation in RIPK1 expression. This postulation was supported by our correlative analysis of methylation status and RIPK1 mRNA expression profiles that showed a significant association between the increase in methylated promoter and the reduction in RIPK1 expression. To our knowledge this is the first study to show an association between the downregulation of RIPK1 expression and a change in promoter methylation.

Results obtained through the analysis of TCGA data provided correlative evidence to support our hypothesis. Therefore, to obtain causal evidence, using a model system we treated our PCI-15B metastatic cells with a DMT inhibitor, 5-aza-2'-deoxycytidine, and found a significant increase in the levels of RIPK1. These data supported our hypothesis that the change in promoter methylation may, at least partially, be the mechanistic cause of downregulated RIPK1 expression. Though it was recently shown that both RIPK1 and RIPK3 are down-regulated during tumor progression of colon cancer, it was also shown that the expression was suppressed by hypoxia, but not by epigenetic DNA modification (*197*). However, a more recent study showed that RIPK3 is downregulated in breast cancer from genomic methylation near its transcriptional start site (*204*). Our data suggest that promoter methylation could be the mechanistic cause of RIPK1 mRNA downregulated during tumor progression. However, the

exact mechanism of how this methylated region controls RIPK1 expression remains to be determined.

Based on ChIP-seq results provided by The Encyclopedia of DNA Elements (ENCODE), the methylated site that we identified in the RIPK1 promoter is occupied by the transcription factor ARID3A in various cell lines. It is therefore possible that the enhanced methylation found in tumor cells reduces ARID3A binding to RIPK1 promoter resulting in reduced RIPK1 transcription. Although ARID3A is known to be involved in transcriptional regulation of various genes related to lymphocyte development, it is not clear how DNA-methylation in the ARID3A-binding site changes its transcriptional ability (*223*). It is possible that enhanced methylation in the RIPK1 promoter found in tumor cells might change its ability to transcribe RIPK1. It is notable in this regard that enhanced expression levels of ARID3A is known to provide better prognosis for colon cancer (*224*).

5.0 AIM 3: INVESTIGATE THE BIOLOGICAL CONSEQUENCES OF RIPK1 DOWNREGULATION IN HNSCC: TUMOR PROGRESSION AND ENHANCED APOPTOTIC RESPONSE TO POLY(I):POLY(C).

5.1 INTRODUCTION

As previously discussed, it has been revealed that despite the role of RIPK1 in promoting necroptosis, it is also vital in epithelial cells to mitigate apoptosis in response to a number of stimuli (*184*, *189–192*). It seems counterintuitive, therefore, to suggest that RIPK1 acts as a suppressor of tumor cell death and that loss of its expression can drive tumorigenesis. However, there is an increasing body of evidence that suggests the latter. Thus far, the following three publications have reported how a loss in RIPK1 expression can give a growth advantage to cancerous cells including 1) overexpression of EGFR (shown to be a vital oncogene in HNSCC), 2) DNA damage-induced p53-independent cell death, and 3) the induction of anoikis resistance (*27*, *198*, *200*, *203*, *218*, *219*). As we observed a loss in RIPK1 throughout tumorigenesis and tumor progression, we sought to determine if this downregulation could be contributing to these characteristics. We hypothesized that silencing of RIPK1 in our primary HNSCC derived cell lines would enhance the metastatic phenotype of malignant HNSCC.

As described before, the acquired ability of a cancer cell to undergo migration and invasion into distant metastatic sites is one of the hallmarks of cancer (*31*, *32*). This process

contributes to the EMT, whereby it mimics the normal physiological processes of cell movement such as embryonic morphogenesis, would healing and immune-cell trafficking (*225–227*). Tumor cell migration is an active process that results from a continuous cycle of the interdependent steps polarization, elongation, pseudopod formation and ECM attachment, followed by contraction (*227*). This process is thought to be regulated by the motility-inducing chemokines and growth factors that induce and maintain migration by signal transduction through PI3K (*228*). As RIPK1 has been shown to contribute to PI3K signaling through upregulated EGFR expression, we hypothesized that RIPK1 silencing may increase the rate of migration in the primary derived HNSCC cells.

RIPK1 downregulation may be advantageous for the primary tumor to develop metastatic characteristics as others have suggested. However, because of the role of RIPK1 in activating TLR3-NF-κB pro-survival signaling, we sought to determine if the downregulation of RIPK1 was responsible for the enhanced apoptosis that we previously observed in metastatic HNSCC. This would be an exciting finding as it has implications for the use of RIPK1 as a potential biomarker for patients whose tumors would be more susceptible to an apoptotic response to treatment with TLR3 ligands.

5.2 RESULTS

5.2.1 Modulation of RIPK1 expression changes *in vitro* tumor-promoting properties.

To define the *in vitro* consequences of RIPK1 downregulation on cellular properties, we used RNA interference to silence RIPK1 expression in the PCI-15A primary tumor derived cell line.

Similarly, to examine the role of RIPK1 in the previously observed apoptotic response, we created clones stably expressing a RIPK1 construct in PCI-15B, a cell line derived from a metastatic tumor. We then analyzed the expression of RIPK1 in these cell lines containing ectopic changes and found that there was a restored expression of RIPK1 in the cell line derived from a metastatic tumor and, conversely, clones with shRNA knock-down of RIPK1 expression had comparable to the expression of RIPK1 in metastatic cells (**Figure 12**).

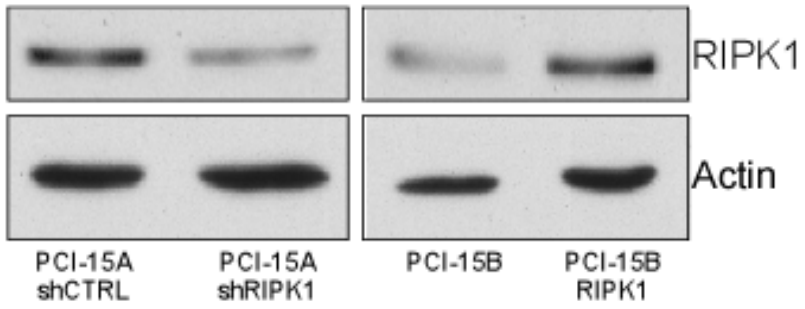

Figure 12 Ectopic changes in the expression of RIPK1 in primary and metastatic HNSCC derived cell lines: After silencing RIPK1 in the primary and restoring the expression of RIPK1 in metastatic derived tumor cell lines, we analyzed the expression RIPK1. Untreated lysates from the PCI-15A & B cells with ectopic changes to RIPK1 levels were immunoblotted for the expression of RIPK1 and Actin.

We used 2D scratch (**Figure 13A**) and 3D transwell migration assays (**Figure 13B**) in the PCI-15A shRIPK1 cell line to determine if a loss in the expression of RIPK1 could contribute to the abilities of tumor cells to metastasize. We observed that the 2D wound healing was significantly more efficient in the PCI-15A shRIPK1 cells than in the shCTRL, indicating that decreased RIPK1 expression increases the migration rate of PCI-15A cells. Similarly, when the same cell line (PCI-15A-shRIPK1) was used in a 3D migration assay in a transwell chamber, there was an enhanced migration of the cells through the fibronectin coated membrane compared to the control cell.

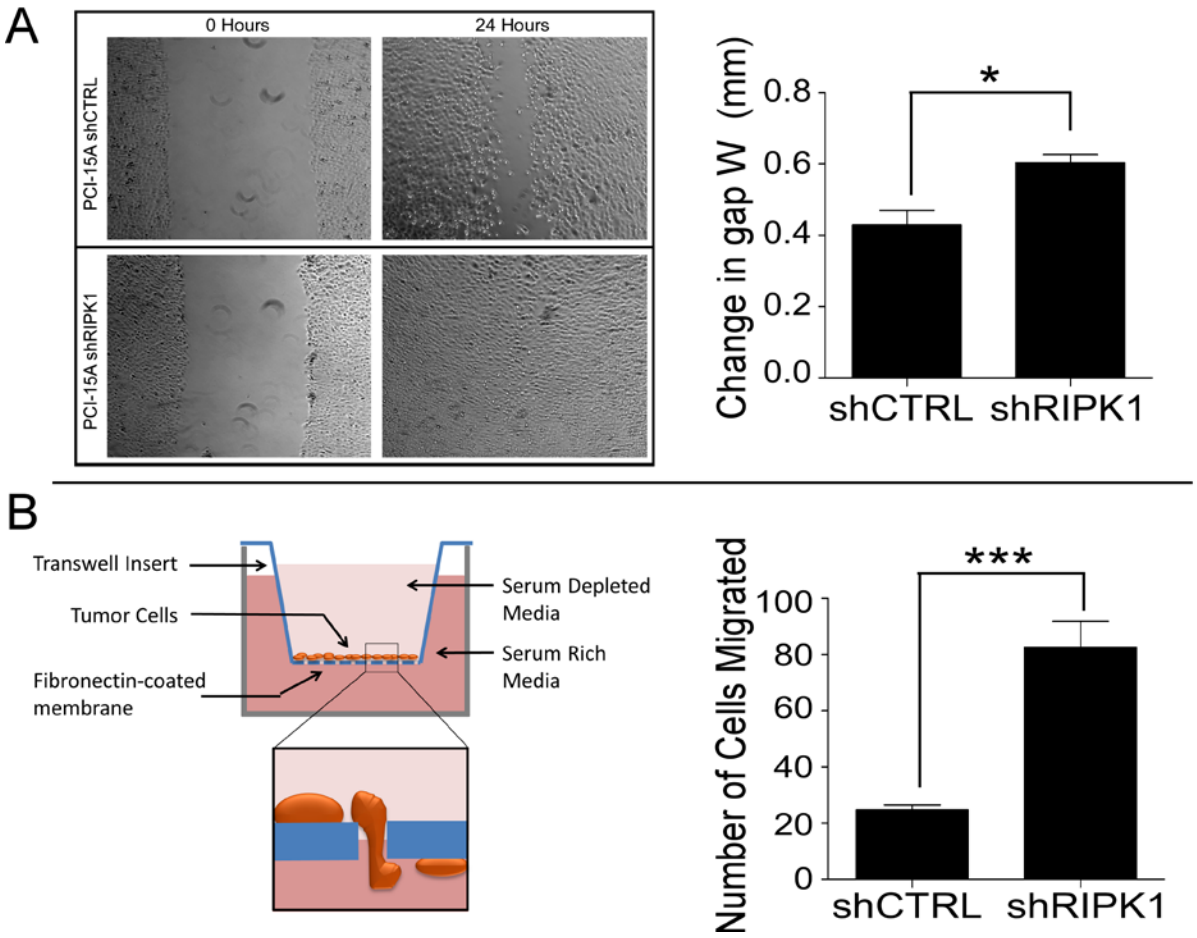

Figure 13 Silencing of RIPK1 in primary derived HNSCC cell lines enhances the rate of migration: (A) Cell migration of PCI-15A primary cell lines stably expressing RIPK1 shRNA in a 2D scratch assay (A). 2D migration was quantified as the measured (mm) difference between the scratched gap at 0 hours and at 24 hours (A, lower). Cell migration was also measured in these cells using a 3D transwell migration filter assay (B) The left panel provides a schematic of the 3D transwell migration assay. In this assay cells were serum starved for 24 hours before seeding into transwell, (Right Panel) 3D migration was quantified based on the number of cells that migrated through a porous membrane coated with fibronectin.

Anoikis is a form of apoptosis that results from loss of cell adhesion to the ECM (*202*). Thus, anoikis plays an important protective role in preventing actively proliferating cells from re-attachment and growth in inappropriate environments (*229*). Resistance to anoikis is a common feature of the carcinoma epithelial-mesenchymal transition and is necessary for transformed cells to survive under "anchorage independent" growth conditions (*202*). *In vivo*, anoikis resistance would result in loss of apoptotic signals after detachment of keratinocytes from the basement

membrane and allow these cells to survive during the migration and invasion into distant organs (*229*). Using an anoikis-resistance assay (**Figure 14A)** we validated the work on OSCC from Kamarajan *et al,* who showed that RIPK1 downregulation enhances anoikis resistance. We found that PCI-15A cells expressing shRNA to RIPK1 were less capable of reattaching and recovering after being cultured in an anoikis inducing environment (**Figure 14B**) (*198*). These data suggest that in addition to previous observations, we found that RIPK1 downregulation may enhance the anoikis-resistance characteristics of metastatic tumors.

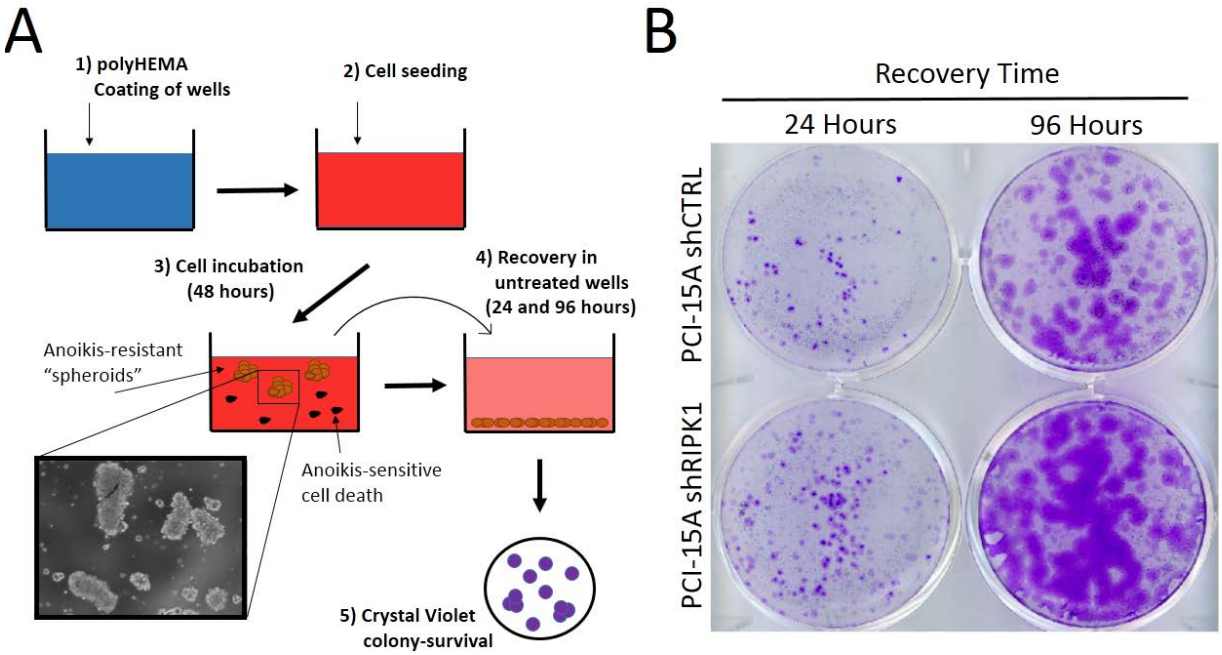

Figure 14 Silencing of RIPK1 expression enhanced the anoikis resistance: A schematic for the anoikis resistance assay that we used is provided (A). In this experiment cells were plated in poly-HEMA coated wells for 48 hours to prevent attachment. After 48 hours the cells were collected and transferred to uncoated plates to allow for reattachment and recovery. After 24 and 96 hours of recovery the wells were fixed with methanol, stained with crystal violet and imaged. (B) PCI-15A shRIPK1 cells were more anoikis-resistant than shRNA control cells.

Finally, we also tested the changes in EGFR expression with ectopic changes of RIPK1 expression to validate the previous study from Ramnarain *et al* (*27*). We observed that the

expression of EGFR increased in our shRIP1 stable knockdown cells and, conversely, if we ectopically expressed RIPK1 there was a significant decrease in the expression of EGFR (**Figure 15**).

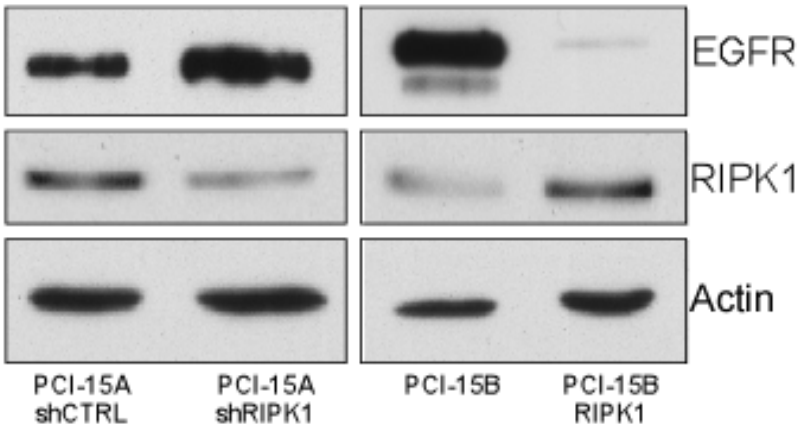

Figure 15 Modulation of RIPK1 expression inversely correlates to the expression of EGFR: Untreated lysates from the PCI-15A & B cells with ectopic changes to RIPK1 levels were immunoblotted for the expression of RIPK1, EGFR and Actin.

5.2.2 Ectopic expression of RIPK1 in OSC-19 cells in a mouse model.

Silencing RIPK1 expression in HNSCC cell lines enhanced metastatic phenotypes and expression of RIPK1 decreased the expression of EGFR, an important oncogene in HNSCC. We hypothesized that if we ectopically expressed RIPK1 in a metastatic cell line it would decrease the rate of metastasis in these cells. We were able to obtain a cell line, OSC-19-luciferase, which has been used previously in HNSCC orthotopic xenograft mouse models and has been shown to metastasize in 70% of mice tested. We validated the reduced expression of RIPK1 and enhanced EGFR levels in the OSC-19-luciferase parental cells by comparing the protein levels to our characterized PCI-15A/15B cells (**Figure 16A**). We found a similar quantity of these proteins

the OSC-19 cells as our PCI-15B metastatic cells. Additionally, we validated the stable expression of the RIPK1 construct in these cells by immunoblotting for RIPK1-flag (**Figure 16B**). By introducing this cell line into the tongues of nude mice, through intramuscular injection, we hypothesized that there would be a significant decrease in the initial rate and/or overall metastasis in the cell lines expressing RIPK1. However, when we tested the migration of these cells from the initial injection site into the mouse cervical lymph node, we observed no difference between the pcDNA3-CTRL expressing and pcDNA-RIPK1 expressing tumors (**Figure 16C**).

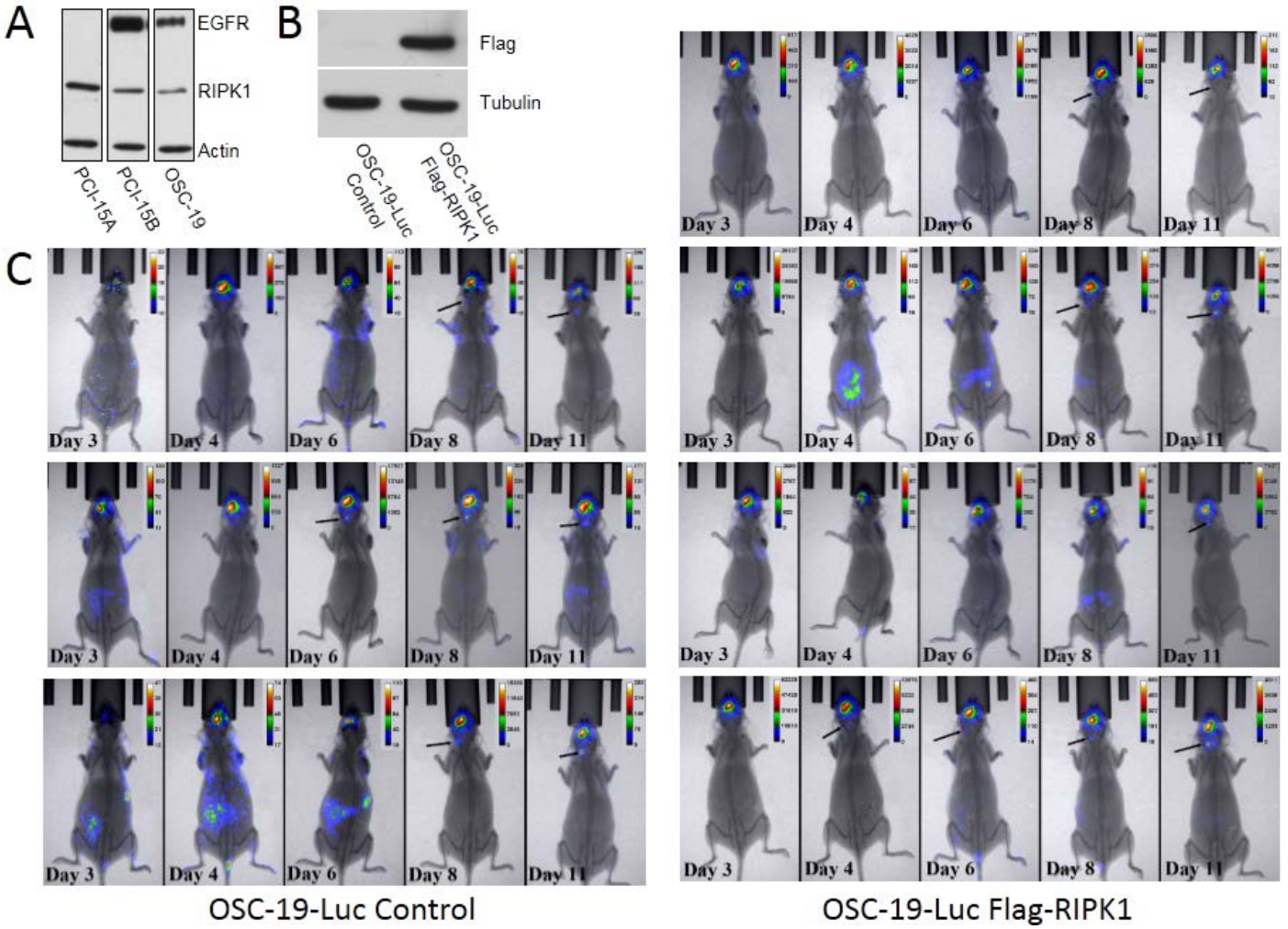

Figure 16 Stable expression of RIPK1 in the OSC-19-luc HNSCC cell line does not suppress lymph node metastasis in the orthotopic xenograph mouse model: (A) Lysates from the OSC-19 and PCI-15A & B cells were immunoblotted for the expression of EGFR and RIPK1. (B) Lysates from the OSC-19-CTRL and ODC-19-luc-RIPK1-flag were immunoblotted for Flag expression. (C) OSC-19 metastatic HNSCC cell lines expressing pcDNA3-CTRL or pcDNA-RIPK1 were injected into the tongues of nude mice and the cervical lymph node metastasis was observed over the next 11 days by imaging with a bioluminescence imaging system (IVIS 100). Cervical lymph node metastasis is indicated by the black arrows.

5.2.3 Ectopic changes in RIPK1 expression modulates dsRNA-mediated apoptosis

Cleaved poly(ADP-ribose) polymerase (c-PARP) was used as a measure of apoptosis in response to poly(I):poly(C) treatment in these experiments. PARP is a nuclear protein that functions to recognize DNA damage such as single strand breaks and signals for the cell to repair the associated damage. During apoptosis the PARP protein is inactivated by caspase 3 cleavage into an 89- and 24-kDa fragment which contain the active site and the DNA-binding domain of the enzyme, respectively (33). We therefore used an antibody to the 89kDa cleavage product (c-PARP) as an indicator of caspase 3 activity, which is indicative of apoptosis (33). In the past, we validated the use of c-PARP as an indicator of apoptosis in our cell model using both a cell viability assay and a 3/7 caspase glo (Promega) and annexinV/propidium iodine staining and observed the same enhancement or apoptosis in the metastatic cells (data not shown). However, in these experiments we did not use these techniques to validate our results. Additionally, full-length PARP levels are often used as an internal control to ensure that changes in C-PARP levels are not caused by deregulation of the total PARP expression. However, a caveat of these experiments is that we did not measure total PARP.

As shown in **Figure 17A** as the concentration of poly(I):poly(C) increases in PCI-15A-shCTRL cells there is no change in the amount of apoptosis (c-PARP lanes 2-4 vs. lane 1), however there is a significant increase in the apoptotic response to poly(I):poly(C) when the expression of RIPK1 is knocked-down in these cells with shRNA (c-PARP lanes 6-8 vs. lane 5). Similarly in **Figure 17B** we found that when we restored the expression of RIPK1 in the PCI-15B metastatic cell line we observed that there was no longer an enhanced apoptotic response to poly(I):poly(C) (lanes 5-8 vs. lanes 1-4). In addition, we restored the expression of RIPK1 in a

highly metastatic cell line OSC-19 to ensure that our observation was not an artifact of this paired cell line (data not shown) and we observed the same phenotype. These data indicate that ectopic changes in RIPK1 expression correlate to the hypothesized changes in the apoptotic response to poly(I):poly(C) treatment.

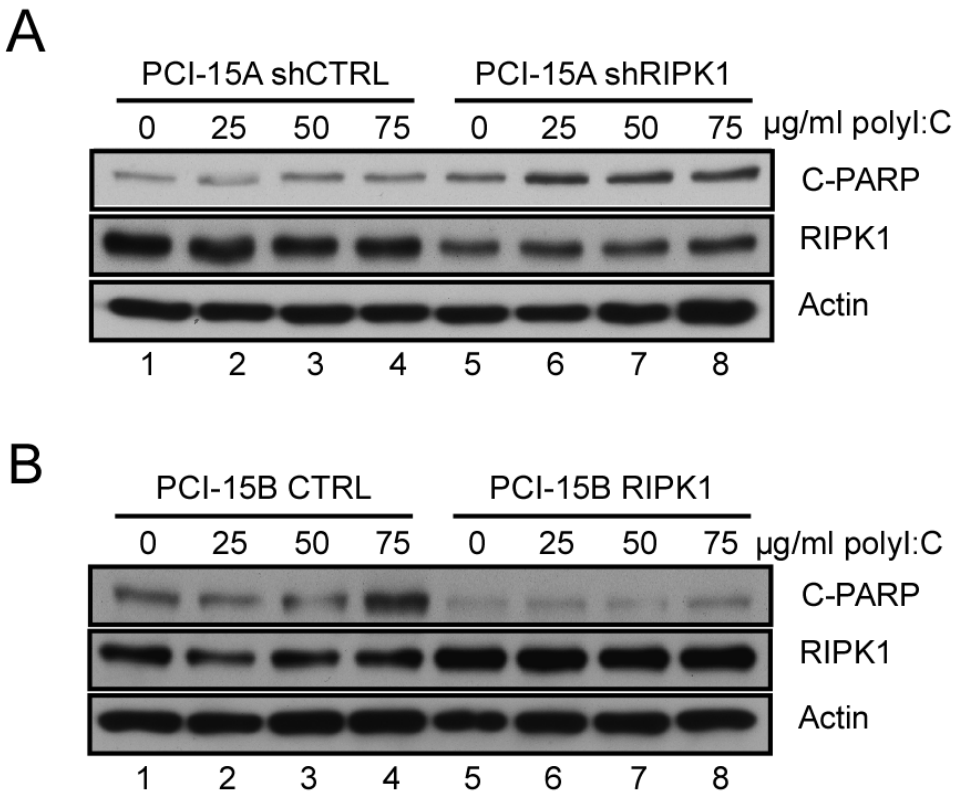

Figure 17 Ectopic changes in RIPK1 expression modulates dsRNA-mediated apoptosis: PCI-15A primary cell lines were stably transduced with RIPK1 shRNA (A). These cells were treated with increasing amounts of poly(I):poly(C) before whole-cell lysates were analyzed by Western blot using antibodies for cleaved PARP and actin as a loading control. Additionally RIPK1 expression was restored in PCI-15B metastatic HNSCC cell line by transducing with a RIPK1 expression construct (B).

To validate these findings we created PCI-15B metastatic cells expressing RIPK1 under a tetracycline-inducible promoter to determine if there was a dose response to poly(I):poly(C) treatment (**Figure 18**). We observed that as we increased the concentration of doxycycline there was an increase in the expression of RIPK1 (lanes 3-6 vs. lane 1 and 2) and a correlative

decrease in the apoptotic response to poly(I):poly(C) (lanes 4 and 5 vs. lane 2). These data suggest that the downregulation of RIPK1 could result in an exploitable enhanced apoptotic response to TLR3 ligands in metastatic HNSCC.

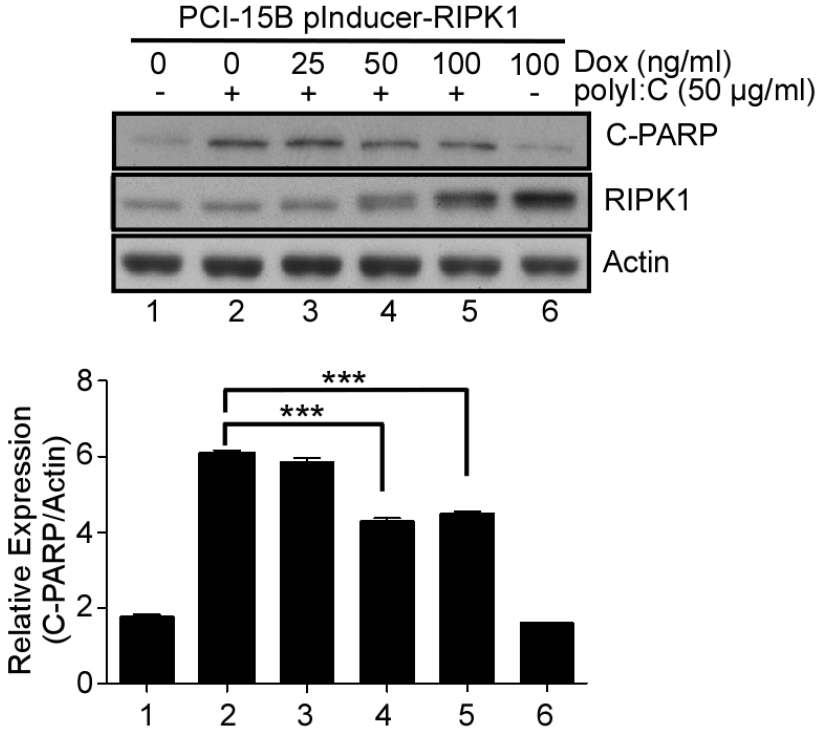

Figure 18 Induced RIPK1 expression mitigated dsRNA-mediated apoptosis: The PCI-15B metastatic cell line were stably transduced with a dox-inducible RIPK1 expression vector. Whole-cell lysates were prepared from cells with an increasing concentration of dox in the presence and absence of 50µg/ml poly(I):poly(C). Cleaved PARP levels were analyzed (bottom graph) using the ImageJ gel quantification software package normalizing to actin levels. Bars represent the mean and SD from triplicate readings of the representative blot provided in (upper panel).

5.2.4 Additive Apoptotic effect of poly(I):poly(C) cotreatment with HNSCC therapies in HNSCC cell lines

We observed an enhanced apoptotic response in the metastatic HNSCC cell lines treated with poly(I):poly(C). Therefore, we hypothesized that cotreatment with poly(I):poly(C) could increase the cell death response to the therapeutics cetuximab and cisplatin. We found that there was an increase in apoptosis after treatment with either of these drugs in the presence of poly(I):poly(C),

as indicated by cleaved PARP in both primary and metastatic cell lines (**Figure 19**). These treatments appeared to have a synergistic effect, as the levels of cleaved PARP after cotreatment were more than that expected from combining the levels of apoptosis in individual treatments.

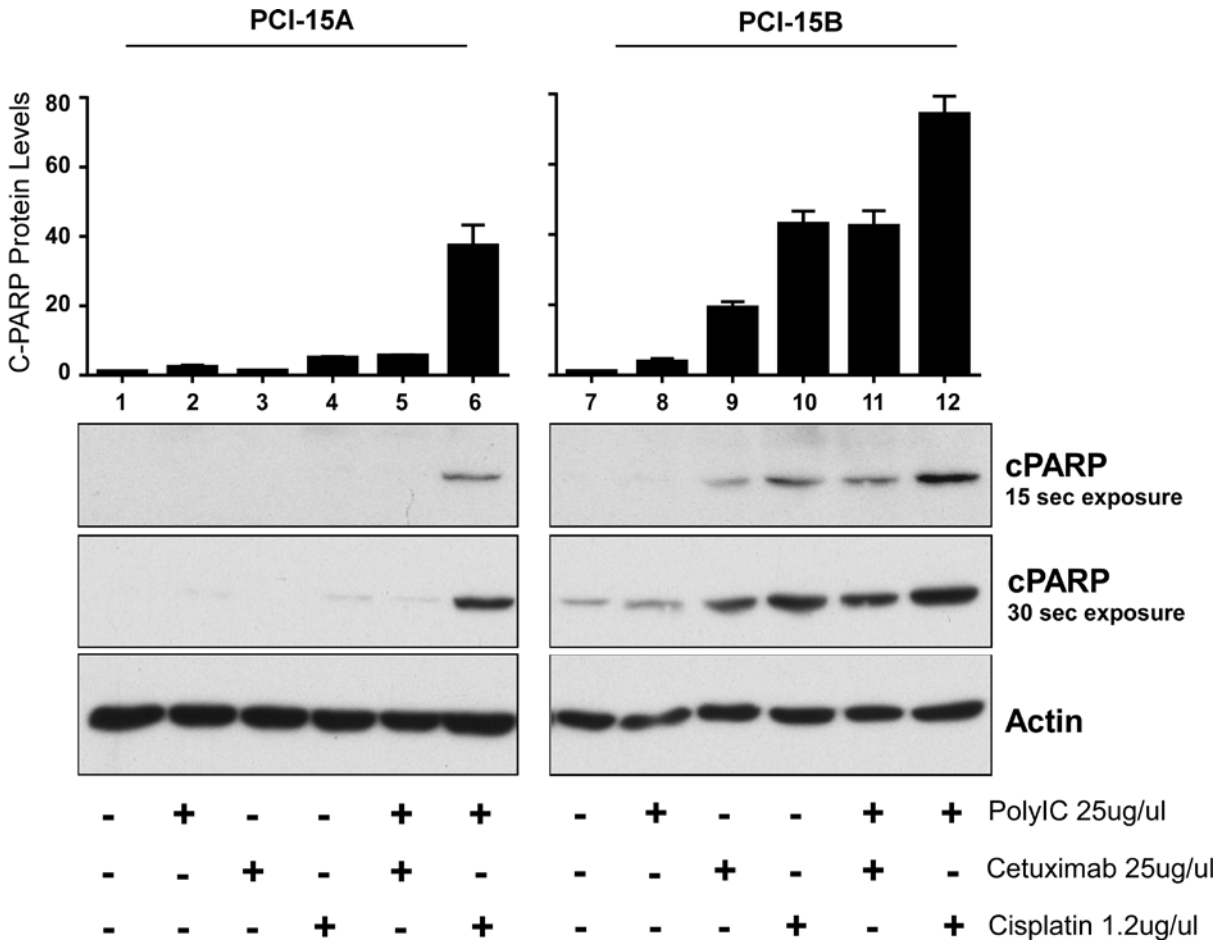

Figure 19 Additive apoptotic effect with polyI:C cotreatments: PCI-15A (primary) and PCI-15B (metastatic) HNSCC cell lines were treated with 25 μg/ml of polyI:C in the presence or absence of 10μg/ml cetuximab or 10μg/ml Cisplatin for 24 hours before whole-cell lysates were analyzed by Western blot using antibodies for cleaved PARP and actin as a loading control. Additionally the PCI-15B cells were treated with an increasing amount of polyI:C in the presence of 10μg/ml cetuximab.

5.3 DISCUSSION

We tested the metastatic potential of modulating RIPK1 expression by measuring the growth promoting properties in HNSCC. We found that knockdown of the RIPK1 expression with shRNA increases the rate of migration in HNSCC cell lines derived from a primary tumor, extending the notion that RIPK1 may act as a suppressor of tumor progression. Thus, our findings align with others who have shown RIPK1 expression is reduced during the tumor progression (*27*, *203*). Recently it was shown that there is an inverse relationship between RIPK1 and EGFR expression in breast cancer (*27*). We also found that ectopic changes in RIPK1 in our HNSCC derived cell lines inversely correlated with the expression of EGFR. It was suggested that RIPK1 binds to and sequesters Sp1, a potent EGFR transcription factor, causing a downregulation of the expression of EGFR. This may partially explain why RIPK1 expression is reduced in the tumor progression of HNSCC as EGFR levels are upregulated in the majority of HNSCC tumors. The regulatory role of RIPK1 on EGFR expression may partially explain the enhanced rates of migration that we observed after silencing RIPK1 expression in our primary derived cell lines.

In addition, Kamarajan *et al.* recently revealed that RIPK1 and sirtuin-3 (SIRT3), a NAD-dependent deacetylase that is known to regulate cell survival, metabolism, and tumorigenesis, have an opposite expression profile in OSCC (*198*). They showed that silencing RIPK1 expression increased the expression of SIRT3 and resistance to anoikis. Additionally, they showed that growing OSCC cells grown in anoikis promoting conditions caused a down-regulation of RIPK1 (*198*). Our data validates this study as silencing RIPK1 increased the resistance to anoikis in our primary HNSCC derived cell line. However, further investigation is

required to conclusively delineate the mechanistic role of RIPK1 in modulating EGFR and anoikis resistance in HNSCC.

We found that when we treated the modified HNSCC cell lines with poly(I):poly(C) there was reduced apoptosis in the metastatic cells that ectopically expressed RIPK1 and an increase in apoptosis in the primary cells where RIPK1 expression was partially silenced. This finding suggested that the loss of RIPK1 expression during tumor progression increases the sensitivity to treatment with synthetic TLR3 ligands. We believe that the implications of these findings are that RIPK1 expression or promoter methylation can be used as a potential biomarker for the use of TLR3 ligands as adjuvants for treating metastatic HNSCC.

To test the efficacy of TLR3 ligands as potent immuno-adjuvants in metastatic cells, we treated the autologous paired cell lines with poly(I):poly(C) in the presence or absence of the common HNSCC therapeutics cetuximab or cisplatin. We observed that there was a more than additive apoptotic effect when we cotreated both the primary, and more significantly, the metastatic cell lines. Together these findings advocate for in vivo studies to evaluate the effects of cotreatment on primary cells that have metastasized into lymph tissue. Additionally it would be worth investigating the levels of RIPK1 in HNSCC or additional cancer patients who have undergone cotreatment with retrospective gene array studies or that are currently being treated with poly(I):poly(C).

Since we observed that a decrease in the expression of RIPK1 in primary cells contributes to their metastatic phenotype, we hypothesized that restoring the expression of RIPK1 in metastatic cells would decrease their potential to metastasize. As a corollary of this hypothesis, if we ectopically expressed RIPK1 in a metastatic cell line, it would decrease the rate of metastasis in these cells.

Previous studies characterizing HNSCC cells lines in orthotopic murine models of oral tongue cancer revealed that there was no observable cervical lymph node metastasis of PCI-15A and PCI-15B cells (*230*). However, we were able to obtain a cell line, OSC-19-luc, which has been used in previous studies and has been shown to metastasize in 70% of mice tested (*230*). As we observed similar RIPK1 and EGFR protein quantities in the OSC-19 metastatic cell lines relative to PCI-15B cells, we expected that there would be a reduction in the growth promoting properties with ectopic RIPK1 expression. However, a caveat of this experiment is that we did not fully characterize these OSC-19-luc-RIPK1 cells in our migration and anoikis resistance assays.

By introducing this cell line into the tongues of nude mice, through intramuscular injection, we hypothesized there would be a significant decrease in the initial rate and/or overall metastasis in the cell lines expressing RIPK1. However, we did not observe a significant change in the rate of metastasis between control cells and cells expressing RIPK1. This finding was surprising, as we were not expecting the control cells to metastasize in all of the mice we tested. It is possible that there were technical limitations in these experiments. For example, we injected twice as many cells ($1x10^5$ in our study versus $5x10^4$) as the study that showed a 70% rate of metastasis (*230*). Also we discovered, through later characterization, that there were differences in the expression of luciferase between the control and RIPK1 expressing cells. Another confounding factor is that we did not characterize these cells, and it is plausible that the overexpression of RIPK1 in the OSC-19 cells was not sufficient to change their metastatic properties. It is likely that there are more chromosome abnormalities enhancing the metastatic phenotype of OSC-19 cells in the nude mouse model as they contain a disruptive p53 mutations, whereas our PCI-15A/B cell lines express WT p53 (*208*). Unfortunately, no syngeneic model

exists for HNSCC in mice. However, it could be possible to use another carcinogenesis model such as a mouse syngeneic prostate cancer model. The advantage of demonstrating this phenotype in a mouse model was that we could test the effectiveness of poly(I):poly(C) to eliminate metastatic cells that have downregulated RIPK1 expression.

6.0 FINAL DISCUSSION

Detailed understanding of the molecular mechanisms regulating tumor immunity and immunosuppression have led to the development of novel cancer immunotherapeutic approaches. The early efforts of immunotherapy were focused on enhancing the amplitude and responsiveness of effector T cells to target tumor cells by providing antigen for dendritic cell cross-presentation (*231*). However, this therapy had limitations as neoantigen-specific effector T cells often become exhausted (*232*). This exhaustion is attributed to persistent stimulation with antigen and the activation of immuno-checkpoints, both of which are crucial for maintaining self-tolerance (*232*). Consequently, the attention of immunotherapy shifted focus to targeting these inhibitory immune-checkpoint proteins, cytotoxic T-lymphocyte-associated antigen 4 (CTLA4) and programmed cell death protein 1 (PD1), which are often overexpressed on exhausted T cells (*233*). However, it has also been reported that the type I IFN response plays a central role in the process of immunosuppression by enhancing the maturation, co-stimulatory activity and by increasing the capacity of dendritic cells to present neoantigens (*104*). Therefore, the significance of the innate immune signaling pathways in the context of immunotherapeutics have attracted attention (*234*). The immunotherapy focus has thus changed to stress the importance of the innate immune receptors, which culminate in the production of IFN and can also directly mediate cell death (*235*). Among the innate immune receptors, because of its ability to strongly induce IFN, TLR3 has attracted close attention (*95, 167–171*).

While examining the role of TLR3 signaling in the metastatic progression of HNSCC, we found that there was an enhanced apoptosis by poly(I):poly(C) treatment in cells derived from metastatic tumors compared to the primary tumor (*156*). Mechanistically this difference was attributed to a defective TLR3-mediated NF-κB activation in metastatic tumor derived cell lines (*156*). We observed that, though IL-1β and TNFα-mediated NF-κB activation remained intact in the metastatic cells, there was a significant reduction in the NF-κB activation upon stimulation with poly(I):poly(C) (*156*). Since RIPK1 is an essential adaptor for TLR3 mediated activation of NF-κB and pro-survival signaling, we compared the expression changes of RIPK1 in cell lines and tumor samples. Our results suggest that RIPK1 expression is reduced during the tumor progression of HNSCC. Considering the classical role of RIPK1 in mediating TNFR signaling, our finding of RIPK1 loss in metastatic tumors was both surprising and counterintuitive. However, as discussed below, recent findings about the multifunctional roles of RIPK1 help reveal a possible explanation of reduced RIPK1 expression during HNSCC tumor progression.

RIPK1 induces TNFR-mediated necroptosis and, as it has recently been shown that TNFR signaling plays a major role in promoting metastasis, it is conceivable that a reduction in RIPK1 expression contributes to tumor survival by mitigating this form of cell death (*236*). However, this is unlikely considering that RIPK1 expression is also required to inhibit TNFR-mediated apoptosis (*197*). Additionally, in the context of TLR signaling, it has been shown that RIPK1 and RIPK3 compete for the RHIM domain in TRIF and that this interaction prevents TLR3-RIPK3 mediated necroptosis (*55*). However, multiple studies have recently emerged that provide insights into the role of RIPK1 in mediating these death pathways that may elucidate tumor development (*184*, *192*).

It was recently shown that RIPK1-null mice die within a few days of birth from systemic inflammation, and that the postnatal lethality was not prevented by deletion of RIPK3 or caspase-8 (*184*, *192*). However, RIPK1-/-, caspase8-/- and RIPK3-/- triple-knockout mice survive into adulthood, affirming the crucial role RIPK1 plays in preventing both TNFα-caspase 8 mediated apoptosis and TLR3-RIP3 necroptosis (*184*, *192*). Rickard *et al.* demonstrated that the systemic inflammation in RIPK1 null mice was caused by a NF-κB-independent RIPK3-MLKL necroptotic release of inflammatory signals IL-33 and IL-1α (*184*). This finding revealed that in addition to NF-κB-mediated inflammation, RIPK1 also participates in limiting inflammatory signals. As RIPK1 expression is required to prevent TLR3-RIPK3 mediated necrosis, reduced RIPK1 expression during the tumor progression of HNSCC may contribute to the necrotic release of IL-33 into the tumor microenvironment. The expression of IL-33 has been shown to be correlated with poor prognosis in HNSCC, ovarian cancer, breast, lung and gastric cancers (*237–240*). Also IL-33 was recently shown to increase the invasiveness of HNSCC (*241*).

Furthermore, it is well-established that inflammatory signals released from dying cells initiate the adaptive immune response by providing antigen and inflammatory signals for dendritic cells which then activate CD8+ T cells through a process called antigen cross-priming. As a follow-up to the triple-knockout experiments, Yatim et al. showed that necroptotic, but not apoptotic cell death was essential for the effective cross-priming of DCs (*219*). Moreover, they showed that RIPK1-NF-κB activation during necroptosis was required to protect mice from tumor challenge (*219*). In light of these results, it is conceivable that, while RIPK1 downregulation contributes to TNF and TLR mediated apoptosis and necroptosis respectively, the loss of NF-κB signaling in TLR3-RIPK3 mediated necroptosis may prevent the elimination

of tumors by the adaptive immune response. However, further investigation is required to determine if the reduction in RIPK1 we observed in HNSCC contributions to avoiding immune destruction.

In addition to its crucial role in activating NF-kB signaling, RIPK1 has been identified as an essential regulator in determining cell fate in response to several signaling pathways (*182*). Numerous inflammatory cytokines, PAMPs, DAMPs and genotoxic stresses culminate in apoptosis and necroptosis mediated by the expression of RIPK1 (*182*). Among these pathways, it was revealed that RIPK1 is required for PARP-1 mediated cell death in response to reactive oxygen species and DNA damaged in a p53-independent mechanism (*242*). This may partially explain why it would be advantageous for HNSCC tumors to down-regulate RIPK1 expression as mutated p53 and high chromosome instability is observed in the majority of these tumors. Furthermore, it was shown that RIPK1 interacts with the CD95/Fas death and focal adhesion kinase (FAK) survival signaling pathways to mediate anoikis in oral squamous cell carcinoma (OSCC) (*203*). Therefore, a loss in RIPK1 expression could facilitate the resistance to anoikis, enhancing the metastatic potential of HNSCC.

Given this duality of RIPK1 in promoting and limiting inflammatory signals as well as preventing and contributing to cell death, it is unsurprising that RIPK1 has been found to be both up- and down-regulated in cancers (*27*, *193–198*). For instance, it was recently shown that enhanced expression of RIPK1 is associated with the growth and invasion of human gallbladder carcinoma and that the silencing of RIPK1 inhibited the tumor growth of a gallbladder cell line in a subcutaneous xenograft mouse model (*193*). Additionally, RIPK1 expression was shown to be increased in human non-small cell lung cancer, contributed to the transformation of human bronchial epithelial cells and that RIPK1 expression increased in a cigarette smoke-exposed

mouse lung model (*194*). RIPK1 up-regulation was also shown to contribute to the growth and invasive properties in melanoma and colorectal adenocarcinoma (*195*, *196*). However, RIPK1 expression has been shown to also be down-regulated in several other types of cancer including breast, OSCC, and colon cancer (*27*, *197*, *198*).

Our investigation reveals that RIPK1 down-regulation contributes to tumor metastasis in HNSCC as RIPK1 silencing in primary derived cell lines enhances the metastatic phenotype. These findings align with others who have shown RIPK1 expression is reduced during the tumor progression (*27*, *203*). Recently, Ramnarain *et al.* showed that there is an inverse correlation between the RIP1 and the EGFR levels in breast cancer cells (*27*). Upon further investigation they revealed that RIPK1 regulates the expression of EGFR by suppressing Sp1 activity, a potent transcription factor for EGFR expression (*27*). Here we show that ectopic changes in RIPK1 also caused an inverse expression of EGFR in HNSCC. Up-regulated EGFR expression may shed light to elucidate how reduced RIPK1 expression is advantageous for tumors. The regulatory role of RIPK1 on EGFR expression may also partially explain the enhanced rates of migration that we observed after silencing RIPK1 expression in our primary derived cell lines. In addition to the RIPK1-EGFR inverse relationship, Kamarajan *et al.* recently revealed that RIPK1 and SIRT3, a NAD-dependent deacetylase that is known to regulate cell survival, metabolism, and tumorigenesis, have an opposite expression profile in OSCC (*198*). They showed that silencing RIPK1 expression increased the expression of SIRT3 and resistance to anoikis (*198*). Additionally, they showed that growing OSCC cells grown in anoikis promoting conditions caused a down-regulation of RIPK1 (*198*). Our data validates this study as silencing RIPK1 increased the resistance to anoikis in our primary HNSCC derived cell line. However, further

investigation is required to conclusively delineate the mechanistic role of RIPK1 in modulating EGFR and anoikis resistance in HNSCC.

We reconcile the differential findings of RIPK1 up- and down-regulated expression during tumor progression given the multiple, often opposing, roles of RIPK1 (*27*, *193–198*). RIPK1 expression may enhance cell survival, inflammation and proliferation as well as contribute to cell death through necroptosis (*190–192, 197, 219*). It is conceivable that RIPK1 contributes to either cell death or survival responses depending on the molecular landscape of the tumor including the expression of interacting proteins and presence of signaling molecules in the tumor microenvironment. For example, ligands present in the mucosal aerodigestive microenvironment may no longer be present in the primary tumor or sterile nodal site of metastatic cells. Additionally, it is plausible that the expression of RIPK1 may be altered throughout tumor development, as previous reports have demonstrated that RIPK1 is up-regulated in the early stages of bladder cancer and down-regulated in later stages (*243*). This may explain the observed increase in RIPK1 levels after tumor progression in several of our matched patient samples, though the overall RIPK1 expression levels were reduced in HNSCC. An additional confounding factor is that many of these patients have received radiation and chemical based treatment and it is conceivable that tumor tissues and the derived cell lines are clonally selected for altered RIPK1 expression. For example, it was shown that RIP1 and RIP3 regulate radiation-induced programmed necrosis in glioblastoma and therefore the down-regulation of these proteins can be associated with radiation resistant cells (*244*).

Our methylation data suggests a novel mechanistic cause of the RIPK1 down-regulation. We discovered a significant correlation between the reduction of RIPK1 and an increase in promoter methylation in a CpG island -868 bases from the transcription start site in matched

patient samples. We also show that treatment of a metastatic derived cell line with a hypomethylating agent rescues the expression of RIPK1. Taken together these data suggests that epigenetic changes through promoter methylation may be responsible for the downregulation of RIPK1 mRNA transcript during HNSCC tumorigenesis. As previously discussed, the ENCODE database ChIP-seq results show that the hypermethylated CpG island in RIPK1 is occupied by the transcription factor ARID3A in various cell lines. The hypermethylated region we identified may effect ARID3A binding to the promoter resulting in reduced RIPK1 transcription. However, there is no data available on the role of promoter methylation and ARID3A activity to support this conjecture. Although studies have shown that RIPK1 is downregulated in tumor progression this is the first study to our knowledge that proposes a mechanism in HNSCC. It was recently shown by Moriwaki *et al.* that, although RIPK1 and RIPK3 are downregulated in colon cancer, the down-regulation was associated with hypoxia rather than hypermethylation (*197*). We did not test for hypoxia driven changes in the expression levels of RIPK1 in our cell lines, but this would be interesting as the role of hypoxia in contributing to HNSCC metastasis is well-established (*151*).

Finally our results show that the reduction of RIPK1 expression during tumorigenesis and tumor progression, specifically in cells derived from metastatic tumors, is responsible for the enhanced apoptosis by poly(I):poly(C) treatment. In this context, our finding that the expression levels of RIPK1 regulates the apoptotic response to poly(I):poly(C), may provide an important indicator for its *in vivo* efficacy. As the downregulation of RIPK1 expression contributes to the metastatic tumor progression of HNSCC, but is essential for TLR3-NF-κB survival, we believe the results described here may open new prospects for using dsRNA to target metastatic tumor cells. In support of this theory, we show that there is a more significant apoptotic effect when we

cotreated both the primary, and more significantly, the metastatic cell lines with common HNSCC therapeutics cetuximab or cisplatin. These findings suggest that down-regulation or promoter methylation of RIPK1 can be used as a potential biomarker for treating patients with synthetic poly(I):poly(C).

In light of using the reduction of RIPK1 expression as an indicator of improved chemotherapeutic efficacy, we hypothesize there may be druggable targets to enhance the response of patient tumors to poly(I):poly(C). It was recently shown that treatment of breast cancer cells with 2-deoxy-d-glucose (2-DG), a glycolysis inhibitor, or 17-dimethylaminoethylamino-17-demethoxygeldanamycin, an Hsp90 inhibitor, causes a down-regulation of RIPK1 (*245*, *246*). Interestingly these studies showed that the down-regulation of RIPK1 from these treatments increases the apoptotic sensitivity of cells to TRAIL ligand (*245*, *246*). It may also be possible to target NF-kB activation to enhance the effect of poly(I):poly(C). One of the promising NF-κB activation inhibitors, Bortezomib, has been shown to inhibit proliferation and directly induce apoptosis in HNSCC (*247*, *248*). It would be interesting to reproduce these findings by treating HNSCC cell lines with these therapies in combination with poly(I):poly(C).

In summary, our results suggest that epigenetic changes during tumor progression promotes downregulation of RIPK1 expression. This reduced expression enhances the metastatic potential of the tumor cell to evade anoikis-induced cell death, and may contribute to tumor progression by enhancing the ability of the tumor cell to migrate. Nevertheless, because of the dual role RIPK1 plays in augmenting both cell death and survival signaling, these findings could suggest a therapeutically exploitable means to provide better efficacy for the poly(I):poly(C) adjuvant therapy. This work suggests RIPK1 as a potential candidate tumor suppressor protein

and, given the promiscuity of RIPK1 in several additional pathways, provides a new avenue of investigation to broaden our understanding of tumor progression of HNSCC. Taken together, our results reveal several important aspects of RIPK1 function in the context of tumorigenesis. First, our *in vivo* and *in vitro* data suggest despite the loss in NF-kB prosurvival signaling, downregulation of RIPK1 is correlated with tumor progression. Second, ectopic downregulation of RIPK1 enhances metastatic properties of cells, suggesting its crucial function in maintaining cellular integrity. Third, the differential levels of RIPK1 in various stages of tumor progression may significantly influence the outcome of pro-survival NF-κB signaling, which is prominently activated in tumors (*247*).

APPENDIX A: UNIQUE ANTIVITAL ROLES OF THE 2',5'-OLIGOADENYLATE SYNTHETASE ISOZYMES

Work described in this section was completed by authors Kevin Dylan McCormick, Veit Hornung, and Saumendra N. Sarkar and represents a substantial portion of the graduate work completed by Kevin McCormick during his graduate studies

A.1 INTRODUCTION

The 2′,5′-oligoadenylate synthetase (OAS) are interferon stimulated genes (ISGs) that interact with viral dsRNA present in the cytosol and induce a potent antiviral innate immune response. The *OAS1-3* genes all contain at least one nucleotidyltransferase domain (NTase), which functions as a template-independent RNA polymerase. Upon binding to dsRNA, the OAS1-3 proteins synthesize 2′,5′-linked oligoadenylates, the second messengers which activate the antiviral effector molecule ribonuclease L (RNase L) (*249*, *250*). RNase L binds to the OAS synthesized 2′,5′-oligos, dimerizes and then degrades both cellular and viral mRNA, causing an inhibition of protein synthesis (*250*). The RNase L-dependent antiviral role of the human OAS isoforms have been shown against several virus families (detailed in Table 3) (*251*). However, recent findings have revealed that OAS may have antiviral properties independent of both the NTase enzymatic and RNase L activities.

Table 3 Previously reported virus-specific antiviral activity of the OAS family

Virus	*OAS1* *(p42,p46, p48)*	*OAS2* *(p69/p72)*	*OAS3* *(p100)*	*OASL* *(a,b,c,d)*	*References*
Reoviridae					
Rotavirus	**No OAS isoforms were directly tested Rota virus activates and blocks RNase L**				(*252*)
Flaviviridae					
Hepatitis C Virus	**p46 Inhibits p42 and p48 NE**	**P69/p72 NE**	**p100 Inhibits**	**a,b Inhibits c,b NT**	(*253*, *254*)
Dengue Virus	**p42 and p46 Inhibits, p48 NE**	**P69/p72 NE**	**p100 Inhibits**	**a,b NE c,d NT**	(*255–257*)
West Nile Virus	**No OAS isoforms were directly tested WNV activates and blocks RNase L**				
Herpesviridae					
Human cytomegalovirus	**Inhibits isoform unspecified**	**NT**	**NT**	**NT**	(*258*)
Herpes simplex virus	**No OAS isoforms were directly tested RNase L deficiency enhances infection**				(*259*)
Picornaviridae					
Encephalomyocarditis virus	**NT**	**p69 and p72 Inhibits**	**NT**		(*260–262*)
Coxsackievirus	**No OAS isoforms were directly tested against CV, however RNase L deficiency enhances infection**				(*263*, *264*)
Togaviridae					
Chikungunya	**NT**	**NT**	**p100 Inhibits**	**NT**	(*265*)

NE = isoform has no effect, NT = not tested

In humans, the OAS family is made up of four genes OAS1, OAS2, OAS3 and OASL comprising a total of 10 alternatively spiced gene products OAS1 (*p42/p46/p48*), OAS2 (*p69/ p71*), OAS3 (*p100*) and OASL (*OASLa-d*). The OAS family in mice is more complex and contains a total of eight OAS1 isoforms (*mOas1a-h*), one isoform of mOas2 and mOAS3, and two isoforms of mOasL (mOasL1 and mOasL2) **Figure 20**. Unlike the three isoforms of OAS1 in humans, which arise from splicing variations generated through alternative splicing, the eight mouse OAS1 isoforms were presumably caused through gene duplication events and have generated some redundancies (*266*). The discovery of the numerous OAS repeats has puzzled

researchers for some time as there are differences in the antiviral nature of these proteins and isoforms that have yet to be explained. Recent findings have revealed that the OAS protein family exhibits enzyme-independent antiviral properties in addition to the canonical RNase L activity (*267*). Although it is well-established that human OAS1 has a potent antiviral effect against *flaviviruses*, the severity of infection depends on polymorphism-driven splice-variant isoforms (*257*, *268–273*). The difference in OAS1 isoform antiviral activity cannot be explained by its enzymatic activity alone as all of the OAS1 isoforms activate RNase L (*274*).

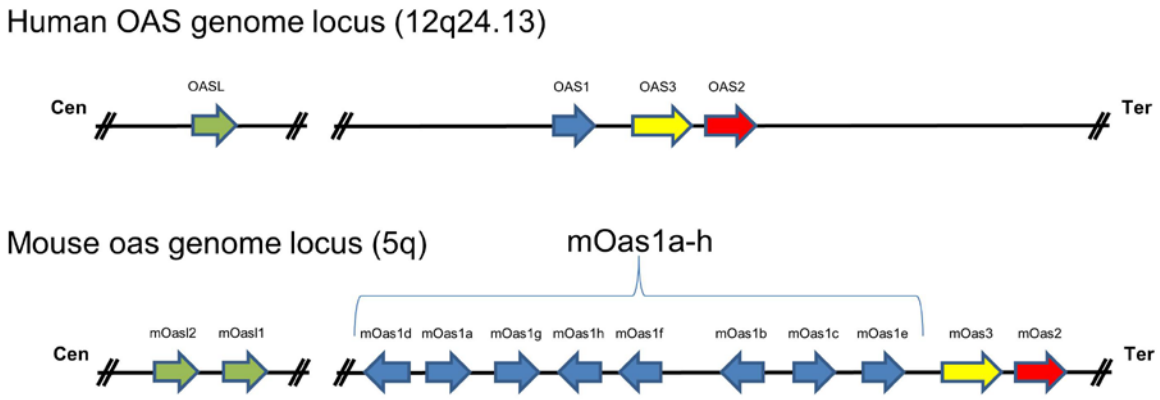

Figure 20 Schematic map showing chromosomal locations of the human and mouse OAS genes: (figure adapted from the works from Eskildsen *et al.* and Kakuta *et al.* (*275*, *276*))

Studies have emerged to elucidate the NTase-independent anti-viral mechanisms of OAS1. For example, a splice variant of OAS1, isoform 3 (also known as, p48, or 9-2), was shown to contain a Bcl-2 homology 3 (BH3) domain (*277*). Consequently, upon expression, OAS1 interacts with anti-apoptotic proteins Bcl-2 and Bclx(L) to induce apoptosis, presumably, in a type-I interferon response mechanism (*277*). In addition, as OAS1 has been shown to be present in the sera of *flaviviruses* (hepatitis C virus) infected individuals and the levels correlate to the success of treating these patients with pegylated IFNα (*278*, *279*), Kristiansen et al.

showed that this exogenous OAS1 can protect cells from virus infection (*280*). They found that exogenous OAS1 enters into cells and leads to an antiviral state independently of RNase L or IFN induction (*280*).

Moreover, it was shown by a number of groups that the virulence of West Nile Virus (WNV) in mice is dependent on mOas1b (*281–284*). More specifically, it was shown that lab strains of mice are extremely sensitive to WNV, whereas wild caught mice are resistant (*281*). Through cross breading and genotyping, it was discovered that a premature stop codon in *mOas1* gene in lab mice cause them to be more permissive to WNV infection. This is intriguing as it has been shown that the full-length mOas1b lacks a functional NTase domain and is therefore enzymatically null. Additionally, it was shown that the difference in WNV infection is not dependent on RNase L (*285*). Thus, an enzyme-independent mechanism must exist for at least one of the mOas1 proteins that has been evolutionarily selected for gene duplication.

To shed light on the RNase L independent antiviral mechanisms of OAS, a recent study proposed that the OAS proteins may directly mediate innate immune signaling (*286*). It was shown that OASL, lacks a catalytically active NTase domain and therefore does not activate RNase L, but nonetheless contributes to the innate immune antiviral state (*286*). Remarkably, it was shown that the OASL protein contains an ubiquitin-like domain, interacting with both dsRNA and RIG-I which circumvents the necessity of RIG-I to be poly-ubiquitinated (*286*). The antiviral mechanism of OASL was therefore suggested to enhance the sensing and downstream IFN induction to viral dsRNA.

We hypothesized that in addition to the NTase-independent role of OASL in RIG-I signaling, the additional OAS proteins could be modulating innate immune signaling which could explain the enzymatic-independent antiviral effects that others have observed with

mOas1b. While investigating the roles of OAS proteins in innate immune signaling, we found that the type-II IFN signaling is defective in the THP-1 OAS1 knock-out cell lines as indicated by IRF1 induction. This is an intriguing finding as the importance of IFNγ signaling and IRF1 induction have been shown to be vital for a robust antiviral response to WNV *in vivo* (*287*). Additionally, it has been shown that IRF-1 regulates adaptive immune responses as *IRF-1*-null mice show diminished levels of $CD8^+$ T cells in peripheral lymphoid organs, due to decreased class I HLA expression and impaired selection in the thymus (*287–290*).

A.2 MATERIALS AND METHODS

A.2.1 CELL LINES

The human monocytic cell line THP-1 and the THP-1 OAS 1, 2 and 3 knockouts were obtained from Veit Hornung from the Institute of Clinical Chemistry and Clinical Pharmacology, University of Bonn, Bonn, Germany.

A.2.2 CRISPR/CAS9 KNOCKOUT

A detailed protocol for the generation of THP-1 knockouts using the CRISPR/Cas9 system has been described (*291*). For the effective knockout of a gene using this system the sgRNAs must be selected preferably from the first critical coding regions of the gene of interest. Because the THP-1 cells are difficult to transfect, they must either be transduced, or in this case, they were electroporated. For electroporation the THP-1 cells were first seeded at a density of $2x10^5$

cells/ml and incubated for 24 hours in a 37 degree incubator for 24 hours. After incubation $2x10^6$ cells are resuspended in 250µl of OPTI-MEM mixed with 2.5µg of the plasmids pCMV-mCherry-T2A-Cas9 and pLKO.1-sgRNA_OAS1/2/3-CMV-GFP in a 4mm cuvette. The cells are then electroporated using an exponential pulse at 250V and 950 uF. The cells are then transferred to 6 well plates and allowed to recover for 2 days. These cells are then FACS sorted for mCherry positive cells before plating in 96 well –limiting dilution format. Because the electroporation efficiency varies between experiments, three different cell densities are chosen for the limiting dilutions 200 cells/ml, 100 cells/ml and 50 cells/ml. Sequential 1:1 dilutions of this suspension are made and 100µl is plated in the 96 well plates. The clones are grown for two weeks and grown clones are picked and re-plated in 96 wells in duplicate; using one well for further cultivation and one for subsequent genotyping.

A.2.3 ANTIBODIES AND REAGENTS

Antibodies against OAS1 were purchased from Cell Signaling Technology (Beverly, MA) and actin from Santa Cruz Biotechnology (cat.# sc-47778 Dallas, TX). Antibodies for phoso-STAT1 (P-Tyr701) were purchased from Cell signaling (#9171) and total STAT1 from Santa Cruz Biotechnology (SC-345 Dallas, TX). IRF1 antibody was also purchased from IRF1 (C-20) Santa Cruz Biotechnology (sc-497 Dallas, TX) The IFNγ was purchased from Miltenyi Biotec (130-096-873).

A.2.4 WESTERN BLOTTING ANALYSIS

To prepare whole cell lysates, cells were washed in ice-cold PBS, scraped, collected in lysis buffer (20 mM HEPES pH 7.4, 1 % Triton-X 100, 150 mM NaCl, 1.5 mM MgCl2, 12.5 mM b-glycerophosphate, 2 mM EGTA, 10 mM NaF, 2 mM DTT, 1 mM Na3VO4, 1 mM PMSF plus 1x protease inhibitors). Equal amounts of protein extracts were subjected to 8% SDS–polyacrylamide gel electrophoresis and transferred onto a polyvinylidene difluoride membrane. Membrane was blocked with 5% nonfat dry milk and incubated with primary antibody and subsequently with horseradish peroxidase–conjugated secondary antibody for 1 hour at room temperature. After washing, membranes were exposed onto film and then developed.

A.2.5 QUANTITATIVE PCR ANALYSIS OF GENE EXPRESSION

Total RNA was purified using Trizol reagent (Invitrogen) and treated with DNase I (DNA Free kit, Ambion, Foster City, CA). Total RNA (1µg) was used for reverse transcription using iScript cDNA synthesis kit (Bio-Rad, Hercules, CA) and subjected to real-time PCR using a CFX96 real time system (Bio-Rad) according to manufacturer's instructions. Primers for IRF1 (forward 5'-CTGGGCTTCACACAGTCTCA-3' reverse 5'-GTCGATCCTGGAACACTGGT-3'), STAT1 (forward 5'-CATCCGGTACACTCGCACAG reverse 5'- AAAAGGAGCCAGATCCCAAGA) and RPL32 were as previously reported (*217*).. PCR amplification of each gene was normalized to that of RPL32

A.2.6 VIRUS INFECTION AND FLOW CYTOMETRY ANALYSIS

We used a recombinant vesicular stomatitis virus (Indiana strain) encoding full-length enhanced green fluorescent protein (eGFP) in frame into the hinge region of the VSV phosphoprotein (VSV-GFP) (*292*). For the VSV-GFP infection, a total of $2x10^6$ THP-1 cells were seeded in 12 well plates. The cells were treated with 1000 U/ml of IFNγ or IFNα for 18 hours before infection with VSV-GFP virus. Aliquots were then taken from the infected wells beginning at the initial sign of infection at 4 hours (monitored by fluorescence microscopy), then at 6, 8 and 10 hours post-infection. The aliquots containing infected cells were spun down in a microcenTRIFuge for 5 minutes at 800gs. The cells were washed with 1XPBS and repelleted. After the wash, the cells were resuspended in 4% paraformaldehyde for 5 minutes at room temperature. The cells were then rewashed and stored at 4 degrees until analyzed by flow. The GFP positive cells were quantified using a BD ACCURI C6 Flow Cytometer using the percentage of infection at 0 hours PI as a control for baseline.

A.3 RESULTS

A.3.1 IFNγ signaling was defective in the THP-1 OAS1 knockout cell lines.

During our screening of innate immune signaling in THP-1 cells that were OAS1, 2 and 3 knockout, we found that IFNγ stimulated IRF1 induction was defective in the THP-1 OAS1 and, to a lesser extent, the OAS2 knockout cells **Figure 21A**. This finding was interesting as we observed that the response to IFNα was intact in all of the cell clones (data not shown). We used

a second clonal isolate of OAS1 knockout to validate the IFNγ-IRF1 result and we also observed less induction of IRF1 in these cell lines **Figure 21B**. To investigate the induction kinetics we stimulated these cells with IFNγ during increasing time points and we found that the initial rate of IRF1 induction is reduced as well as the peak levels **Figure 21C**.

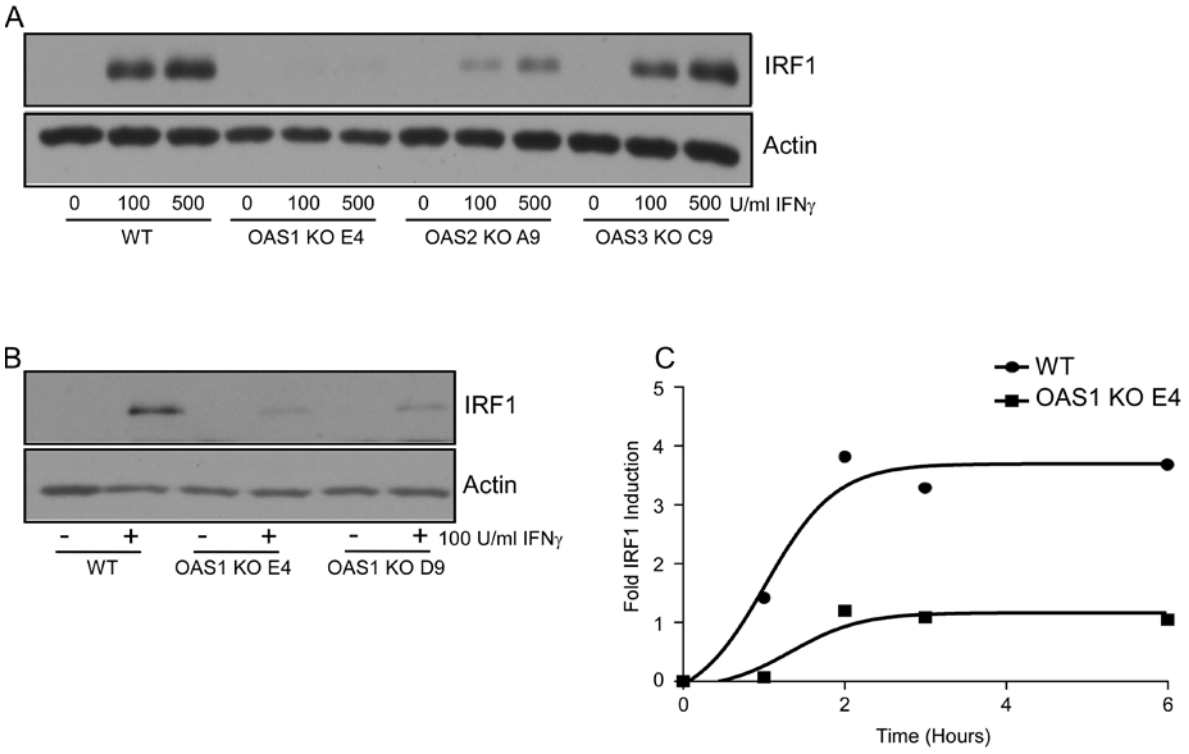

Figure 21 Loss of IRF1 induction in OAS1 knockout cell lines in response to IFNγ signaling: IRF1 induction was used to measure response to Type-I interferon stimulation. (A) WT and OAS1, 2 and 3 KO THP-1 cells were treated with IFNγ for 8 hours before whole cell lysates were analyzed by western blot. IRF1, was used as a readout for IFNγ signaling. (B) The defect in IRF1 induction was validated using an additional OAS1 knockout clone. (C) The WT and OAS1 knockout THP-1 cells were treated with 500U/ml of IFNγ for the indicated times. IRF1protein production was then quantified by western blotting followed by LiCOR and reported as fold change over Actin.

A.3.2 Downstream mediators of the IFNγ pathway are intact in OAS1 knockout cells.

To investigate the mechanistic defect in IRF1 induction upon IFNγ stimulation we analyzed the total STAT1 induction as well as the phosphorylated STAT1. There was no significant difference

in the total *STAT1* mRNA levels and protein production between the WT and OAS1 KO cells (**Figure 22A**). This is an interesting finding as, in addition to IRF1, STAT1 has also been shown to be an IFNγ-stimulated gene and therefore this suggests that there is specificity in the effect of OAS1 on IFNγ induced genes and not all the IFNγ stimulated genes were affected. Additionally we observed no significant difference in the levels of phosphorylated STAT1 suggesting again that the loss of IRF1 induction is downstream of gene expression regulation (**Figure 22A**). Indeed, when we analyzed the mRNA induction of *IRF1* there was also no significant difference between these cell lines suggesting that the total protein levels are being downregulated by a post-transcriptional mechanism (**Figure 22B&C**).

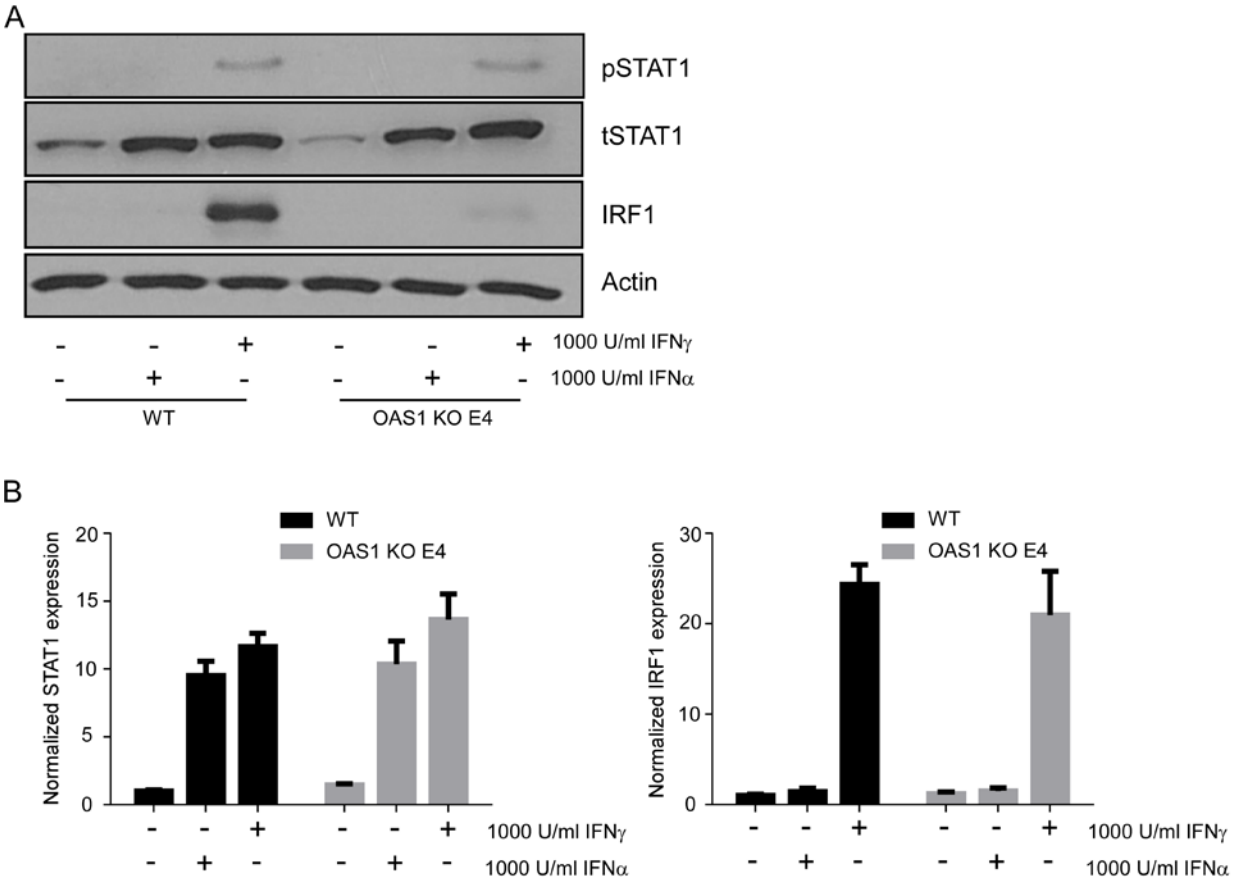

Figure 22 IFNGR downstream mediators are intact in OAS1 knockout cells: WT and OAS1 knockout cells were treated with the 1000U/ml of either IFNα or IFNγ for 8 hours and then lysates and mRNA were extracted from the cell pellets. (A) Whole-cell lysates were immunoblotted with anti-phosphorylated-STAT1, anti-total STAT1 and anti-IRF1 induction. Similarly in (B) the total mRNA was extracted and the levels of STAT1 and IRF1 induction were quantified by qRT-PCR.

A.3.3 Inhibition of the proteasome restores the induction of IRF1 upon IFNγ stimulation

There are several possible causes of the lack of protein production in the OAS1 KO cells including translational regulation. One of the possible causes for the loss of IRF1 protein in response to IFNγ in OAS1 KO cells is that there is an enhanced protein degradation of IRF1. To test if IRF1 is being degraded in the OAS1 KO cells, we stimulated the WT and OAS1 KO cells with IFNγ in the presence or absence of the proteasome inhibitor MG132. MG132 cotreatment

resulting in an increased level of IRF1 (~50%) indicating that proteosomal degradation could be at least partially responsible for the loss of IRF1 in OAS1 KO cells (**Figure 23**).

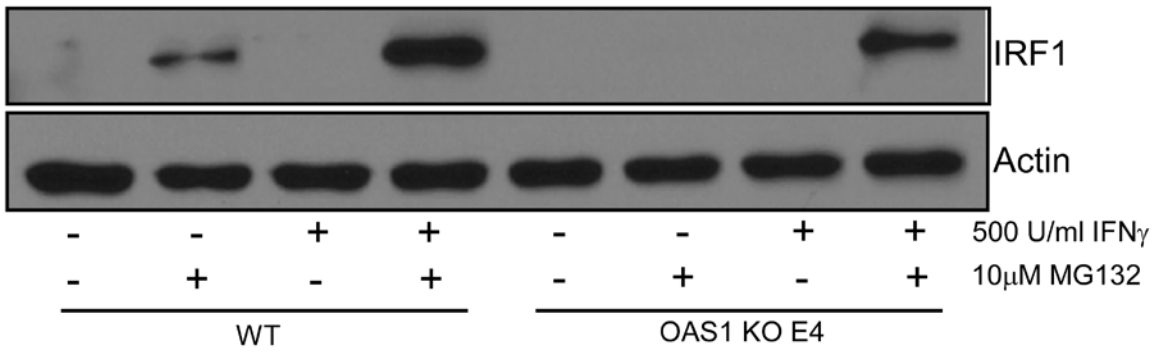

Figure 23 IRF1 proteasome degradation rate is increased in the OAS1 knockout cells: WT and OAS1 KO cells were stimulated with IFNγ in the presence or absence of the proteasome inhibitor MG132 for 6 hours before the cells were lysed and immunoblotted for the induction of IRF1 and actin.

A.3.4 Ectopic expression of mOas1b increases IRF1 stability upon IFNγ stimulation

RAW264.7 cells are derived from BALB/c mice that have been shown to express a truncated form of mOas1b, causing them to be sensitive to WNV. The mechanism of this enhanced sensitivity has not yet been elucidated. Additionally, it has been demonstrated that IRF1 plays a key role in controlling the WNV viral load within an infected mouse (*287*). Because of the lack of IRF1 induction and stability in THP-1 cells that have OAS1 deleted, we hypothesized that restoration of the full length mOas1b in the mouse cells would increase the stability of IRF1. We transfected the RAW264.7 cells with plasmids encoding the mOas1b and mOas1g and observed that in the presence of cyclohexamide, which blocks global translation, there is an increase in the steady-state levels of IRF1 in mOas1b transfected, but not control or mOas1g transfected cells

(**Figure 24**). These results indicate that mice expressing a truncated form of mOas1b may be more susceptible to infection because of the loss of IRF1 stability.

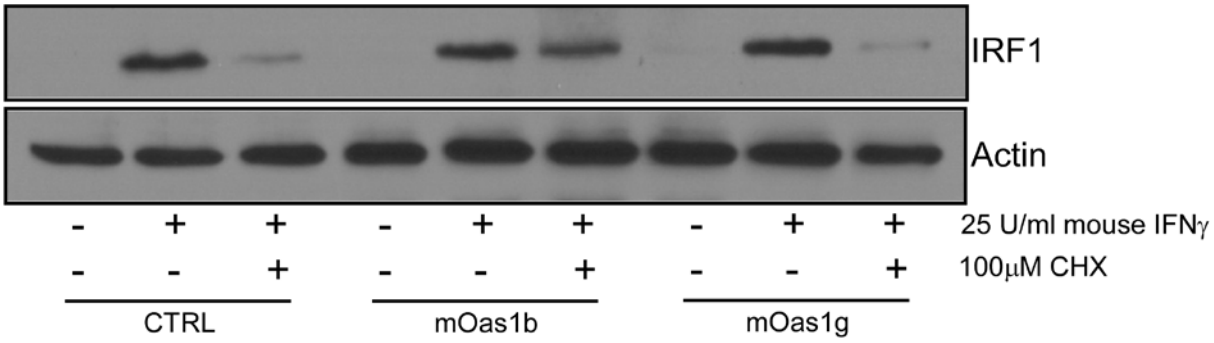

Figure 24 IRF1 protein stability was increased in RAW cells expressing mOas1b: Raw cells were transfected with the indicated plasmids for 48 hours and then treated with 25 U/ml of mouse IFNγ. After 2 hours treatment the cells were washed and either left untreated or treated with cycloheximide. After additional 2 hours incubation the cells were immunoblotted for mouse IRF1 and actin.

A.3.5 IFNγ pretreatment of THP-1 OAS1 knockout cells elicited a less protective response against VSV-GFP infection.

As previously mentioned, the mutated from of mOas1b has been shown to be responsible for WNV susceptibility in mice and IFNGR and IRF1 knockout mice have also been shown to be sensitive to WNV infection. As we observed a defect in IFNγ signaling in the OAS1 knockout cell lines, we wanted to test the antiviral activity in OAS1 knockout cells after priming with IFNγ. Because the sensitivity of VSV to IFNγ has been demonstrated in a number of studies, we reasoned that it would be a valid system to initially test the antiviral relevance of the defective IFNγ signaling in OAS1 knockout cell lines. To this end, we pretreated WT and OAS1 knockout cell lines with increasing concentrations of IFNα or IFNγ for 18 hours before infecting with VSV at an MOI of 1. Virus production was then monitored at 4, 6, 8 and 10 hours post infection by

GFP expression using flow cytometry (**Figure 25**). There were less GFP positive cells at 10 hours post infection in the IFNγ pretreated OAS1 knockout cell lines than in the WT, however as expected we observed an equal level of protection in the IFNα in both cell types.

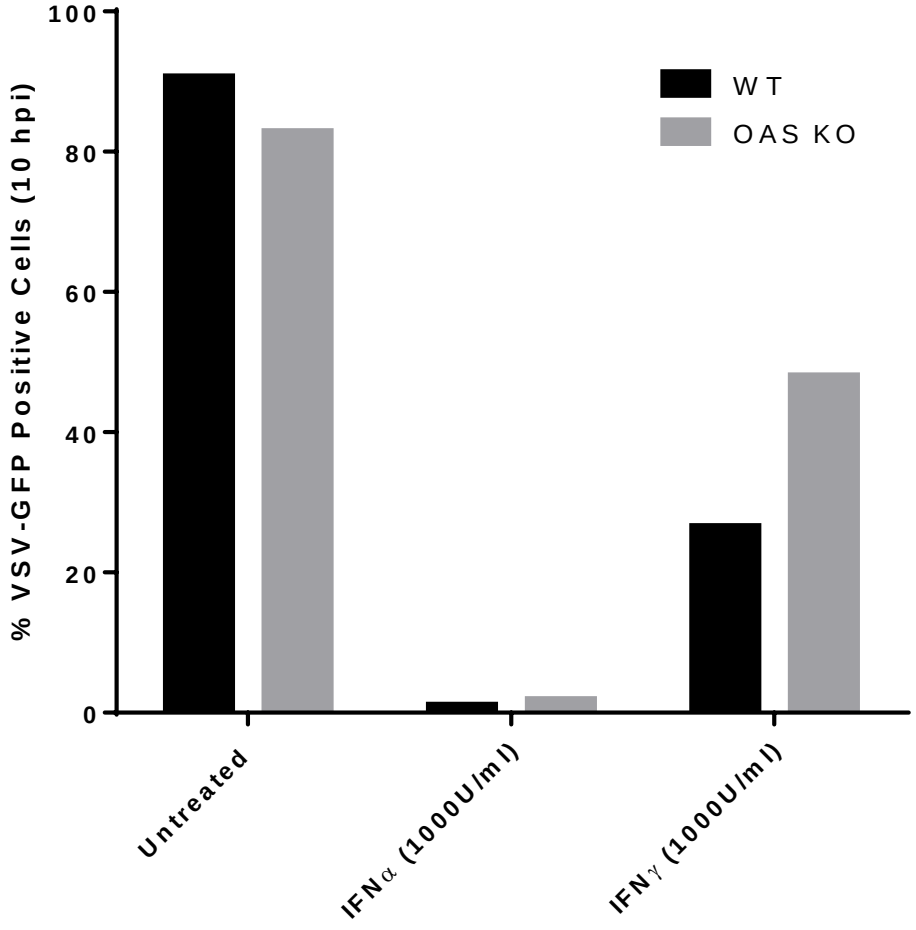

Figure 25 IFNγ pretreatment of THP-1 OAS1 KO cells elicited a less protective response against VSV-GFP: WT and OAS1 knockout cell lines were treated with 1000U/ml of IFNα or IFNγ for 18h before infecting with VSV-GFP (Indiana strain) at an MOI of 1. At ten hours post infection, the cells were PFA fixed and % infection was reported as the number of cells that were GFP positive quantified by flow cytometry relative to gated total live cells.

A.4 DISCUSSION

The recent discovery that mouse susceptibility to WNV can be traced to a premature stop codon mutation in *mOaslb,* an ortholog of OAS1, is an exciting finding given that this protein lacks an enzymatically active NTase domain. This suggests that there could be novel antiviral mechanisms for this ISG that are independent of the canonical RNaseL activation, however, the molecular mechanism of this antiviral activity has yet to be elucidated.

We found that the IFNγ induction of IRF1 is defective in human cells that lack the OAS1 protein. This defect appears to be downstream of IFNγ signaling as there was no significant difference in STAT1 phosphorylation and induction or IRF1 mRNA transcription between WT and OAS1 knockout cells. This finding suggests that OAS1 was somehow effecting the production, stability or degradation of IRF1 protein. When we inhibited proteasome within the cells with MG132 and treated the cells with IFNγ, we observed a restoration of IRF1 in the OAS1 knockout cells suggesting that OAS1 could be preventing the premature degradation of IRF1 by the proteasome. Additionally when we restored the expression of full length mOas1b to RAW cells derived from mice with a truncated mOas1b, there was a decrease in the degradation of IRF1 upon treatment with the translation inhibitor cyclohexamide indicating that it could be responsible for the increased sensitivity to WNV infection.

We believe that the increased of IRF1 degradation could explain why mice with a truncated form of mOasl are more susceptible to WNV as a number of studies have shown that both IFNγ and IRF1 are essential to controlling virus infection and dissemination (*287*). There are a number of ways OAS1 could be interfering with the proteasomal degradation of IRF1 including the regulation the polyubiquitination of IRF1, through interaction of OAS with the E3 ligase or physical impairment of the E3 ubiquitin ligase to interact with IRF1. Also possible, but

less likely as the effect seems IRF1 specific, is the ability of OAS1 to directly interact with the proteasome and prevent IRF1 degradation. In addition, it is possible that the OAS proteins are effecting more IFNγ induced genes or, more broadly, that the other OAS isozymes also have innate or adaptive immune modulatory activities independent of the enzymatic activity.

Recently it was discovered that there are polymorphisms in the OAS1 gene that are associated with more severe infection with the *flaviviruses* HCV, dengue and WNV (*257*, *268*–*273*). It was later determined that the polymorphisms that are associated with the severe forms of these diseases are at exon splicing acceptor sites and that the base changes dictate the OAS1 isoform message that will be translated (*268*). These findings suggest that there are differences in the antiviral activity of the human OAS1 isoforms, however to date there is no evidence suggesting a difference in the RNase L role of these isoforms as they all have NTase activity. We hypothesize that there is an isoform-specific effect of OAS1 on IRF1 stability that could be responsible for the difference in susceptibility of humans to these viruses. We have cloned the three isoforms of OAS1 and we are in the process of restoring the expression of each into the THP-1 cells that have OAS1 knocked out to examine this hypothesis.

Because of the importance of IFNγ signaling and its relationship to IRF1 induction in the context of innate as well as adaptive immunity, these findings have implications in not only infectious diseases including viruses, bacteria and protozoa as well as non-communicable diseases such as cancer. This suggests that the OAS proteins should be investigated more rigorously for their involvement in additional enzyme-independent mechanisms.

There are many unanswered questions that remain to be addressed from this work. It will be interesting to investigate the mechanism of how OAS1 is enhancing the stability or inhibiting the degradation of IRF1. There are a number of possibilities including direct interaction between

OAS1 and IRF1 that preventing ubiquitination or the interaction with proteins that mediate the proteosomal degradation of IRF1. Additionally we would like to validate our model *in vivo* with mOas1b truncated mice to determine if there are decreased levels of IRF1 in response to virus and if this is the factor responsible for sensitivity. Finally, it will be interesting to investigate the alternatively spiced OAS1 isoforms to determine if the previously observed polymorphism associated flavivirus susceptibility/sensitivity is associated with this phenomenon.

APPENDIX B: SV40 LARGE T ANTIGEN INDUCTION OF ISGS IS DEPENDENT ON THE LT-INITIATED DNA-DAMAGE RESPONSE

Work described in this section was published in The Journal of Immunology (J Immunol. 2014 June 15; 192(12): 5933-5942) by authors Adriana Forero, Nicholas S. Giacobbi, Ole V. Gjoerup, Kevin D. McCormick, Christopher J. Bakkenist, James M. Pipas, and Saumendra N. Sarkar.

B.1 INTRODUCTION

Upon infection, polyomaviruses (PyV) such as simian virus 40 (SV40) encode for an early protein known as Large T antigen that mediates the control of viral DNA replication, host cell proliferation and both viral and host gene expression (*293*). Because of the ability of PyV to interfere with the host cell cycle, the viral proteins, especially LT, have been associated with cell transformation through its interaction with p53 and pRB (*294–296*). The multiple functions of LT are determined by its interaction with and manipulation of a number of host proteins and pathways, however because of limitations in the knowledge of PyV, the pathogenesis and transformative properties of these viruses are not completely understood.

It has previously been shown that the expression of SV40 LT alone is sufficient to activate both the ataxia-telangiectasia mutated (ATM) and ATM and Rad3-related (ATR) DNA-damage response (DDR) pathways (*297*). The activation of these DDR pathways act to enhance viral genome replication however, at the time this study was published, the cellular consequences of this DDR activation had not been fully elucidated. Additionally it has been shown that SV40 LT expression can induce a robust interferon response in host cells with the marked induction of type I interferon (IFN) and the downstream expression of interferon stimulated genes (ISGs) (*298*). Here we provide causal evidence that links these two actions whereby the activation of DDR through the expression of SV40 LT triggers the stimulation of ISGs.

B.2 MATERIALS AND METHODS

B.2.1 CELLS AND REAGENTS

BJ/TERT cells and derived cell lines were cultured in DMEM with 20% medium 199 (Invitrogen, Carlsbad, CA), 10% FBS, and Pen/Strep. The following Abs were used in this study for immunoblot analysis: SV LT (pAb 416 and 419) (*299*), ISG56 (*139*), and OASL (Abgent, San Diego, CA) (*297*).

B.2.2 PLASMIDS AND VIRUS

Retroviral plasmids pLBNCX and pLBNCX-LT and plasmid pCMV-LT encoding SV40 LT cDNA have been previously described (doi: 10.1128/JVI.01515-08, 10.1101/gad.11.9.1098). Retroviral vectors pLBNCX and pLBNCX-LT were transfected into ($1x10^7$) packaging cell line (293-Ampho) using Fugene 6 (Roche, Mannheim, Germany) following manufacturer's guidelines and processed, as previously described (*297*, *300*).

B.2.3 QUANTITATIVE PCR ANALYSIS OF GENE EXPRESSION

Total RNA was purified using Trizol reagent (Invitrogen) and treated with DNase I (DNA Free kit, Ambion, Foster City, CA). Total RNA (1µg) was used for reverse transcription using iScript cDNA synthesis kit (Bio-Rad, Hercules, CA) and subjected to real-time PCR using a CFX96 real time system (Bio-Rad) according to manufacturer's instructions (*297*).

B.3 RESULTS AND DISCUSSION

It has previously been reported that deletion of amino acids 89–97 in LT (dl89–97) results in the ablation of its binding to Bub1 and a reduction in the activation of DDR by LT (*301*). To provide genetic evidence to support the involvement of LT-mediated DDR in inducing IFNβ, we analyzed OASL and ISG60 protein expression in cells stably transduced with either full length LT, dl89–97 or vector control (**Figure 26A**). For dI89–97 mutant expressing cells we used two different batches of BJ/TERT cells, which were generated independently at two different times (dI89–97(I) and dI89–97(II)). As previously observed, LT expression resulted in a robust induction of both ISG60 and OASL expression. However, dl89–97 expression resulted in attenuated ISG induction in both cell lines expressing dI89–97 (**Figure 26A**). The reduction in ISG expression was accompanied by diminished IFNβ, ISG60 and OASL mRNA induction in dl89–97 expressing cells (**Figure 26B**) (*297*). These findings suggest that, even in the absence of viral infection, LT induces the DRR mediated IFN response in fibroblast cells.

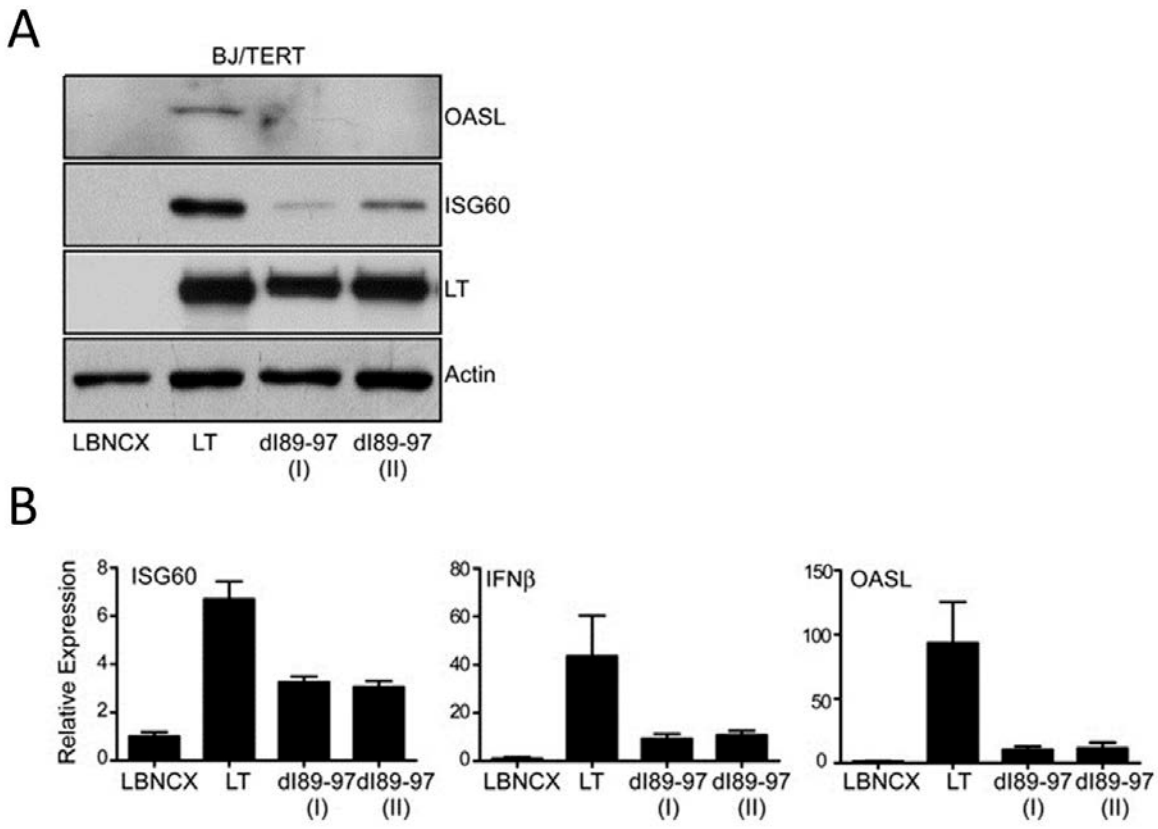

Figure 26 SV40 LT ISG induction is dependent on DDR activation: (A) Analysis of induction of ISGs by LT mutants defective in DDR induction. Lysates were prepared from BJ/TERT cells stably expressing either the wt LT or LT dI89-97. Expression of OASL, ISG60, LT, and Actin was detected by immunoblot analysis. (B) Analysis of type I IFN and ISG mRNA induction by LT mutant. Total RNA was harvested from BJ/TERT cells expressing LT, dI89-97, or empty vector. ISG60, IFNβ, and OASL mRNA expression was determined by qRT-PCR. Expression of target genes was normalized to the housekeeping gene RPL32 and reported relative to the enhancement observed over empty vector expressing cells (value 1).

APPENDIX C: IRF4 REDUCED EXPRESSION INDUCES LYTIC REACTIVATION OF KSHV IN PRIMARY EFFUSION LYMPHOMA CELLS

Work in this section was published in

Virology (Virology. 2014 June; 0: 4-10.) by Adriana Forero,

Kevin D. McCormick, Frank J. Jenkins and Saumendra N. Sarkar.

C.1 INTRODUCTION

The long term persistence of Kaposi Sarcoma-associated Herpesvirus (KSHV) has been associated with Primary Effusion Lymphoma (PEL) (*302*). The host-pathogen interactions between infected B cells and KSHV that determine the switch between latent and lytic stages of the viral replication cycle and the precise mechanism of how KSHV may contribute to tumorigenesis have not been fully elucidated. Specifically, it is known that the interplay between host cell innate immune pathways and viruses contribute to the replication cycle and the outcome of viral persistence.

The KSHV replication transactivator (RTA) is a sequence-specific DNA binding protein that recognizes and binds to RRE containing viral gene promoters, as well as ISRE and ISRE-like sequences found in the promoter regulatory regions of cellular ISGs (*303*, *304*). It is thought that the transition of KSHV from latency to lytic replication is controlled by RTA, which is necessary to initiate gene transcription, virion formation and cell death (*303*). However the host cell signaling pathways that effect the expression of RTA remain elusive.

Previously, *Forero et al.* found that the ectopic expression of IRF4 in PEL cells resulted in the inhibition of TPA stimulated RTA expression (*305*). This finding was interesting as IRF4 expression has been associated with cellular transformation. However it remained to be determined if a change in IRF4 expression, through downregulation, would increase the lytic virus cycle and result in active virus production. Here we demonstrated that a down-regulation of IRF4 expression in PEL cells elicited a robust RTA expression as expected from our previous results. This RTA induction yielded a significant increase in the amount of KSHV virions produced in the PEL cells.

C.2 MATERIALS AND METHODS

C.2.1 Nuclear Extraction Protocol for the KSHV replication transactivator (RTA) expression assay

BCBL-l stably expressing inducible shCTRL or shIRF4 were seeded in 6 well plates ($1x10^6$ cells/well) in the presence or absence of Dox (100ng/ml). After 24 hours the cells were transferred into 15ml conical tubes and pelleted at 300gs for 5 minutes. The supernatant was then removed, the cells were suspended in 1ml of 1XPBS and transferred into microcenTRIFuge tubes. The cells were then washed with PBS an additional 2X. After washing, the cell pellet was re-suspended in 100µl of a hypotonic buffer, pelleted at 1000RPMs and then re-suspended in RIPA buffer. The cells were then pulse sonicated for 1 second. After sonication, the cells were pelleted at maximum speed for 10 minutes. The lysates were then immunoblotted for Tubulin, DRBP76, IRF4 and RTA.

C.2.2 Quantitative real-time PCR assay for KSHV production

BCBL-l stably expressing inducible shCTRL or shIRF4 were seeded in T25 ($2x10^6$ cells/flask) flasks in the presence (1 sample) or absence (2 samples) of Dox (100ng/ml). After 72 hours the cells were treated with TPA (15ng/ml), co-treated with TPA (15ng/ml) and Dox (100ng/ml) or left untreated (mock) as indicated in **Figure 27B**. After 72 hours incubation with TPA, the supernatants containing cells were collected and the cells were pelleted by cenTRIFuging at 1200RPMs for 10 minutes in 50ml conical tubes. The supernatants were then transferred to Beckman SW-28 Ultra-Clear cenTRIFuge tubes (cat# 344058) and the samples were diluted to

36ml with 1xPBS to prevent the collapse of the tubes. The samples were then centrifuged , to pellet the KSHV, at 12,000rpm for 3 hours using a Beckman Optima L80K cenTRIFuge. After ultra-centrifugation , the supernatant was discarded and the pellet (often invisible) was resuspended in 500µl 1xPBS. We then used Ambion's DNA-free™ DNase treatment (50µl 10X buffer and 1µl rDNaseI incubated at 37C for 30 minutes) to remove any intracellular KSHV DNA that may have been released during cell pelleting and could have potentially contaminated our extracellular virus. We then used the phenol-chloroform technique to denature the KHSV and purify the containing DNA. Briefly, we combined equal parts (500µl) phenol-chloroform pH=8.0 (Omnipure cat#6680) to our pellets diluted in 1xPBS and after a brief vortexing, we centrifuged the samples for 10 minutes at 14,000g. The top aqueous layer was removed and transferred to a new tube containing 1ml 100% ethanol and 50µl 3M sodium acetate (1/10 original volume). The samples were then incubated overnight at -20^{o}C and then the DNA was pelleted by centrifugation at 14,000g for 15 minutes, the pellets were then washed with 500µl 70% ethanol and resuspended in 100µl nuclease free water. To quantify the KSHV DNA, we then used the AmpliTaq Gold 360 Master Mix (cat#4398876) according to the manufactures instructions with primers and a probe targeting the k8 region of the KSHV genome (real-time PCR forward primer 5'-GTC TCT TGG ACA AGC TCG CTG TT-3', reverse primer 5'-AGT GAG CAT GGC AGA TGT TCG T-3'; and probe 5'-FAM-CGG TCT GTG AAA CGG TCA TTG ACC TTA C –TAM (as described in Qu et al. 2010)).

C.3 RESULTS AND DISCUSSION

Previously we reported that ectopic expression of IRF4 resulted in the inhibition of TPA-stimulated RTA (encoded by ORF50) transcription in PEL cells (Forero et al., 2013). To determine whether depletion of IRF4 affects RTA expression in PEL cells, we examined RTA protein synthesis in Dox (100 ng/ml) treated BCBL-1 sh-IRF4 and observed an increase in the nuclear accumulation of RTA (**Figure 27**). We have now observed that there is an inverse relationship between the expression of IRF4 and the expression and downstream activity of RTA. Together these finding suggest with that IRF4 plays a role regulating the switch between KSHV latency and reactivation.

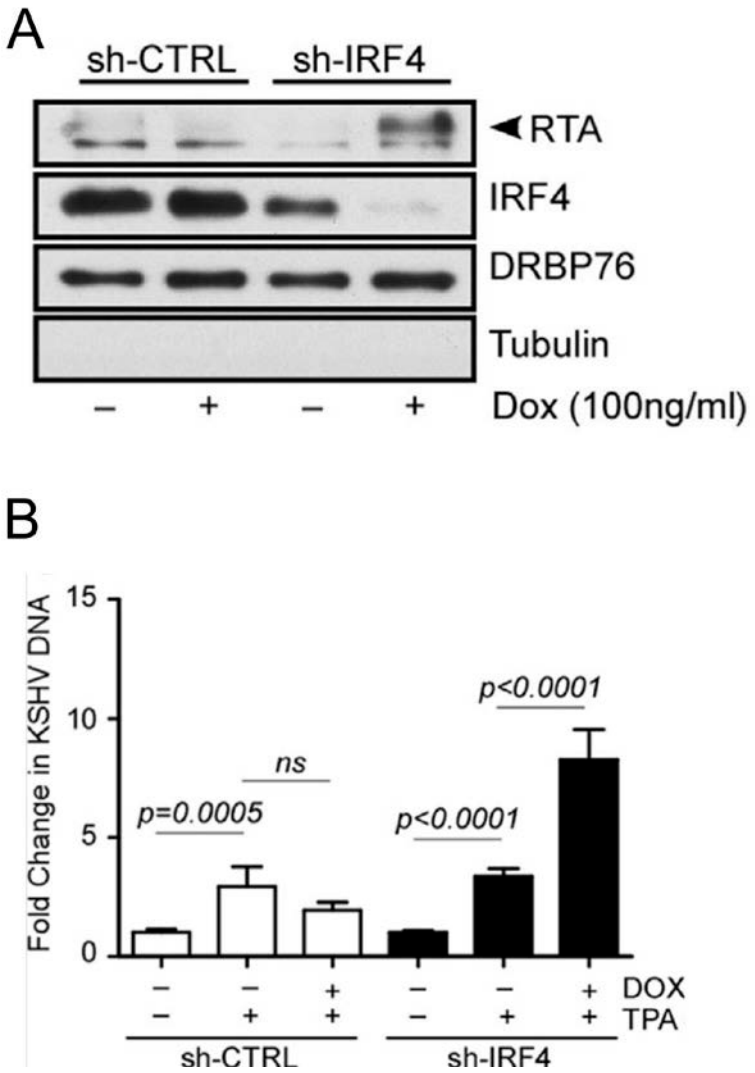

Figure 27 Loss of IRF4 results in a robust induction of KSHV lytic gene expression and viral reactivation: (A) Nuclear accumulation of KSHV replication transactivator (RTA) expression follows loss of IRF4. Nuclear fractions were prepared from cell treated with Dox for 72 h. Fractions were resolved by SDS-PAGE and immunoblotted with antibodies against IRF4, RTA, DRBP76 (nuclear marker), and Tubulin (cytoplasmic marker). (B) KSHV virion production following IRF4 silencing. BCBL-1 sh-CTRL and sh-IRF4 cells were stimulated with Dox for 72 h followed by stimulation with TPA (15 ng/ml) or Dox and TPA for an additional 72 h. KSHV DNA released into the supernatant was measured by probed-based qPCR. Results are expressed as fold change with respect to their respective untreated cells (value 1).

APPENDIX D: LIST OF ABBREVIATIONS

Table 4 Table of Abbreviations

ALT	alternative lengthening of telomeres
ATM	ataxia-telangiectasia mutated
ATR	ATM and Rad3-related
BCBL	body-cavity-based lymphoma
CBP	(cyclic-AMP-responsive-element-binding protein (CREB)-binding protein)
CBP	cyclic-AMP-responsive-element-binding protein (CREB)-binding protein
cFLIP	Cellular FLICE-like inhibitory protein
CHX	cyclohexamide
CIN	Chromosome Instability
CLR	C-type lectin receptors
cMET	MET Proto-Oncogene Receptor Tyrosine Kinase
cPARP	Cleaved-poly ADP ribose polymerase
CRT	chemoradiotherapy
CTL	cytotoxic T lymphocyte

CXCL1	chemokine (C-X-C motif) ligand 1
DAMPs	Damage Associated Molecular Patterns
DD	death domain
DDR	DNA-damage response
DISC	death-inducing signaling complex
DRBP	double-stranded RNA binding protein
DV	Dengue virus
ECD	ectodomain
ECL	Enhanced Chemiluminescence
ECM	Extracellular matrix
EGFR	Epithelial Growth Factor Receptor
EMCV	Encephalomyocarditis virus
EMT	Epithelial–mesenchymal transition
FADD	FAS-associated death domain protein
FAK	focal adhesion complex
GAGs	glycosaminoglycans
GM-CSF	granulocyte/monocyte-colony stimulating factor
HCV	hepatitis C virus
HFN	Human Fibronectin
HLA	human leukocyte antigen

HNSCC	Head and Neck Squamous Cell Carcinoma
HPV	Human papillomavirus
IAP	inhibitor of apoptosis proteins
IFN	Interferon
IKKε	IκB kinase-related kinase-ε
IL	interleukin
IRF1	Interferon Regulatory Factor 1
IRF3	Interferon Regulatory Factor 3
ISG	Interferon Stimulated gene
ISRE	interferon-stimulated response elements
IκB	Inhibitor of κB
KSHV	Kaposi's sarcoma-associated herpesvirus
KSHV	Kaposi Sarcoma-associated Herpesvirus
LRR	leucine-rich repeats
LT	Large T antigen
MAPK	mitogen-activated protein kinase
MAPK	Mitogen-activated protein kinase
MEFs	mouse embryonic fibroblast cells
MMPs	matrix metalloproteases
MOI	Multiplicity of infection

NF-κB	Nuclear Factor κB
NK	Natural killer cell
NLR	nucleotide-binding oligomerization domain-like receptors
NTase	Nucleotidyltransferase
OAS	2'-5'-oligoadenylate synthase
PAMPs	Pathogen Associated Molecular Patterns
PARP	poly(ADP-ribose) polymerase
PCI	Pittsburgh Cancer Institute
PEL	Primary Effusion Lymphoma
PEL	Primary Effusion Lymphoma
PI3K	Phosphatidylinositol 3,4,5-Trisphosphate
PKC	Phospholipase C
Poly(I):poly(C)	Polyinosinic:polycytidylic acid
PRR	Pattern Recognition Receptors
PTEN	Phosphatidylinositol 3,4,5-Trisphosphate 3-Phosphatase
PyV	polyomaviruses
RHIM	RIP homotypic interaction motif
RIPK1	Receptor Interacting Protein Kinase 1
RLR	retinoic acid-inducible gene 1 like receptor
RNase L	ribonuclease L

RRE	Rev response element
RTA	KSHV replication transactivator
RTA	KSHV replication transactivator
SCC	Squamous cell carcinoma
SIRT3	sirtuin-3
STAT1	signal transducer and activator of transcription 1
TBK1	TANK-binding kinase 1
TERT	Telomerase reverse transcriptase
TERT	Telomerase
TGFβ	Tumor Growth Factor β
TIR	Toll-IL-1 receptor
TLR	Toll Like Receptor
TNF	Tumor Necrosis Factor
TPA	Tissue plasminogen activator
TRADD	TNFR1-associated death domain protein
TRAIL	TNFα related apoptosis-inducing ligand receptor
TRI	signaling type I receptor
TRIF	TIR domain-containing adaptor
TRII	TGFB binding type II receptor
UMSCC	University of Michigan SCC

VEGF	Vascular Growth Factor Receptor
WNV	West Nile virus
β2m	beta2-microglobulin

BIBLIOGRAPHY

1. R. Weinburg, *The Biology of Cancer* (Garland Science, New York, second., 2014).

2. R. T. Greenlee, T. Murray, S. Bolden, P. A. Wingo, Cancer statistics, 2000. *CA. Cancer J. Clin.* **50**, 7–33 (2000).

3. M. Hashibe *et al.*, Consortium. **33** (2011), doi:10.1158/1055-9965.EPI-08-0347.Interaction.

4. K. D. Hunter, E. K. Parkinson, P. R. Harrison, Profiling early head and neck cancer. *Nat. Rev. Cancer*. **5**, 127–135 (2005).

5. G. P. Pfeifer *et al.*, Tobacco smoke carcinogens, DNA damage and p53 mutations in smoking-associated cancers. *Oncogene*. **21**, 7435–51 (2002).

6. M. S. Swanson, N. Kokot, U. K. Sinha, The Role of HPV in Head and Neck Cancer Stem Cell Formation and Tumorigenesis. *Cancers (Basel).* **8** (2016), doi:10.3390/cancers8020024.

7. F. Pezzuto *et al.*, Update on Head and Neck Cancer: Current Knowledge on Epidemiology, Risk Factors, Molecular Features and Novel Therapies. *Oncology*. **89**, 125–36 (2015).

8. J. B. Vermorken, P. Specenier, Optimal treatment for recurrent/metastatic head and neck cancer. *Ann. Oncol.* **21 Suppl 7**, vii252–61 (2010).

9. A. Jemal, F. Bray, J. Ferlay, Global Cancer Statistics: 2011. *CA Cancer J Clin*. **49**, 1,33–64 (1999).

10. L. A. Torre *et al.*, Global Cancer Statistics, 2012. *CA a cancer J. Clin.* **65**, 87–108 (2015).

11. J. Ferlay *et al.*, Estimates of worldwide burden of cancer in 2008: GLOBOCAN 2008. *Int. J. Cancer*. **127**, 2893–917 (2010).

12. C. C. R. Ragin, F. Modugno, S. M. Gollin, CRITICAL REVIEWS IN ORAL BIOLOGY & MEDICINE The Epidemiology and Risk Factors of Head and Neck Cancer : a Focus on Human Papillomavirus, 3–5 (2006).

13. A. Garg, P. Chaturvedi, P. C. Gupta, A review of the systemic adverse effects of areca nut or betel nut. *Indian J. Med. Paediatr. Oncol.* **35**, 3–9 (2014).

14. N. Vigneswaran, M. D. Williams, Epidemiologic Trends in Head and Neck Cancer and Aids in Diagnosis. *Oral Maxillofac. Surg. Clin. North Am.* **26**, 123–141 (2014).

15. P. M. Weinberger *et al.*, Human papillomavirus-active head and neck cancer and ethnic health disparities. *Laryngoscope*. **120**, 1531–7 (2010).

16. E. Majchrzak *et al.*, Oral cavity and oropharyngeal squamous cell carcinoma in young adults: a review of the literature. *Radiol. Oncol.* **48**, 1–10 (2014).

17. J. N. Myers, T. Elkins, D. Roberts, R. M. Byers, Squamous cell carcinoma of the tongue in young adults: increasing incidence and factors that predict treatment outcomes. *Otolaryngol. Head. Neck Surg.* **122**, 44–51 (2000).

18. A. K. Chaturvedi, E. A. Engels, W. F. Anderson, M. L. Gillison, Incidence trends for human papillomavirus-related and -unrelated oral squamous cell carcinomas in the United States. *J. Clin. Oncol.* **26**, 612–9 (2008).

19. H. Weinstock, S. Berman, W. Cates, Sexually transmitted diseases among American youth: incidence and prevalence estimates, 2000. *Perspect. Sex. Reprod. Health*. **36**, 6–10.

20. G. D'Souza, A. Dempsey, The role of HPV in head and neck cancer and review of the HPV vaccine. *Prev. Med. (Baltim).* **53**, S5–S11 (2011).

21. A. R. Kreimer, G. M. Clifford, P. Boyle, S. Franceschi, Human papillomavirus types in head and neck squamous cell carcinomas worldwide: a systematic review. *Cancer Epidemiol. Biomarkers Prev.* **14**, 467–75 (2005).

22. R. Zeitlin, H. P. Nguyen, D. Rafferty, S. Tyring, Advancements in the Management of HPV-Associated Head and Neck Squamous Cell Carcinoma. *J. Clin. Med.* **4**, 822–31 (2015).

23. A. Duray, D. Lacremans, S. Demoulin, P. Delvenne, S. Saussez, Prognosis of HPV-positive head and neck cancers: implication of smoking and immunosuppression. *Adv. Cell. Mol. Otolaryngol.* **2** (2014), doi:10.3402/acmo.v2.25717.

24. C. Scully, S. Porter, ABC of oral health. Swellings and red, white, and pigmented lesions. *BMJ*. **321**, 225–8 (2000).

25. S. Syrjänen, Human papillomavirus (HPV) in head and neck cancer. *J. Clin. Virol.* **32 Suppl 1**, S59–66 (2005).

26. P. T. Hennessey, W. H. Westra, J. A. Califano, Human Papillomavirus and Head and Neck Squamous Cell Carcinoma: Recent Evidence and Clinical Implications. *J. Dent. Res.* **88**, 300–306 (2009).

27. D. B. Ramnarain *et al.*, RIP1 links inflammatory and growth factor signaling pathways by regulating expression of the EGFR. *Cell Death Differ*. **15**, 344–353 (2008).

28. M. S. Lawrence *et al.*, Comprehensive genomic characterization of head and neck squamous cell carcinomas. *Nature*. **517**, 576–582 (2015).

29. C. R. Leemans, B. J. M. Braakhuis, R. H. Brakenhoff, The molecular biology of head and neck cancer. *Nat. Rev. Cancer*. **11**, 9–22 (2011).

30. A. Psyrri, T. Y. Seiwert, A. Jimeno, Molecular pathways in head and neck cancer: EGFR, PI3K, and more. *Am. Soc. Clin. Oncol. Educ. Book*, 246–55 (2013).

31. D. Hanahan, R. A. Weinberg, Hallmarks of Cancer: The Next Generation. *Cell*. **144**, 646–674 (2011).

32. D. Hanahan, R. A. Weinberg, The hallmarks of cancer. *Cell*. **100**, 57–70 (2000).

33. D. J. B. Ashley, The two “hit” and multible “hit” theories of carcinogenesis. *Br J Cancer*. **June 23**, 313–238 (1969).

34. C. O. NORDLING, A new theory on cancer-inducing mechanism. *Br. J. Cancer*. **7**, 68–72 (1953).

35. J. R. Grandis, D. J. Tweardy, Elevated levels of transforming growth factor alpha and epidermal growth factor receptor messenger RNA are early markers of carcinogenesis in head and neck cancer. *Cancer Res.* **53**, 3579–84 (1993).

36. B. Ozanne, C. S. Richards, F. Hendler, D. Burns, B. Gusterson, Over-expression of the EGF receptor is a hallmark of squamous cell carcinomas. *J. Pathol.* **149**, 9–14 (1986).

37. and T. Y. J. Ishitoya, M. Toriyama, N. Oguchi, K. Kitamura, M. Ohshima, K. Asano, Gene amplification and overexpression of EGF receptor in squamous cell carcinomas of the head and neck. *Br J Cancer.* **59**, 559–562 (1989).

38. J. M. Curry *et al.*, Tumor microenvironment in head and neck squamous cell carcinoma. *Semin. Oncol.* **41**, 217–34 (2014).

39. H. Li, D. Xu, B.-H. Toh, J.-P. Liu, TGF-beta and cancer: is Smad3 a repressor of hTERT gene? *Cell Res.* **16**, 169–73 (2006).

40. P. M. Siegel, J. Massagué, Cytostatic and apoptotic actions of TGF-beta in homeostasis and cancer. *Nat. Rev. Cancer*. **3**, 807–21 (2003).

41. A. B. Roberts, A. Russo, A. Felici, K. C. Flanders, Smad3: a key player in pathogenetic mechanisms dependent on TGF-beta. *Ann. N. Y. Acad. Sci.* **995**, 1–10 (2003).

42. S. Bayne, J.-P. Liu, Hormones and growth factors regulate telomerase activity in ageing and cancer. *Mol. Cell. Endocrinol.* **240**, 11–22 (2005).

43. H. Yang, S. Kyo, M. Takatura, L. Sun, Autocrine transforming growth factor beta suppresses telomerase activity and transcription of human telomerase reverse transcriptase in human cancer cells. *Cell Growth Differ.* **12**, 119–27 (2001).

44. J. S. Long, K. M. Ryan, New frontiers in promoting tumour cell death: targeting apoptosis, necroptosis and autophagy. *Oncogene*. **31**, 5045–60 (2012).

45. S. Mansilla, L. Llovera, J. Portugal, Chemotherapeutic targeting of cell death pathways. *Anticancer. Agents Med. Chem.* **12**, 226–38 (2012).

46. P. Vandenabeele, W. Declercq, F. Van Herreweghe, T. Vanden Berghe, The role of the kinases RIP1 and RIP3 in TNF-induced necrosis. *Sci. Signal.* **3**, re4 (2010).

47. A. Degterev *et al.*, Chemical inhibitor of nonapoptotic cell death with therapeutic potential for ischemic brain injury. *Nat. Chem. Biol.* **1**, 112–9 (2005).

48. L. Galluzzi *et al.*, Molecular definitions of cell death subroutines: recommendations of the Nomenclature Committee on Cell Death 2012. *Cell Death Differ.* **19**, 107–120 (2012).

49. S. Fulda, A. M. Gorman, O. Hori, A. Samali, Cellular Stress Responses: Cell Survival and Cell Death. *Int. J. Cell Biol.* **2010**, 1–23 (2010).

50. S. Elmore, Apoptosis: A Review of Programmed Cell Death. *Toxicol. Pathol.* **35**, 495–516 (2007).

51. D. R. McIlwain, T. Berger, T. W. Mak, Caspase functions in cell death and disease. *Cold Spring Harb. Perspect. Biol.* **5**, a008656 (2013).

52. S. W. Lowe, Apoptosis in cancer. *Carcinogenesis*. **21**, 485–495 (2000).

53. X. Piao *et al.*, c-FLIP maintains tissue homeostasis by preventing apoptosis and programmed necrosis. *Sci. Signal.* **5**, ra93 (2012).

54. X. Li *et al.*, Overexpression of cFLIP in head and neck squamous cell carcinoma and its clinicopathologic correlations. *J. Cancer Res. Clin. Oncol.* **134**, 609–15 (2008).

55. W. J. Kaiser *et al.*, Toll-like receptor 3-mediated necrosis via TRIF, RIP3, and MLKL. *J. Biol. Chem.* **288**, 31268–79 (2013).

56. Z. G. Liu, Molecular mechanism of TNF signaling and beyond. *Cell Res.* **15**, 24–7 (2005).

57. B. Beutler, A. Cerami, Tumor necrosis, cachexia, shock, and inflammation: a common mediator. *Annu. Rev. Biochem.* **57**, 505–18 (1988).

58. J. Folkman, Role of angiogenesis in tumor growth and metastasis. *Semin. Oncol.* **29**, 15–8 (2002).

59. J. Folkman, The role of angiogenesis in tumor growth. *Semin. Cancer Biol.* **3**, 65–71 (1992).

60. R. J. Eisma, J. D. Spiro, D. L. Kreutzer, Vascular endothelial growth factor expression in head and neck squamous cell carcinoma. *Am. J. Surg.* **174**, 513–7 (1997).

61. T. G. Dray, N. J. Hardin, R. A. Sofferman, Angiogenesis as a prognostic marker in early head and neck cancer. *Ann. Otol. Rhinol. Laryngol.* **104**, 724–9 (1995).

62. H. Mineta, Prognostic value of vascular endothelial growth factor (VEGF) in head and neck squamous cell carcinomas. *Br. J. Cancer*. **83**, 775–781 (2000).

63. M. L. Poeta *et al.*, TP53 mutations and survival in squamous-cell carcinoma of the head and neck. *N. Engl. J. Med.* **357**, 2552–61 (2007).

64. O. G. Opitz *et al.*, Cyclin D1 overexpression and p53 inactivation immortalize primary oral keratinocytes by a telomerase-independent mechanism. *J. Clin. Invest.* **108**, 725–32 (2001).

65. J. G. Rheinwald *et al.*, A two-stage, p16(INK4A)- and p53-dependent keratinocyte senescence mechanism that limits replicative potential independent of telomere status. *Mol. Cell. Biol.* **22**, 5157–72 (2002).

66. J. Califano *et al.*, Genetic progression model for head and neck cancer: implications for field cancerization. *Cancer Res.* **56**, 2488–92 (1996).

67. H. Yamaguchi, J. Wyckoff, J. Condeelis, Cell migration in tumors. *Curr. Opin. Cell Biol.* **17**, 559–564 (2005).

68. S. Markwell, S. Weed, Tumor and Stromal-Based Contributions to Head and Neck Squamous Cell Carcinoma Invasion. *Cancers (Basel).* **7**, 382–406 (2015).

69. L. J. et a;. Alberts B, Johnson A, *The Extracellular Matrix of Animals* (Garland Science, ed. 4th, 2002; http://www.ncbi.nlm.nih.gov/books/NBK26810/).

70. H. S. Leong *et al.*, Invadopodia Are Required for Cancer Cell Extravasation and Are a Therapeutic Target for Metastasis. *Cell Rep.* **8**, 1558–1570 (2014).

71. E. L. Rosenthal, L. M. Matrisian, Matrix metalloproteases in head and neck cancer. *Head Neck*. **28**, 639–648 (2006).

72. E. L. Rosenthal *et al.*, Role of the plasminogen activator and matrix metalloproteinase systems in epidermal growth factor- and scatter factor-stimulated invasion of carcinoma cells. *Cancer Res.* **58**, 5221–30 (1998).

73. Y. Imanishi *et al.*, Clinical significance of expression of membrane type 1 matrix metalloproteinase and matrix metalloproteinase-2 in human head and neck squamous cell carcinoma. *Hum. Pathol.* **31**, 895–904 (2000).

74. T. Yoshizaki *et al.*, Increased expression of membrane type 1-matrix metalloproteinase in head and neck carcinoma. *Cancer*. **79**, 139–44 (1997).

75. D. E. Bassi, H. Mahloogi, R. Lopez De Cicco, A. Klein-Szanto, Increased furin activity enhances the malignant phenotype of human head and neck cancer cells. *Am. J. Pathol.* **162**, 439–47 (2003).

76. D. E. Bassi *et al.*, Elevated furin expression in aggressive human head and neck tumors and tumor cell lines. *Mol. Carcinog.* **31**, 224–32 (2001).

77. N. Muñoz *et al.*, Epidemiologic classification of human papillomavirus types associated with cervical cancer. *N. Engl. J. Med.* **348**, 518–27 (2003).

78. F. Stubenrauch, L. A. Laimins, Human papillomavirus life cycle: active and latent phases. *Semin. Cancer Biol.* **9**, 379–86 (1999).

79. N. Dyson, P. M. Howley, K. Münger, E. Harlow, The human papilloma virus-16 E7 oncoprotein is able to bind to the retinoblastoma gene product. *Science*. **243**, 934–7 (1989).

80. B. A. Werness, A. J. Levine, P. M. Howley, Association of human papillomavirus types 16 and 18 E6 proteins with p53. *Science.* **248**, 76–9 (1990).

81. N. Keen, R. Elston, L. Crawford, Interaction of the E6 protein of human papillomavirus with cellular proteins. *Oncogene*. **9**, 1493–9 (1994).

82. J. M. Huibregtse, M. Scheffner, P. M. Howley, A cellular protein mediates association of p53 with the E6 oncoprotein of human papillomavirus types 16 or 18. *EMBO J.* **10**, 4129–35 (1991).

83. R. Klaes *et al.*, Detection of high-risk cervical intraepithelial neoplasia and cervical cancer by amplification of transcripts derived from integrated papillomavirus oncogenes. *Cancer Res.* **59**, 6132–6 (1999).

84. N. Wentzensen, S. Vinokurova, M. von Knebel Doeberitz, Systematic review of genomic integration sites of human papillomavirus genomes in epithelial dysplasia and invasive cancer of the female lower genital tract. *Cancer Res.* **64**, 3878–84 (2004).

85. K. Shibuya, C. D. Mathers, C. Boschi-Pinto, A. D. Lopez, C. J. Murray, Global and regional estimates of cancer mortality and incidence by site: II. Results for the global burden of disease 2000. *BMC Cancer*. **2**, 37 (2002).

86. C. D. Mathers, K. Shibuya, C. Boschi-Pinto, A. D. Lopez, C. J. L. Murray, Global and regional estimates of cancer mortality and incidence by site: I. Application of regional cancer survival model to estimate cancer mortality distribution by site. *BMC Cancer*. **2**, 36 (2002).

87. P. Georges, Chemotherapy advances in locally advanced head and neck cancer. *World J. Clin. Oncol.* **5**, 966 (2014).

88. J.-P. Pignon, A. le Maître, E. Maillard, J. Bourhis, MACH-NC Collaborative Group, Meta-analysis of chemotherapy in head and neck cancer (MACH-NC): an update on 93 randomised trials and 17,346 patients. *Radiother. Oncol.* **92**, 4–14 (2009).

89. F. Petrelli *et al.*, Concomitant platinum-based chemotherapy or cetuximab with radiotherapy for locally advanced head and neck cancer: a systematic review and meta-analysis of published studies. *Oral Oncol.* **50**, 1041–8 (2014).

90. J. B. Vermorken *et al.*, Platinum-based chemotherapy plus cetuximab in head and neck cancer. *N. Engl. J. Med.* **359**, 1116–27 (2008).

91. J. A. Bonner *et al.*, Radiotherapy plus cetuximab for locoregionally advanced head and neck cancer: 5-year survival data from a phase 3 randomised trial, and relation between cetuximab-induced rash and survival. *Lancet. Oncol.* **11**, 21–8 (2010).

92. T. Y. Seiwert *et al.*, The MET Receptor Tyrosine Kinase Is a Potential Novel Therapeutic Target for Head and Neck Squamous Cell Carcinoma. *Cancer Res.* **69**, 3021–3031 (2009).

93. J. A. Sparano *et al.*, Randomized phase III trial of marimastat versus placebo in patients with metastatic breast cancer who have responding or stable disease after first-line chemotherapy: Eastern Cooperative Oncology Group trial E2196. *J. Clin. Oncol.* **22**, 4683–90 (2004).

94. S. R. Bramhall *et al.*, A double-blind placebo-controlled, randomised study comparing gemcitabine and marimastat with gemcitabine and placebo as first line therapy in patients with advanced pancreatic cancer. *Br. J. Cancer*. **87**, 161–167 (2002).

95. B. Salaun *et al.*, TLR3 as a biomarker for the therapeutic efficacy of double-stranded RNA in breast cancer. *Cancer Res.* **71**, 1607–1614 (2011).

96. S. Sharma, L. Zhu, TLR3 agonists and proinflammatory antitumor activities. *Expert Opin. …*. **17**, 481–483 (2013).

97. G. P. Dunn, L. J. Old, R. D. Schreiber, The Immunobiology of Cancer Immunosurveillance and Immunoediting. *Immunity*. **21**, 137–148 (2004).

98. L. Zitvogel, A. Tesniere, G. Kroemer, Cancer despite immunosurveillance: immunoselection and immunosubversion. *Nat. Rev. Immunol.* **6**, 715–27 (2006).

99. G. P. Dunn, L. J. Old, R. D. Schreiber, The three Es of cancer immunoediting. *Annu. Rev. Immunol.* **22**, 329–60 (2004).

100. D. S. Chen, I. Mellman, Oncology Meets Immunology: The Cancer-Immunity Cycle. *Immunity*. **39**, 1–10 (2013).

101. J. Neefjes, M. L. M. Jongsma, P. Paul, O. Bakke, Towards a systems understanding of MHC class I and MHC class II antigen presentation. *Nat. Rev. Immunol.* (2011), doi:10.1038/nri3084.

102. S.-R. Woo, L. Corrales, T. F. Gajewski, Innate Immune Recognition of Cancer. *Annu. Rev. Immunol.* **33**, 445–474 (2015).

103. A. S. Dighe, E. Richards, L. J. Old, R. D. Schreiber, Enhanced in vivo growth and resistance to rejection of tumor cells expressing dominant negative IFN gamma receptors. *Immunity*. **1**, 447–56 (1994).

104. M. S. Diamond *et al.*, Type I interferon is selectively required by dendritic cells for immune rejection of tumors. *J. Exp. Med.* **208**, 1989–2003 (2011).

105. K. Schroder, Interferon- : an overview of signals, mechanisms and functions. *J. Leukoc. Biol.* **75**, 163–189 (2003).

106. D. H. Kaplan *et al.*, Demonstration of an interferon gamma-dependent tumor surveillance system in immunocompetent mice. *Proc. Natl. Acad. Sci. U. S. A.* **95**, 7556–61 (1998).

107. C. S. Tannenbaum, T. A. Hamilton, Immune-inflammatory mechanisms in IFNgamma-mediated anti-tumor activity. *Semin. Cancer Biol.* **10**, 113–23 (2000).

108. E. Padovan, G. C. Spagnoli, M. Ferrantini, M. Heberer, IFN-alpha2a induces IP-10/CXCL10 and MIG/CXCL9 production in monocyte-derived dendritic cells and enhances their capacity to attract and stimulate CD8+ effector T cells. *J. Leukoc. Biol.* **71**, 669–76 (2002).

109. R. D. Schreiber, L. J. Old, M. J. Smyth, Cancer Immunoediting: Integrating Immunity's Roles in Cancer Suppression and Promotion. *Science (80-.).* **331**, 1565–1570 (2011).

110. J. A. Aguirre-Ghiso, Models, mechanisms and clinical evidence for cancer dormancy. *Nat. Rev. Cancer*. **7**, 834–46 (2007).

111. G. T. Motz, G. Coukos, Deciphering and reversing tumor immune suppression. *Immunity*. **39**, 61–73 (2013).

112. R. L. Ferris, Immunology and Immunotherapy of Head and Neck Cancer. *J. Clin. Oncol.* **33**, 3293–304 (2015).

113. J. M. Bernstein, C. R. Bernstein, C. M. L. West, J. J. Homer, Molecular and cellular processes underlying the hallmarks of head and neck cancer. *Eur. Arch. Otorhinolaryngol.* **270**, 2585–93 (2013).

114. M. Campoli, S. Ferrone, HLA antigen changes in malignant cells: epigenetic mechanisms and biologic significance. *Oncogene*. **27**, 5869–5885 (2008).

115. J. R. Grandis *et al.*, Human leukocyte antigen class I allelic and haplotype loss in squamous cell carcinoma of the head and neck: clinical and immunogenetic consequences. *Clin. Cancer Res.* **6**, 2794–802 (2000).

116. M. D. Turner, B. Nedjai, T. Hurst, D. J. Pennington, Cytokines and chemokines: At the crossroads of cell signalling and inflammatory disease. *Biochim. Biophys. Acta - Mol. Cell Res.* **1843**, 2563–2582 (2014).

117. C. Allen, P. Clavijo, C. Van Waes, Z. Chen, Anti-Tumor Immunity in Head and Neck Cancer: Understanding the Evidence, How Tumors Escape and Immunotherapeutic Approaches. *Cancers (Basel).* **7**, 2397–2414 (2015).

118. G. Dong, Z. Chen, T. Kato, C. Van Waes, The host environment promotes the constitutive activation of nuclear factor-kappaB and proinflammatory cytokine expression during metastatic tumor progression of murine squamous cell carcinoma. *Cancer Res.* **59**, 3495–504 (1999).

119. S. Basith, B. Manavalan, T. H. Yoo, S. G. Kim, S. Choi, Roles of toll-like receptors in cancer: a double-edged sword for defense and offense. *Arch. Pharm. Res.* **35**, 1297–316 (2012).

120. V. Gosu, S. Basith, O.-P. Kwon, S. Choi, Therapeutic applications of nucleic acids and their analogues in Toll-like receptor signaling. *Molecules.* **17**, 13503–29 (2012).

121. S. Akira, K. Takeda, Toll-like receptor signalling. *Nat. Rev. Immunol.* **4**, 499–511 (2004).

122. G. Chen, M. H. Shaw, Y.-G. Kim, G. Nuñez, NOD-Like Receptors: Role in Innate Immunity and Inflammatory Disease. *Annu. Rev. Pathol. Mech. Dis.* **4**, 365–398 (2009).

123. L. A. J. O'Neill, D. Golenbock, A. G. Bowie, The history of Toll-like receptors — redefining innate immunity. *Nat. Rev. Immunol.* **13**, 453–460 (2013).

124. A. Chaturvedi, S. K. Pierce, How Location Governs Toll-Like Receptor Signaling. *Traffic.* **10**, 621–628 (2009).

125. L. A. J. O'Neill, A. G. Bowie, The family of five: TIR-domain-containing adaptors in Toll-like receptor signalling. *Nat. Rev. Immunol.* **7**, 353–64 (2007).

126. B. Manavalan, S. Basith, S. Choi, Similar Structures but Different Roles - An Updated Perspective on TLR Structures. *Front. Physiol.* **2**, 41 (2011).

127. J. L. Slack, Identification of Two Major Sites in the Type I Interleukin-1 Receptor Cytoplasmic Region Responsible for Coupling to Pro-inflammatory Signaling Pathways. *J. Biol. Chem.* **275**, 4670–4678 (2000).

128. N. J. Gay, M. Gangloff, A. N. R. Weber, Toll-like receptors as molecular switches. *Nat. Rev. Immunol.* **6**, 693–8 (2006).

129. J. K. Bell, J. Askins, P. R. Hall, D. R. Davies, D. M. Segal, The dsRNA binding site of human Toll-like receptor 3. *Proc. Natl. Acad. Sci. U. S. A.* **103**, 8792–7 (2006).

130. M. Matsumoto, H. Oshiumi, T. Seya, Antiviral responses induced by the TLR3 pathway. *Rev. Med. Virol.* **21**, 67–77 (2011).

131. H. Oshiumi, M. Matsumoto, K. Funami, T. Akazawa, T. Seya, TICAM-1, an adaptor molecule that participates in Toll-like receptor 3-mediated interferon-beta induction. *Nat. Immunol.* **4**, 161–7 (2003).

132. K. Funami *et al.*, Spatiotemporal Mobilization of Toll/IL-1 Receptor Domain-Containing Adaptor Molecule-1 in Response to dsRNA. *J. Immunol.* **179**, 6867–6872 (2007).

133. M. Matsumoto *et al.*, Subcellular Localization of Toll-Like Receptor 3 in Human Dendritic Cells. *J. Immunol.* **171**, 3154–3162 (2003).

134. H. Häcker *et al.*, Specificity in Toll-like receptor signalling through distinct effector functions of TRAF3 and TRAF6. *Nature*. **439**, 204–207 (2006).

135. S. Sankar, H. Chan, W. J. Romanow, J. Li, R. J. Bates, IKK-i signals through IRF3 and NFkappaB to mediate the production of inflammatory cytokines. *Cell. Signal.* **18**, 982–93 (2006).

136. K. A. Fitzgerald *et al.*, IKKepsilon and TBK1 are essential components of the IRF3 signaling pathway. *Nat. Immunol.* **4**, 491–6 (2003).

137. S. Sharma *et al.*, Triggering the interferon antiviral response through an IKK-related pathway. *Science*. **300**, 1148–51 (2003).

138. M. Tatematsu *et al.*, A molecular mechanism for Toll-IL-1 receptor domain-containing adaptor molecule-1-mediated IRF-3 activation. *J. Biol. Chem.* **285**, 20128–36 (2010).

139. S. N. Sarkar *et al.*, Novel roles of TLR3 tyrosine phosphorylation and PI3 kinase in double-stranded RNA signaling. *Nat. Struct. & Mol. Biol.* **11**, 1060–1067 (2004).

140. K. Honda, T. Taniguchi, IRFs: master regulators of signalling by Toll-like receptors and cytosolic pattern-recognition receptors. *Nat. Rev. Immunol.* **6**, 644–658 (2006).

141. B. K. Weaver, K. P. Kumar, N. C. Reich, Interferon regulatory factor 3 and CREB-binding protein/p300 are subunits of double-stranded RNA-activated transcription factor DRAF1. *Mol. Cell. Biol.* **18**, 1359–68 (1998).

142. M. Yoneyama *et al.*, Direct triggering of the type I interferon system by virus infection: activation of a transcription factor complex containing IRF-3 and CBP/p300. *EMBO J.* **17**, 1087–95 (1998).

143. W. Suhara *et al.*, Analyses of virus-induced homomeric and heteromeric protein associations between IRF-3 and coactivator CBP/p300. *J. Biochem.* **128**, 301–7 (2000).

144. N. Grandvaux *et al.*, Transcriptional Profiling of Interferon Regulatory Factor 3 Target Genes: Direct Involvement in the Regulation of Interferon-Stimulated Genes. *J. Virol.* **76**, 5532–5539 (2002).

145. S. Chattopadhyay *et al.*, Viral apoptosis is induced by IRF-3-mediated activation of Bax. *EMBO J.* **29**, 1762–73 (2010).

146. Z. Jiang, T. W. Mak, G. Sen, X. Li, Toll-like receptor 3-mediated activation of NF- B and IRF3 diverges at Toll-IL-1 receptor domain-containing adapter inducing IFN-. *Proc. Natl. Acad. Sci.* **101**, 3533–3538 (2004).

147. M. C. Gauzzi, M. Del Cornò, S. Gessani, Dissecting TLR3 signalling in dendritic cells. *Immunobiology*. **215**, 713–723 (2010).

148. Z. Jiang *et al.*, Poly(dI{middle dot}dC)-induced Toll-like Receptor 3 (TLR3)-mediated Activation of NFkappa B and MAP Kinase Is through an Interleukin-1 Receptor-associated Kinase (IRAK)-independent Pathway Employing the Signaling Components TLR3-TRAF6-TAK1-TAB2-PKR. *J. Biol. Chem.* **278**, 16713–16719 (2003).

149. C. Wang *et al.*, No Title. *Nature*. **412**, 346–351 (2001).

150. M. Sasai *et al.*, Cutting Edge: NF-kappaB-activating kinase-associated protein 1 participates in TLR3/Toll-IL-1 homology domain-containing adapter molecule-1-mediated IFN regulatory factor 3 activation. *J. Immunol.* **174**, 27–30 (2005).

151. M. Yamamoto *et al.*, Cutting edge: a novel Toll/IL-1 receptor domain-containing adapter that preferentially activates the IFN-beta promoter in the Toll-like receptor signaling. *J. Immunol.* **169**, 6668–72 (2002).

152. N. Cusson-Hermance, Rip1 Mediates the Trif-dependent Toll-like Receptor 3- and 4-induced NF- B Activation but Does Not Contribute to Interferon Regulatory Factor 3 Activation. *J. Biol. Chem.* **280**, 36560–36566 (2005).

153. E. Meylan *et al.*, RIP1 is an essential mediator of Toll-like receptor 3-induced NF-kappa B activation. *Nat. Immunol.* **5**, 503–7 (2004).

154. Z. He *et al.*, Functional toll-like receptor 3 expressed by oral squamous cell carcinoma induced cell apoptosis and decreased migration. *Oral Surg. Oral Med. Oral Pathol. Oral Radiol.* **118**, 92–100 (2014).

155. N. Nomi, S. Kodama, M. Suzuki, Toll-like receptor 3 signaling induces apoptosis in human head and neck cancer via survivin associated pathway. *Oncol. Rep.* **24**, 225–31 (2010).

156. N. Umemura *et al.*, Defective NF-κB signaling in metastatic head and neck cancer cells leads to enhanced apoptosis by double-stranded RNA. *Cancer Res.* **72**, 45–55 (2012).

157. C. Rydberg, A. Månsson, R. Uddman, K. Riesbeck, L.-O. Cardell, Toll-like receptor agonists induce inflammation and cell death in a model of head and neck squamous cell carcinomas. *Immunology*. **128**, e600–11 (2009).

158. R. Pries *et al.*, Induction of c-Myc-dependent cell proliferation through toll-like receptor 3 in head and neck cancer. *Int. J. Mol. Med.* **21**, 209–15 (2008).

159. H.-C. Chuang, C.-C. Huang, C.-Y. Chien, J.-H. Chuang, Toll-like receptor 3-mediated tumor invasion in head and neck cancer. *Oral Oncol.* **48**, 226–32 (2012).

160. S. E. Pike *et al.*, Vasostatin, a Calreticulin Fragment, Inhibits Angiogenesis and Suppresses Tumor Growth. *J. Exp. Med.* **188**, 2349–2356 (1998).

161. S. E. Pike *et al.*, Calreticulin and calreticulin fragments are endothelial cell inhibitors that suppress tumor growth. *Blood*. **94**, 2461–8 (1999).

162. T. Matijević, J. Pavelić, Poly(I:C) treatment influences the expression of calreticulin and profilin-1 in a human HNSCC cell line: a proteomic study. *Tumour Biol.* **33**, 1201–8 (2012).

163. Z. Ding, D. Gau, B. Deasy, A. Wells, P. Roy, Both actin and polyproline interactions of profilin-1 are required for migration, invasion and capillary morphogenesis of vascular endothelial cells. *Exp. Cell Res.* **315**, 2963–73 (2009).

164. K. Zeljic *et al.*, Association of TLR2, TLR3, TLR4 and CD14 genes polymorphisms with oral cancer risk and survival. *Oral Dis.* **20**, 416–24 (2014).

165. B. Salaun, I. Coste, M.-C. Rissoan, S. J. Lebecque, T. Renno, TLR3 can directly trigger apoptosis in human cancer cells. *J. Immunol.* **176**, 4894–901 (2006).

166. A. Paone *et al.*, Toll-like receptor 3 regulates angiogenesis and apoptosis in prostate cancer cell lines through hypoxia-inducible factor 1 alpha. *Neoplasia*. **12**, 539–49 (2010).

167. H.-C. Jeung *et al.*, Phase III trial of adjuvant 5-fluorouracil and adriamycin versus 5-fluorouracil, adriamycin, and polyadenylic-polyuridylic acid (poly A:U) for locally advanced gastric cancer after curative surgery: final results of 15-year follow-up. *Ann. Oncol.* **19**, 520–6 (2008).

168. N. Kemeny *et al.*, Randomized trial of standard therapy with or without poly I:C in patients with superficial bladder cancer. *Cancer*. **48**, 2154–7 (1981).

169. J. Lacour *et al.*, Adjuvant treatment with polyadenylic-polyuridylic acid (Polya.Polyu) in operable breast cancer. *Lancet (London, England)*. **2**, 161–4 (1980).

170. A. I. Chin *et al.*, Toll-like receptor 3-mediated suppression of TRAMP prostate cancer shows the critical role of type I interferons in tumor immune surveillance. *Cancer Res.* **70**, 2595–603 (2010).

171. G. Gambara *et al.*, TLR3 engagement induces IRF-3-dependent apoptosis in androgen-sensitive prostate cancer cells and inhibits tumour growth in vivo. *J. Cell. Mol. Med.* **19**, 327–339 (2015).

172. ClinicalTrials.gov, (available at https://clinicaltrials.gov/ct2/results?term=hiltonol&Search=Search).

173. T. M. Glavan, J. Pavelic, The exploitation of Toll-like receptor 3 signaling in cancer therapy. *Curr. Pharm. Des.* **20**, 6555–64 (2014).

174. A. H. Boulares *et al.*, Role of Poly (ADP-ribose) Polymerase (PARP) Cleavage in Apoptosis. **274**, 22932–22940 (1999).

175. D. Ofengeim, J. Yuan, Regulation of RIP1 kinase signalling at the crossroads of inflammation and cell death. *Nat. Rev. Mol. Cell Biol.* **14**, 727–736 (2013).

176. H. H. Park *et al.*, The death domain superfamily in intracellular signaling of apoptosis and inflammation. *Annu. Rev. Immunol.* **25**, 561–86 (2007).

177. D. Vercammen, P. Vandenabeele, R. Beyaert, W. Declercq, W. Fiers, Tumour necrosis factor-induced necrosis versus anti-Fas-induced apoptosis in L929 cells. *Cytokine*. **9**, 801–8 (1997).

178. N. Holler *et al.*, Fas triggers an alternative, caspase-8-independent cell death pathway using the kinase RIP as effector molecule. *Nat. Immunol.* **1**, 489–95 (2000).

179. M. Kalai *et al.*, Tipping the balance between necrosis and apoptosis in human and murine cells treated with interferon and dsRNA. *Cell Death Differ.* **9**, 981–994 (2002).

180. Y. Ma, V. Temkin, H. Liu, R. M. Pope, NF- B Protects Macrophages from Lipopolysaccharide-induced Cell Death: THE ROLE OF CASPASE 8 AND RECEPTOR-INTERACTING PROTEIN. *J. Biol. Chem.* **280**, 41827–41834 (2005).

181. M.-C. Michallet *et al.*, TRADD Protein Is an Essential Component of the RIG-like Helicase Antiviral Pathway. *Immunity*. **28**, 651–661 (2008).

182. N. Festjens, T. Vanden Berghe, S. Cornelis, P. Vandenabeele, RIP1, a kinase on the crossroads of a cell's decision to live or die. *Cell Death Differ.* **14**, 400–410 (2007).

183. W. W.-L. Wong *et al.*, RIPK1 is not essential for TNFR1-induced activation of NF-κB. *Cell Death Differ.* **17**, 482–487 (2010).

184. J. A. Rickard *et al.*, RIPK1 Regulates RIPK3-MLKL-Driven Systemic Inflammation and Emergency Hematopoiesis. *Cell*. **157**, 1175–1188 (2014).

185. M. A. Kelliher *et al.*, The death domain kinase RIP mediates the TNF-induced NF-kappaB signal. *Immunity*. **8**, 297–303 (1998).

186. D. Panayotova-Dimitrova *et al.*, cFLIP regulates skin homeostasis and protects against TNF-induced keratinocyte apoptosis. *Cell Rep.* **5**, 397–408 (2013).

187. S. Kreuz, D. Siegmund, P. Scheurich, H. Wajant, NF-kappaB inducers upregulate cFLIP, a cycloheximide-sensitive inhibitor of death receptor signaling. *Mol. Cell. Biol.* **21**, 3964–73 (2001).

188. L. Zhang *et al.*, TRAIL activates JNK and NF-κB through RIP1-dependent and -independent pathways. *Cell. Signal.* **27**, 306–14 (2015).

189. W. J. Kaiser *et al.*, RIP1 suppresses innate immune necrotic as well as apoptotic cell death during mammalian parturition. *Proc. Natl. Acad. Sci.* **111**, 7753–7758 (2014).

190. N. Takahashi *et al.*, RIPK1 ensures intestinal homeostasis by protecting the epithelium against apoptosis. *Nature*. **513**, 95–99 (2014).

191. M. Dannappel *et al.*, RIPK1 maintains epithelial homeostasis by inhibiting apoptosis and necroptosis. *Nature*. **513**, 90–94 (2014).

192. C. P. Dillon *et al.*, RIPK1 Blocks Early Postnatal Lethality Mediated by Caspase-8 and RIPK3. *Cell*. **157**, 1189–1202 (2014).

193. G. Zhu *et al.*, Expression of the RIP-1 gene and its role in growth and invasion of human gallbladder carcinoma. *Cell. Physiol. Biochem.* **34**, 1152–65 (2014).

194. W. Chen *et al.*, RIP1 maintains DNA integrity and cell proliferation by regulating PGC-1α-mediated mitochondrial oxidative phosphorylation and glycolysis. *Cell Death Differ.* **21**, 1061–70 (2014).

195. X. Y. Liu *et al.*, RIP1 Kinase Is an Oncogenic Driver in Melanoma. *Cancer Res.* **75**, 1736–48 (2015).

196. H.-X. You, Y.-H. Zhou, S.-Y. Tan, T.-H. She, Effects of silencing RIP1 with siRNA on the biological behavior of the LoVo human colon cancer cell line. *Oncol. Lett.* **7**, 2065–2072 (2014).

197. K. Moriwaki, J. Bertin, P. J. Gough, G. M. Orlowski, F. K. Chan, Differential roles of RIPK1 and RIPK3 in TNF-induced necroptosis and chemotherapeutic agent-induced cell death. *Cell Death Dis.* **6**, e1636 (2015).

198. P. Kamarajan *et al.*, Receptor-interacting protein (RIP) and Sirtuin-3 (SIRT3) are on opposite sides of anoikis and tumorigenesis. *Cancer*. **118**, 5800–10 (2012).

199. Y. Lin *et al.*, Tumor Necrosis Factor-induced Nonapoptotic Cell Death Requires Receptor-interacting Protein-mediated Cellular Reactive Oxygen Species Accumulation. *J. Biol. Chem.* **279**, 10822–10828 (2004).

200. G. M. Hur, Y.-S. Kim, M. Won, S. Choksi, Z. Liu, The death domain kinase RIP has an important role in DNA damage-induced, p53-independent cell death. *J. Biol. Chem.* **281**, 25011–7 (2006).

201. H.-M. Shen *et al.*, Essential Roles of Receptor-Interacting Protein and TRAF2 in Oxidative Stress-Induced Cell Death. *Mol. Cell. Biol.* **24**, 5914–5922 (2004).

202. S. M. Frisch, Disruption of epithelial cell-matrix interactions induces apoptosis. *J. Cell Biol.* **124**, 619–626 (1994).

203. P. Kamarajan, J. Bunek, Y. Lin, G. Nunez, Y. L. Kapila, Receptor-interacting protein shuttles between cell death and survival signaling pathways. *Mol. Biol. Cell.* **21**, 481–8 (2010).

204. G.-B. Koo *et al.*, Methylation-dependent loss of RIP3 expression in cancer represses programmed necrosis in response to chemotherapeutics. *Cell Res.* **25**, 707–725 (2015).

205. C. J. Lin *et al.*, Head and neck squamous cell carcinoma cell lines: established models and rationale for selection. *Head Neck.* **29**, 163–88 (2007).

206. H.-B. Jie *et al.*, CTLA-4^{+} Regulatory T Cells Increased in Cetuximab-Treated Head and Neck Cancer Patients Suppress NK Cell Cytotoxicity and Correlate with Poor Prognosis. *Cancer Res.* **75**, 2200–10 (2015).

207. D. S. Heo *et al.*, Biology, cytogenetics, and sensitivity to immunological effector cells of new head and neck squamous cell carcinoma lines. *Cancer Res.* **49**, 5167–75 (1989).

208. D. Sano *et al.*, Disruptive TP53 mutation is associated with aggressive disease characteristics in an orthotopic murine model of oral tongue cancer. *Clin. Cancer Res.* **17**, 6658–70 (2011).

209. M. Zhao *et al.*, Assembly and initial characterization of a panel of 85 genomically validated cell lines from diverse head and neck tumor sites. *Clin. Cancer Res.* **17**, 7248–64 (2011).

210. V. Patel *et al.*, Decreased lymphangiogenesis and lymph node metastasis by mTOR inhibition in head and neck cancer. *Cancer Res.* **71**, 7103–12 (2011).

211. J. E. Duex, A. Sorkin, RNA interference screen identifies Usp18 as a regulator of epidermal growth factor receptor synthesis. *Mol. Biol. Cell*. **20**, 1833–44 (2009).

212. R. J. Kimple *et al.*, Enhanced radiation sensitivity in HPV-positive head and neck cancer. *Cancer Res.* **73**, 4791–800 (2013).

213. R. L. Ferris *et al.*, Human papillomavirus-16 associated squamous cell carcinoma of the head and neck (SCCHN): a natural disease model provides insights into viral carcinogenesis. *Eur. J. Cancer*. **41**, 807–15 (2005).

214. K. L. Meerbrey *et al.*, The pINDUCER lentiviral toolkit for inducible RNA interference in vitro and in vivo. *Proc. Natl. Acad. Sci. U. S. A.* **108**, 3665–70 (2011).

215. J. Zhu *et al.*, High-throughput screening for TLR3-IFN regulatory factor 3 signaling pathway modulators identifies several antipsychotic drugs as TLR inhibitors. *J. Immunol.* **184**, 5768–76 (2010).

216. Cancer Genome Atlas Network, Comprehensive genomic characterization of head and neck squamous cell carcinomas. *Nature*. **517**, 576–82 (2015).

217. S. K. Arepalli, M. Choi, J.-K. Jung, H. Lee, Novel NF-κB inhibitors: a patent review (2011 - 2014). *Expert Opin. Ther. Pat.* **25**, 319–34 (2015).

218. J. Bunek, P. Kamarajan, Y. L. Kapila, Anoikis mediators in oral squamous cell carcinoma. *Oral Dis.* **17**, 355–61 (2011).

219. N. Yatim *et al.*, RIPK1 and NF- B signaling in dying cells determines cross-priming of CD8+ T cells. *Science (80-.).* **350**, 328–334 (2015).

220. J. D. McGhee, G. D. Ginder, Specific DNA methylation sites in the vicinity of the chicken beta-globin genes. *Nature*. **280**, 419–20 (1979).

221. T. Phillips, The Role of Methylation in Gene Expression. *Nat. Educ.* **1**, 116 (2008).

222. A. Videtic Paska, P. Hudler, Aberrant methylation patterns in cancer: a clinical view. *Biochem. Medica*. **25**, 161–176 (2015).

223. M. L. Ratliff, M. Mishra, M. B. Frank, J. M. Guthridge, C. F. Webb, The Transcription Factor ARID3a Is Important for In Vitro Differentiation of Human Hematopoietic Progenitors. *J. Immunol.* **196**, 614–23 (2016).

224. M. Song *et al.*, High expression of AT-rich interactive domain 3A (ARID3A) is associated with good prognosis in colorectal carcinoma. *Ann. Surg. Oncol.* **21 Suppl 4**, S481–9 (2014).

225. A. F. Chambers, A. C. Groom, I. C. MacDonald, Dissemination and growth of cancer cells in metastatic sites. *Nat. Rev. Cancer*. **2**, 563–72 (2002).

226. P. Friedl, E. B. Bröcker, The biology of cell locomotion within three-dimensional extracellular matrix. *Cell. Mol. Life Sci.* **57**, 41–64 (2000).

227. P. Friedl, K. Wolf, Tumour-cell invasion and migration: diversity and escape mechanisms. *Nat. Rev. Cancer*. **3**, 362–374 (2003).

228. P. Devreotes, A. R. Horwitz, Signaling networks that regulate cell migration. *Cold Spring Harb. Perspect. Biol.* **7**, a005959 (2015).

229. A. J. Bretland, J. Lawry, R. M. Sharrard, A study of death by anoikis in cultured epithelial cells. *Cell Prolif.* **34**, 199–210 (2001).

230. C. J. Lin *et al.*, Head and neck squamous cell carcinoma cell lines: Established models and rationale for selection. *Head Neck.* **29**, 163–188 (2007).

231. Y. Zhang, H. C. J. Ertl, Starved and Asphyxiated: How Can CD8+ T Cells within a Tumor Microenvironment Prevent Tumor Progression. *Front. Immunol.* **7** (2016), doi:10.3389/fimmu.2016.00032.

232. J. Crespo, H. Sun, T. H. Welling, Z. Tian, W. Zou, T cell anergy, exhaustion, senescence, and stemness in the tumor microenvironment. *Curr. Opin. Immunol.* **25**, 214–21 (2013).

233. K. M. Mahoney, P. D. Rennert, G. J. Freeman, Combination cancer immunotherapy and new immunomodulatory targets. *Nat. Rev. Drug Discov.* **14**, 561–84 (2015).

234. A. Sistigu *et al.*, Cancer cell–autonomous contribution of type I interferon signaling to the efficacy of chemotherapy. *Nat. Med.* **20**, 1301–1309 (2014).

235. K. Maruyama, Z. Selmani, H. Ishii, K. Yamaguchi, Innate immunity and cancer therapy. *Int. Immunopharmacol.* **11**, 350–7 (2011).

236. S. Acharyya *et al.*, A CXCL1 paracrine network links cancer chemoresistance and metastasis. *Cell*. **150**, 165–78 (2012).

237. X. Tong *et al.*, Interleukin-33 predicts poor prognosis and promotes ovarian cancer cell growth and metastasis through regulating ERK and JNK signaling pathways. *Mol. Oncol.* **10**, 113–25 (2016).

238. K. Ishikawa *et al.*, Expression of interleukin-33 is correlated with poor prognosis of patients with squamous cell carcinoma of the tongue. *Auris. Nasus. Larynx*. **41**, 552–7 (2014).

239. Z.-P. Yang *et al.*, The Association of Serum IL-33 and sST2 with Breast Cancer. *Dis. Markers*. **2015**, 516895 (2015).

240. P. Sun *et al.*, Serum interleukin-33 levels in patients with gastric cancer. *Dig. Dis. Sci.* **56**, 3596–601 (2011).

241. S.-F. Chen *et al.*, The paracrine effect of cancer-associated fibroblast-induced interleukin-33 regulates the invasiveness of head and neck squamous cell carcinoma. *J. Pathol.* **231**, 180–9 (2013).

242. G. M. Hur, The death domain kinase RIP has an essential role in DNA damage-induced NF-kappa B activation. *Genes Dev.* **17**, 873–882 (2003).

243. Z.-Q. Fang *et al.*, Gene expression profile and enrichment pathways in different stages of bladder cancer. *Genet. Mol. Res.* **12**, 1479–89 (2013).

244. A. Das *et al.*, RIP1 and RIP3 complex regulates radiation-induced programmed necrosis in glioblastoma. *Tumour Biol.* (2015), doi:10.1007/s13277-015-4621-6.

245. C. Palacios, A. I. López-Pérez, A. López-Rivas, Down-regulation of RIP expression by 17-dimethylaminoethylamino-17-demethoxygeldanamycin promotes TRAIL-induced apoptosis in breast tumor cells. *Cancer Lett.* **287**, 207–15 (2010).

246. Y. Y. Huang *et al.*, Down-regulation of RIP1 by 2-deoxy-D-glucose sensitizes breast cancer cells to TRAIL-induced apoptosis. *Eur. J. Pharmacol.* **705**, 26–34 (2013).

247. J. A. DiDonato, F. Mercurio, M. Karin, NF-κB and the link between inflammation and cancer. *Immunol. Rev.* **246**, 379–400 (2012).

248. M. Lun *et al.*, Nuclear factor-kappaB pathway as a therapeutic target in head and neck squamous cell carcinoma: pharmaceutical and molecular validation in human cell lines using Velcade and siRNA/NF-kappaB. *Ann. Clin. Lab. Sci.* **35**, 251–8 (2005).

249. A. Zilberstein, A. Kimchi, A. Schmidt, M. Revel, Isolation of two interferon-induced translational inhibitors: a protein kinase and an oligo-isoadenylate synthetase. *Proc. Natl. Acad. Sci. U. S. A.* **75**, 4734–8 (1978).

250. M. J. Clemens, B. R. Williams, Inhibition of cell-free protein synthesis by pppA2’p5'A2'p5'A: a novel oligonucleotide synthesized by interferon-treated L cell extracts. *Cell.* **13**, 565–72 (1978).

251. R. H. Silverman, Viral encounters with 2’,5'-oligoadenylate synthetase and RNase L during the interferon antiviral response. *J. Virol.* **81**, 12720–9 (2007).

252. L. Sánchez-Tacuba, M. Rojas, C. F. Arias, S. López, Rotavirus Controls Activation of the 2’-5'-Oligoadenylate Synthetase/RNase L Pathway Using at Least Two Distinct Mechanisms. *J. Virol.* **89**, 12145–53 (2015).

253. Y.-C. Kwon, J.-I. Kang, S. B. Hwang, B.-Y. Ahn, The ribonuclease L-dependent antiviral roles of human 2’,5'-oligoadenylate synthetase family members against hepatitis C virus. *FEBS Lett.* **587**, 156–64 (2013).

254. M. Ishibashi, T. Wakita, M. Esumi, 2’,5'-Oligoadenylate synthetase-like gene highly induced by hepatitis C virus infection in human liver is inhibitory to viral replication in vitro. *Biochem. Biophys. Res. Commun.* **392**, 397–402 (2010).

255. R.-J. Lin *et al.*, Distinct antiviral roles for human 2’,5'-oligoadenylate synthetase family members against dengue virus infection. *J. Immunol.* **183**, 8035–43 (2009).

256. E. Simon-Loriere *et al.*, High Anti-Dengue Virus Activity of the OAS Gene Family Is Associated With Increased Severity of Dengue. *J. Infect. Dis.* **212**, 2011–20 (2015).

257. K. Alagarasu *et al.*, Polymorphisms in the oligoadenylate synthetase gene cluster and its association with clinical outcomes of dengue virus infection. *Infect. Genet. Evol.* **14**, 390–5 (2013).

258. J. C. G. Tan *et al.*, Inhibition of 2’,5'-Oligoadenylate Synthetase Expression and Function by the Human Cytomegalovirus ORF94 Gene Product. *J. Virol.* **85**, 5696–5700 (2011).

259. K. Al-khatib, B. R. G. Williams, R. H. Silverman, W. Halford, D. J. J. Carr, The murine double-stranded RNA-dependent protein kinase PKR and the murine 2’,5'-oligoadenylate synthetase-dependent RNase L are required for IFN-beta-mediated resistance against herpes simplex virus type 1 in primary trigeminal ganglion culture. *Virology*. **313**, 126–35 (2003).

260. J. Chebath, P. Benech, M. Revel, M. Vigneron, Constitutive expression of (2’-5') oligo A synthetase confers resistance to picornavirus infection. *Nature*. **330**, 587–8.

261. I. Marié, D. Rebouillat, A. G. Hovanessian, The expression of both domains of the 69/71 kDa 2’,5' oligoadenylate synthetase generates a catalytically active enzyme and mediates an anti-viral response. *Eur. J. Biochem.* **262**, 155–65 (1999).

262. A. Ghosh, S. N. Sarkar, G. C. Sen, Cell growth regulatory and antiviral effects of the P69 isozyme of 2-5 (A) synthetase. *Virology*. **266**, 319–28 (2000).

263. M. Flodström-Tullberg *et al.*, RNase L and double-stranded RNA-dependent protein kinase exert complementary roles in islet cell defense during coxsackievirus infection. *J. Immunol.* **174**, 1171–7 (2005).

264. M. Kulka, M. S. Calvo, D. T. Ngo, S. Q. Wales, B. B. Goswami, Activation of the 2-5OAS/RNase L pathway in CVB1 or HAV/18f infected FRhK-4 cells does not require induction of OAS1 or OAS2 expression. *Virology*. **388**, 169–84 (2009).

265. A.-C. Bréhin *et al.*, The large form of human 2',5'-Oligoadenylate Synthetase (OAS3) exerts antiviral effect against Chikungunya virus. *Virology*. **384**, 216–22 (2009).

266. V. Bonnevie-Nielsen *et al.*, Variation in antiviral 2',5'-oligoadenylate synthetase (2'5'AS) enzyme activity is controlled by a single-nucleotide polymorphism at a splice-acceptor site in the OAS1 gene. *Am. J. Hum. Genet.* **76**, 623–33 (2005).

267. H. Kristiansen, H. H. Gad, S. Eskildsen-Larsen, P. Despres, R. Hartmann, The Oligoadenylate Synthetase Family: An Ancient Protein Family with Multiple Antiviral Activities. *J. Interf. Cytokine Res.* **31**, 41–47 (2011).

268. M. K. El Awady *et al.*, Single nucleotide polymorphism at exon 7 splice acceptor site of OAS1 gene determines response of hepatitis C virus patients to interferon therapy. *J. Gastroenterol. Hepatol.* **26**, 843–50 (2011).

269. M. Imran *et al.*, Correlation of OAS1 gene polymorphism at exon 7 splice accepter site with interferon-based therapy of HCV infection in Pakistan. *Viral Immunol.* **27**, 105–11 (2014).

270. R. Thamizhmani, P. Vijayachari, Association of dengue virus infection susceptibility with polymorphisms of 2'-5'-oligoadenylate synthetase genes: a case-control study. *Braz. J. Infect. Dis.* **18**, 548–50.

271. A. W. Bigham *et al.*, Host genetic risk factors for West Nile virus infection and disease progression. *PLoS One*. **6**, e24745 (2011).

272. M. Loeb *et al.*, Genetic variants and susceptibility to neurological complications following West Nile virus infection. *J. Infect. Dis.* **204**, 1031–7 (2011).

273. J. K. Lim *et al.*, Genetic variation in OAS1 is a risk factor for initial infection with West Nile virus in man. *PLoS Pathog.* **5**, e1000321 (2009).

274. R.-J. Lin *et al.*, Distinct Antiviral Roles for Human 2',5'-Oligoadenylate Synthetase Family Members against Dengue Virus Infection. *J. Immunol.* **183**, 8035–8043 (2009).

275. S. Kakuta, S. Shibata, Y. Iwakura, Genomic structure of the mouse 2',5'-oligoadenylate synthetase gene family. *J. Interferon Cytokine Res.* **22**, 981–93 (2002).

276. S. Eskildsen, R. Hartmann, N. O. Kjeldgaard, J. Justesen, Gene structure of the murine 2'-5'-oligoadenylate synthetase family. *Cell. Mol. Life Sci.* **59**, 1212–22 (2002).

277. A. Ghosh, S. N. Sarkar, T. M. Rowe, G. C. Sen, A specific isozyme of 2'-5' oligoadenylate synthetase is a dual function proapoptotic protein of the Bcl-2 family. *J. Biol. Chem.* **276**, 25447–55 (2001).

278. K.-I. Kim *et al.*, 2'-,5'-Oligoadenylate synthetase response ratio predicting virological response to PEG-interferon-alpha2b plus ribavirin therapy in patients with chronic hepatitis C. *J. Clin. Pharm. Ther.* **31**, 441–6 (2006).

279. M. Shindo *et al.*, In vivo interferon system assessed by 2'-5' oligoadenylate synthetase activity in chronic hepatitis C virus patients treated with pegylated interferon and ribavirin. *Hepatol. Res.* **38**, 1213–20 (2008).

280. H. Kristiansen *et al.*, Extracellular 2'-5' oligoadenylate synthetase stimulates RNase L-independent antiviral activity: a novel mechanism of virus-induced innate immunity. *J. Virol.* **84**, 11898–904 (2010).

281. A. A. Perelygin *et al.*, Positional cloning of the murine flavivirus resistance gene. *Proc. Natl. Acad. Sci. U. S. A.* **99**, 9322–7 (2002).

282. A. Kajaste-Rudnitski *et al.*, The 2',5'-oligoadenylate synthetase 1b is a potent inhibitor of West Nile virus replication inside infected cells. *J. Biol. Chem.* **281**, 4624–37 (2006).

283. T. Mashimo *et al.*, A nonsense mutation in the gene encoding 2'-5'-oligoadenylate synthetase/L1 isoform is associated with West Nile virus susceptibility in laboratory mice. *Proc. Natl. Acad. Sci. U. S. A.* **99**, 11311–6 (2002).

284. M. Lucas *et al.*, Infection of mouse neurones by West Nile virus is modulated by the interferon-inducible 2’-5' oligoadenylate synthetase 1b protein. *Immunol. Cell Biol.* **81**, 230–6 (2003).

285. S. V Scherbik, J. M. Paranjape, B. M. Stockman, R. H. Silverman, M. A. Brinton, RNase L plays a role in the antiviral response to West Nile virus. *J. Virol.* **80**, 2987–99 (2006).

286. J. Zhu *et al.*, Antiviral activity of human OASL protein is mediated by enhancing signaling of the RIG-I RNA sensor. *Immunity*. **40**, 936–48 (2014).

287. J. D. Brien *et al.*, Interferon Regulatory Factor-1 (IRF-1) Shapes Both Innate and CD8+ T Cell Immune Responses against West Nile Virus Infection. *PLoS Pathog.* **7**, e1002230 (2011).

288. J. M. Penninger *et al.*, The interferon regulatory transcription factor IRF-1 controls positive and negative selection of CD8+ thymocytes. *Immunity*. **7**, 243–54 (1997).

289. T. Matsuyama *et al.*, Targeted disruption of IRF-1 or IRF-2 results in abnormal type I IFN gene induction and aberrant lymphocyte development. *Cell*. **75**, 83–97 (1993).

290. L. C. White *et al.*, Regulation of LMP2 and TAP1 genes by IRF-1 explains the paucity of CD8+ T cells in IRF-1-/- mice. *Immunity*. **5**, 365–76 (1996).

291. T. Schmidt, J. L. Schmid-Burgk, T. S. Ebert, M. M. Gaidt, V. Hornung, Designer Nuclease-Mediated Generation of Knockout THP1 Cells. *Methods Mol. Biol.* **1338**, 261–72 (2016).

292. S. C. Das, D. Nayak, Y. Zhou, A. K. Pattnaik, Visualization of Intracellular Transport of Vesicular Stomatitis Virus Nucleocapsids in Living Cells. *J. Virol.* **80**, 6368–6377 (2006).

293. J. M. Pipas, SV40: Cell transformation and tumorigenesis. *Virology*. **384**, 294–303 (2009).

294. D. Ahuja, M. T. Sáenz-Robles, J. M. Pipas, SV40 large T antigen targets multiple cellular pathways to elicit cellular transformation. *Oncogene*. **24**, 7729–45 (2005).

295. M. S. Chaurushiya, M. D. Weitzman, Viral manipulation of DNA repair and cell cycle checkpoints. *DNA Repair (Amst).* **8**, 1166–76 (2009).

296. C. Kao, J. Huang, S. Q. Wu, P. Hauser, C. A. Reznikoff, Role of SV40 T antigen binding to pRB and p53 in multistep transformation in vitro of human uroepithelial cells. *Carcinogenesis*. **14**, 2297–302 (1993).

297. A. Forero *et al.*, Simian virus 40 large T antigen induces IFN-stimulated genes through ATR kinase. *J. Immunol.* **192**, 5933–42 (2014).

298. A. V Rathi, P. G. Cantalupo, S. N. Sarkar, J. M. Pipas, Induction of interferon-stimulated genes by Simian virus 40 T antigens. *Virology*. **406**, 202–11 (2010).

299. J. Hein *et al.*, Simian Virus 40 Large T Antigen Disrupts Genome Integrity and Activates a DNA Damage Response via Bub1 Binding. *J. Virol.* **83**, 117–127 (2009).

300. S. Boichuk, L. Hu, J. Hein, O. V. Gjoerup, Multiple DNA Damage Signaling and Repair Pathways Deregulated by Simian Virus 40 Large T Antigen. *J. Virol.* **84**, 8007–8020 (2010).

301. J. Hein *et al.*, Simian virus 40 large T antigen disrupts genome integrity and activates a DNA damage response via Bub1 binding. *J. Virol.* **83**, 117–27 (2009).

302. R. G. Nador *et al.*, Primary effusion lymphoma: a distinct clinicopathologic entity associated with the Kaposi's sarcoma-associated herpes virus. *Blood*. **88**, 645–56 (1996).

303. R. Sun *et al.*, A viral gene that activates lytic cycle expression of Kaposi's sarcoma-associated herpesvirus. *Proc. Natl. Acad. Sci. U. S. A.* **95**, 10866–71 (1998).

304. M. J. Song, H. J. Brown, T. T. Wu, R. Sun, Transcription activation of polyadenylated nuclear rna by rta in human herpesvirus 8/Kaposi's sarcoma-associated herpesvirus. *J. Virol.* **75**, 3129–40 (2001).

305. A. Forero, K. D. McCormick, F. J. Jenkins, S. N. Sarkar, Downregulation of IRF4 induces lytic reactivation of KSHV in primary effusion lymphoma cells. *Virology*. **458-459**, 4–10 (2014).